Dissertation

On

EXPERIMENT AND MODELING OF VERTICAL MILLING CUTTER DEFLECTION DUE TO CUTTING FORCES

Submitted in partial fulfillment of the requirement

for the award of degree of

Master of Engineering

in

Production Engineering

Submitted By

ANKIT THAKUR

Roll No. 801282002

Under the Guidance of

Dr. Tarun Kumar Bera

Assistant Professor

Department of Mechanical Engineering

Thapar University, Patiala

DEPARTMENT OF MECHANICAL ENGINEERING
THAPAR UNIVERSITY
PATIALA-147004, INDIA,

JULY – 2014

This Thesis is dedicated to

My Respected Teacher

Anirban bhattacharya

DECLARATION

I hereby declare that the thesis report entitled **"EXPERIMENT AND MODELING OF VERTICAL MILLING CUTTER DEFLECTION DUE TO CUTTING FORCES"** in the partial fulfillment of the requirements for award of **Master of Engineering** submitted in **Department of Mechanical (Production & Industrial Engineering) Engineering, Thapar University, Patiala,** is a record of my own work carried out under the supervision and guidance of **DR. TARUN KUMAR BERA, Assistant Professor, Department of Mechanical Engineering, Thapar University.** This matter embodied in this report has not been submitted in part or full to any other university or institute for the award of any degree.

Ankit Thakur.

Date: 18/07/2014 **(AnkitThakur)**

This is to certify that above declaration made by the student concerned is correct to the best of my knowledge & belief.

Tarun Kumar Bera

Dr. Tarun Kumar Bera
Assistant Professor
Mechanical Engineering Department
Thapar university, Patiala-147004

Countersigned

by:

DR. AJAY BATISH
Professor & Head
Mechanical Engineering Department
Thapar University, Patiala

DR. S.K. MOHAPATRA
Dean of Academic Affairs
Mechanical Engineering Departmer
Thapar University, Patiala

ACKNOWLEDGEMENT

I would like to express a deep sense of gratitude and thank profusely to my teachers **ANIRBAN BHATTACHARYA** and **Dr. TARUN KUMAR BERA** for their sincere & invaluable guidance, suggestions and attitude, which inspired me to submit thesis report in the present form. Their dynamism and diligent enthusiasm have been highly instrumental in keeping my spirits high. Their flawless and forthright suggestions blended with an innate intelligent application have crowned my task with success.

I am also thankful to **Dr. AJAY BATISH,** Professor and Head, Department of Mechanical Engineering for his encouragement and inspiration for execution of the thesis work.

Ankit Thakur.

ANKIT THAKUR

Roll No. 801282002

ABSTRACT

The purpose of the study was to determine the end mill cutter deflection due to cutting forces which are developed because of different parameters like feed, speed and cutting speed. Firstly, cutting forces are measured by dynamometer during machining and then measurements of the profile of the slot on coordinate measuring machine are done. The results are validated by comparing the actual profile with the desired profile. The two other theoretical methods to obtain the cutter deflection are Bond Graph modeling and Finite Element Analysis (FEA). The theoretical results are validated with the experimental result. The predicted results from FEA and Bond Graph modeling are very close to the experimental study. Though the predictions from FEA and the experimental results are reasonably accurate, Bond Graph modeling is more preferable due to significantly less computational time and space.

Keywords: End mill cutter, Deflection, Cutting forces, Depth of cut, feed, Cutting speed, Finite element analysis, Cantilever beam model

LIST OF ABBREVIATIONS

AI	Artificial intelligence
C	Capacitance
CAD	Computer aided design
CMM	Coordinate measuring machine
CNC	Computer numeric control
DOC	Depth of cut
FEA	Finite element analysis
FEM	Finite element method
GY	Gyrator
HSS	High speed steel
I	Inductance
IGES	Initial graphic exchange specification
R	Resistance
SE	Source of effort
SF	Source of flow
STEP	Standardized graphic exchange file format

NOMENCLATURE

L	Length
A	Area
P	Load
M	Moment
δ_N	Net deflection
F_a	Axial force
F_r	Radial force
F_t	Tangential deflection
U	Stain energy
V	Transverse shear force
B	Width
I_{zz}	Moment of inertia
Du	Deformation
δ_1	Axial deflection
δ_2	Radial deflection
δ_3	Tangential deflection
R_i	Resistance
M_z	Torque

LIST OF FIGURES

Chapter 4: Bond Graph Modeling of Cutter Deflection

Chapter 5: Experimental Study

LIST OF TABLES

TABLE OF CONTENTS

List of abbreviations

AI	Artificial intelligence
C	Capacitance
CAD	Computer aided design
CMM	Coordinate measuring machine
CNC	Computer numeric control
DOC	Depth of cut
FEA	Finite element analysis
FEM	Finite element method
GY	Gyrator
HSS	High speed steel
I	Inductance
IGES	Initial graphic exchange specification
R	Resistance
SE	Source of effort
SF	Source of flow
STEP	Standardized graphic exchange file format

NOMENCLATURE

L	Length
A	Area
P	Load
M	Moment
δ_N	Net deflection
F_a	Axial force
F_r	Radial force
F_t	Tangential deflection
U	Stain energy
V	Transverse shear force
B	Width
I_{zz}	Moment of inertia
Du	Deformation
δ_1	Axial deflection
δ_2	Radial deflection
δ_3	Tangential deflection
R_i	Resistance
M_z	Torque

CHAPTER 1

Introduction

The research on milling cutter deflection is very fine and précised work. The modern days there are so many new machine which done cutting so precisely but if talk in terms of accuracy in microns then some condition and factors affects the accuracy of the cutting like cutting forces, cutting feed, speed etc. Milling is material removal process widely used in industry, so accuracy and precision of cutting is must in it, to know the effect of cutting force on geometry and the inaccuracy in the actual geometry is discussed in this thesis work.

1.1 Background and Motivation

As end milling is versatile process in the milling processes, the accuracy of the cutting is depend upon the tool deflection. For prediction of tool deflection by FEM and bond graph modeling is used and validation of results with experiments.

For better and more accurate results large number of trials with different process parameters is required. Accuracy of the analytical solution may not predict the deflections very accurately whereas, more realistic prediction by FEA requires more computational time.

1.2 Introduction

The research work on milling deflection is important on the bases of accuracy. Cutter deflection consists of different directional deformation such as axial deformation, tangential deformation, and radial deformation due to the cutting force exist during cutting. Also other factor like depth of cut, cutting speed, and feed also effects on the accuracy of the ideal geometry.

1.3 Classification of Milling

Milling can be classified on the basis of their purpose and based on the nomenclature of the machine.

1.3.1 *Peripheral Milling*

Peripheral milling also known as slab milling, to remove the extra material from surface is generated by teeth of the periphery of the cutter and cutter axis rotation is plane parallel to the work piece surface is to machined.

1.3.2 *Face Milling*

Axis of rotation of spindle on which cutter is mounted is perpendicular to the surface of the work piece and tooth are located on the face and periphery of the cutter.

1.3.3 *End Milling*

End milling is commonly used process in industry due to its versatility and the tool is similar like drill bit, only the difference is that it cuts in each direction, where as bit is used for grooving or cut only along the axis of the cutter.

1.4 Nomenclature of Milling Cutter

Cutting angle and its parts has very significant role in terms of tool geometry, below Fig 1.1 shows the common cutter together with its angle and parts.

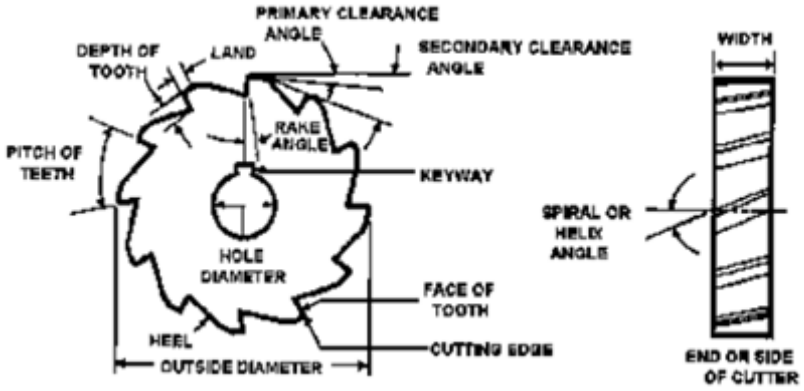

Fig. 1.1 Nomenclature of milling cutter **[Brown, 1914]**

- Pitch of the cutter are resolute by the number of tooth on the periphery of the cutter
- Pitch of the cutter refers to the angular distance between two adjacent tooth.
- Cutting of the work piece is performs by cutting edge.
- Thin surface behind the edge, land is provided on each tooth.
-

- The angle between the tooth face and the center axis of the cutter is known as rake angle. It defines the cutting edge and removes chips from the workpiece during machining or gives path to remove chip from workpiece.
- The angle between the land of the tooth from tangent line to the center line of the cutter is known as the primary clearance angle. The advantage of the angle to prevents from rubbing.
- This angle provides advantages for passage of chips and cutting oils.
- Diameter of the hole clue to determines the size of the arbor.

  [www.macklook.com].

1.5 Geometry of End Mill Cutter

An end mill is most common used milling cutter in industrial application due to its versatility. End mill cutter is resembles with drill bit somewhere but difference is that it provides cutting in the different direction whereas drill bit only performs machining in single direction i.e. along the axis of the bit. The geometry of the end mill cutter is shown in Fig 1.2.

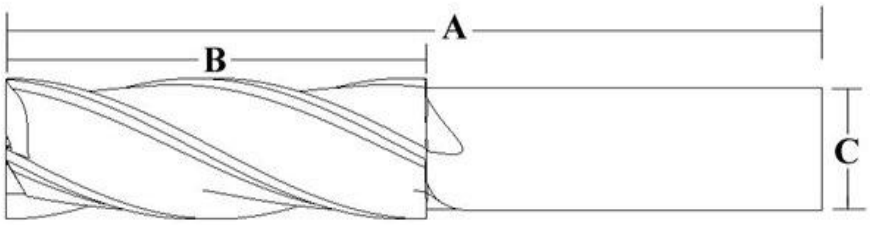

A- Overall Length of End mill Cutter
B- Cutting Length of End mill Cutter
C- Shank Diameter of End Mill Cutter

Fig. 1.2 Geometry of end mill cutter

- **Shank diameter-** It is the body which is used to clamp the cutter in the adapter.
- **Flute length-** It is the part of the cutter which performs the active role during machining , the part contacts with work piece during cutting

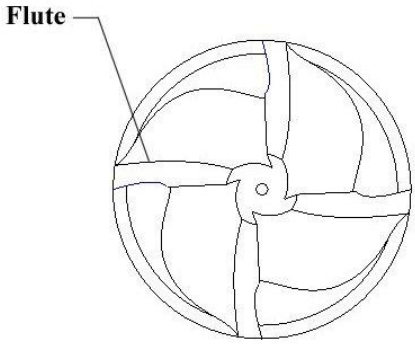

Fig. 1.3 Flute of end mill cutter

- **Flute**- Its is cutting part of the cutter as shown in Fig. 1.3, and space between cutting teeth providing chip space and regrinding capabilities. The number of cutting edges. Sometimes referred to as teeth or gullet.
- **End Mill Technical Features**- During cutting there are some failure due to rubbing and instant load when tool touch the work piece, to avoid such failure there are some angle given to tool geometry as shown below.

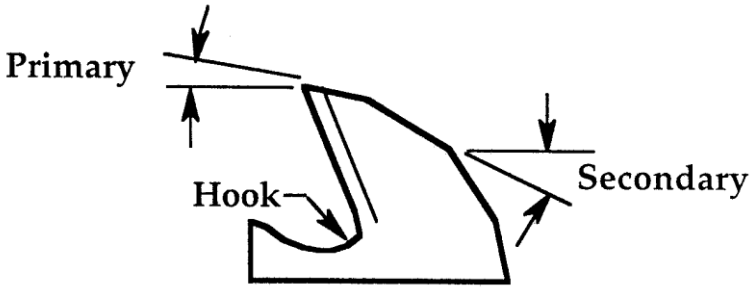

Fig. 1.4 Angles in geometry of end mill

Clearance: Primary (1st angle, 5°-9°) - Relief adjacent to the cutting edge.
Clearance: Secondary (2nd angle, 14°-17°) - Relief adjacent to cutting edge.

- **Rake angle**- The angle between the rake surface to the plane normal to the axis and it provides tool to facilitate machining work with less effort, less cutting force, etc.

In milling practice, the number of teeth in engagement is an important parameter based as which the number of teeth are often designed. Say when the depth of milling is *h*, with a milling cutter of diameter *D* (= 2*R*) and *Z* number of teeth peripherally equispaced, the engagement parameter *K* defined as the number of teeth in action is given by

$$K = \frac{\varphi}{\varepsilon} \tag{1.1}$$

where $\varphi =$ engagement angle for milling cutter, h and $\varepsilon =$ periphal pitch angle.

If it's assumed that for satisfactory cutting action, at least two teeth must be engaged, then

$$Z = \frac{2\pi}{\sqrt{h/_D}} \tag{1.2}$$

If (h/D) is kept between $(1/10)$ and $(1/20)$, the minimum number of teeth will vary between 20 and 28 **[Bhattacharya, 1998]**.

1.6 Cutting Forces in Milling Cutter

There are cutting forces in milling cutter when machined the surface.

- Radial cutting force
- Tangential cutting force

1.6.1 *Significance of the forces*

Significance of various cutting forces in the design of machine cutting tool and deflection of the cutter.

- **Tangential cutting force**

  It gives a torque and power consumption.

  - Design of the cutter, cutting tool
  - Design of the spindle and gear box

- **Radial cutting forces**

  This will cause bending on milling arbor, therefore this will also utilizes for design of machine tool.

1.6.2 *Benefits and Purpose of Determining Cutting Forces*

The aspects of cutting forces concerned

- Magnitude of cutting forces
- Location and direction of action
- Nature/pattern static or dynamic

If it's dynamic then what is frequency and amplitude.

1.6.3 *Determination of the cutting forces facilitates or is needed for*

- Estimation of cutting power consumption for selection of motor during machine tool design
- Structural design of Machine tool, fixture, and tool system.
- Evaluate the role of machining parameter on cutting forces.
- Study machinability characteristics of the work materials.

1.7 Bond Graph Approach for System Modeling

Bond graph is a unified graphical modeling tool which represents power exchanges between different dynamical parts in a system. Bond graph are far more powerful in modeling complex system even with interaction of several energy domains. Bond graph are independent formulation of classical system dynamics which reveal many obscured structures in it, and most significantly stimulate the imagination of the modeler by manifestation of concrete and abstract ideas in integrated forms. A bond graph model is capable of providing physical insight into the dynamic behavior of a system. Bond graph is a physical system can be represented by symbols and lines, identifying the power flow paths.

A bond graph is known as a graphical representation of a physical dynamic system. The difference is that the arcs represent the bi- directional exchange of physical energy while unidirectional represent by those in block diagram and signal-flow graphs. Also, bond graphs are multi domain and domain neutral. It seems that the bond graph modeling is multi domain flawlessly. Links i.e. single port double port and multi port elements are calm of bond. Each bond represents the flow of energy or power. Power variables or pair of variables are known for the flow in each bond, and the product is the immediate power of the bond. Where elements of capacitance and inductance are interconnected by bonds and junctions and make a network structure. Computer can be programmed it systematically by derivation of system equations. The software to make the modeling and simulations are Camp-G, Dymola, ENPORT, SYMBOLS.

The basic idea of a bond graph is that the power transmission between two components by the combination of "effort" and "flow" which have different interpretations in different physical domains. Table 1 gives the interpretations of the effort and the flow variables in different energy domains **[Singh, 2013]**.

Table 1.1 Power variables in different energy domains **[Singh, 2013]**

Systems	Efforts (e)	Flow (f)
Mechanical	Force (N)	Velocity (v)($m \cdot s^{-1}$)
	Torque τ ($N \cdot m$)	Angular velocity ω($rad \cdot s^{-1}$)
Hydraulic	Pressure(p)($N \cdot m^{-2}$)	Volume flow rate $\dot{Q}$ $m^3 \cdot s^{-1}$)
Electrical	Voltage (v)	Current (A)
Thermal	Temperature(K)	Entropy change rate $\dot{s}$ ($W \cdot K^1$)
	Pressure (Pa)	Volume change rate $\dot{v}$
Chemical	Chemical potential (μ)($N \cdot m \cdot mol^{-1}$)	Mass flow rate ($mol \cdot s^{-1}$)

In bond graph the symbol can be recognize into four groups

- Basic one port passive elements *i.e.* inductance (*I*), capacitance (C) and resistance (R).
- Two basic active source element *i.e.* source of effort (Se or SE) and source of flow (Sf or SF).
- Two basic two port elements *i.e.* gyrator (GY) and transformer (TF).
- Two basic junctions constant *i.e.* effort junction (0) and constant flow junction (1) **[Singh, 2013]**.

1.8 Organization of Thesis

The six chapters are included in this thesis work. Overview and all information included into these chapters are given in the following:

A comprehensive literature review is presented in the

Chapter 2 presents literature pertaining to finite element analysis of milling cutter and experimental studies of different cutters. The literature on different condition on which deflection of cutter depend such as feed, cutting speed, depth of cut, are also discussed in this chapter.

Chapter 3 presents the modeling of end mill cutter and finite element analysis with the help of ANSYS software, and discussed about the cutter deflection in various direction due to cutting forces.

Chapter 4 presents the analytical and bond graph modeling of end mill cutter, It includes the development of model by cantilever beam model and give the cutter deflection in various direction due to load.

Chapter 5 presents the details about experimental study of end mill cutter deflection at various condition like feed, speed and depth of cut on vertical milling Computer Numeric Control (CNC), and help to find the actual deflection due to forces exerted on it, the measurement of deflection on very fine instrument called Coordinate Measuring Machine (CMM) and helps us to correlate the results.

Chapter 6 presents the conclusion about all result and validation between Finite Element Method (FEM), Bond Graph, and Experimental Study.

CHAPTER 2

Literature Review

2.1 Introduction

In this chapter literature review addition of cutting forces and tool deflection during machining, after these by using different model technique and tool trajectory to reduce the tool deflection and cutting forces.

2.2 Literature Review

Deflection effect of cutting tool by integrated tool deflection effect for tool path generation in flat end milling without modifying the cutting conditions, the objective was that, a tool path methodology is presented. The cutting forces calculated on the specific cutting pressure k_{t} and k_{r} *i.e.* tangential and radial specific constant. These cutting coefficients are parameters of cutting, cutting velocity, feed rate, tool diameter etc.

The calculations of tool deflection by using FEM and cantilever beam model compared and integrate it in tool path compensation process. In FEM model flat end mill modeled with solid modeling system and analyzed it and in cantilever beam model measured the deflection by both the forces act on beam concentrated and distributed. Then compared with each other both FEM and cantilever beam model, the cantilever beam model approach is better than FEM and it further used to integrate the tool path compensation **[Myeong, 1999]**.

The modeling of tooth trajectory and process geometry in peripheral milling of curved surfaces and deals with variable curvature geometries and true tooth trajectories except constant geometry in past. Calculated feed rate per tooth, entry angle, exit angle, maximum undeformed chip thickness. By using these calculations model a true trajectory. True tooth tranjectory model the process geometry. Process variables vary significantly in both the cases whether it is convex or concave, selection of process parameter values like cutting speed, feed and depth of cut and in modeling, variables like, entry angle, exit angle, feed per tooth along cutter contact path, maximum chip thickness and surface error, and concluded that it is necessary to use a model which considers variation of work piece curvature. Also necessary to model a true trajectory **[Rao, 2004]**.

Two different methods for force analysis *i.e.* mechanistic and mechanics of cutting models, in first calculated cutting force coefficient which are calibrated for certain cutting condition. Three cutting force coefficient in the direction, radial, axial and tangential **[Altintas, 2000; Budak, 1994]**. The maximum torque and power also calculated after one revolution of tool. As the force coefficient affected by chip thickness, since it varies continuously, the average chip thickness is used h_a. As a result this model is very time consuming and number of experiment were taken to find the cutting forces. But it's very high accuracy force prediction for most application. So mechanics of milling approach is used and may reduce the tests. In this technique measured tool angles, velocity and force equilibrium conditions **[Armarego, 1969]**. The modeling of tool done by cantilever beam model, segmented beam model, and finite elements modeling. After the tool is modeled, the clamping stiffness must be known for the total tool deflection **[Rivin, 1999]**. Then structural deformation model of the work piece determined by FEM. Controlling by feed rate scheduling, milling conditions. The results represented that the cutting deflection reduced by 65-78% for variable curved geometries **[Budak, 2005]**.

In case of curved geometries, the process geometry of each tooth is different, and so the cutting forces contributed by each tooth can be calculated by integrating the cutting intensities along the cut portion **[Kline, 1982]**.

$$F_{x_j}(\emptyset) = \frac{K_t f_t R}{4 \tan \beta}\left[-\cos 2\emptyset_j(z) + K_r 2\emptyset_j(z) - K_r \sin 2\emptyset_j(z)\right] \quad (2.1)$$

$$F_{y_j}(\emptyset) = \frac{K_t f_t R}{4 \tan \beta}\left[2\emptyset_j(z) - \sin 2\emptyset_j(z) + K_r \cos 2\emptyset_j(z)\right. \quad (2.2)$$

A cantilever beam deflection model can be used effectively, by using this approach measured a deflection due to cutting forces, it was assume the average cutting force acting at the midpoint along axial depth **[Rao, 2005]**, but it vary with each rotation, hence force center also vary resulting in surface error. At each station normal force produce some error on the surface and it is measure by **[Kline, 1982]**.

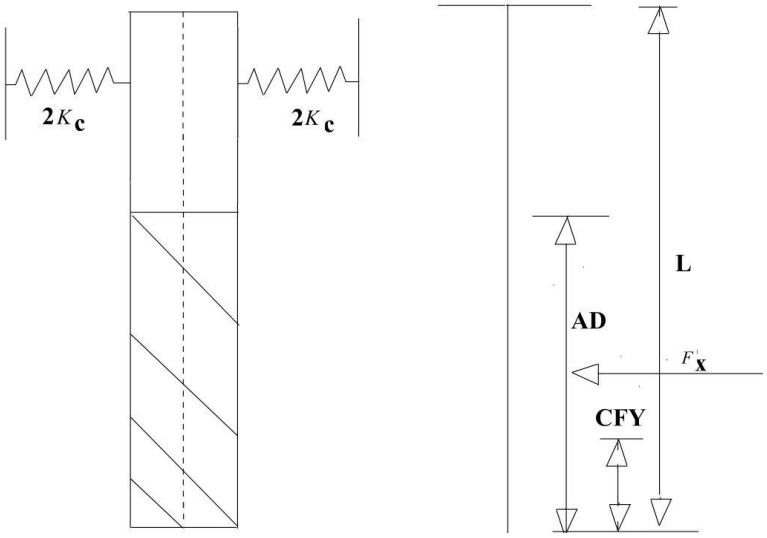

Fig. 2.1 Cutting forces induced tool deflection **[Kline, 1982]**

$$\delta_{\mathrm{N}} = [(CFY - Z)^3 - (L - Z)^3 - 3(L - Z)^2 - (L - CFY)] + \frac{F_{\mathrm{N}}}{K_{\mathrm{c}}} \quad (2.3)$$

This paper concluded that the surface error due to deflection can be reduced by tool compensation by comparing the actual and desired position of tool **[Rao, 2006]**.

The stiffness of the machine tool, tool holder and spindle has same importance in the displacement of tool tip. If the tool is stiff, the flexibility of the machine and tool holder can be higher than that of tool. The ratio of tool deflection between 55% in case of most flexible tool to 30.5% in case of most rigid tool. Also the incorrect setup of tool in the tool holder leads to dimensional error and if number of tooth in the tool, causing different cut and different chip thickness. The origin of the surface error is tool displacement at initial tooth engagement into the part. In three axis the tool axis's is strictly fixed with respect to work piece only feed can be varied and after 15 degree move of cutter evaluation of cutting forces, the error due to cutting forces can be reduced by two similar passes repeating, second pass will remove the stock allowance left by the tool deflection in first cutting pass and it result

the appropriate surface to the theoretical one. This paper concluded that at each control point selecting by CAM users, estimation of forces in every direction 15 degree on the surface tangent plane, the minimum cutting force tool path can be selected which mainly reduce deflection **[Lacalle et al., 2007]**.

The chip formation is essential phenomenon in the cutting process and examine it by physically *i.e.* cutting forces, cutting temp, tool wear, burr, built up edge, chip curling and chip breakage. By using a numerical method FEM **[Tlusty, 1975]**, FDM and artificial intelligence (AI). By using these approaches predicted the cutting forces, cutting temperature, strain, strain rate etc. which are very difficult to predict by experimental methods.

There are three assumptions which was developed by Tlusty **[Tlusty, 1975].**

1. Tangential force proportional to cutting area.
2. Radial force proportional to the tangential cutting force
3. Chip thickness (h)

The deflection of end mill by simplified equation **[Kivanc 2004]**

$$f(x) = deflection_{\max} = c_{\mathrm{E}}^{F_{\mathrm{x}}} \left[\frac{L_1^3}{D_1^4} + \frac{\left(L_2^3 - L_1^3\right)}{D_2^4} \right]^N \tag{2.4}$$

where F_x is applied force and E is the Young's Modulus of elasticity (MPa). Constant *N* is 0.950, 0.965 and 0.974 for 4-flute, 3-flute, 2-flute cutters, respectively **[Kivanc, 2004]**.

There is no universal contact law because modification depend upon the factors that affecting *i.e.* temperature, pressure to do this by starting with a multi-domain modeling approach like bond graphs which build modular models in a hierarchical object-oriented framework.

This work simplified that cutting forces and deflection is depend upon the material properties which are function of strain rate and temperature and in non-linear geometric boundaries free surface chip can be represented and used while theoretical relationships are based on linear geometry boundaries. This paper concluded that material properties in the simulation are function of strain, strain rate, and work piece temperature where as in theoretical relationship, properties are simply defined using the constant material coefficient and in free surface free surface of chip represented **[Saffer et al., 2008]**.

The peripheral milling widely used in aerospace, automobile, die/mould and power generation. It has a capability to generate complex geometry shapes and increase the productivity by increasing feed rate value but due to technical constraint the feed rate value is specific for materials. Feed rate can be increase along RDOC (radial depth of cut) and ADOC

(axial depth of cut) but one limitation if RDOC and ADOC increased above the permissible limit deflection takes place and desired geometry different from actual geometry. So the RDOC and ADOC should be optimum.

The surface error along axial direction is due to inherent variation in milling forces and cutting forces. Where the magnitude of cutting forces depend upon the tool material and geometry, work piece material and geometry , cutting condition etc. but force profile depend upon RDOC and ADOC. It concluded that the magnitude and nature of machined surface due to cutter deflection predicted with acceptable accuracy for all possible cutting condition and variation along axial direction the surface error is not uniform along tool path during machining of curved geometries **[Desai and Rao, 2012]**.

2.3 Summary of Literature Review

After the study of literature review, the aim of the research work, major factors affects tool deflection are due to which the accuracy and productivity become decreases, these factors are cutting force during machining, cutter parameters, tool feed rate, and properties like stain, strain rate.

- The cutting forces minimized by using fine parameter of cutter and feed rate in both radial and axial direction.
- The tool deflection measured by most suitable technique cantilever beam model, there are some other model can find the deflection, segmented beam model, finite element method.
- Chip formation phenomenon is also a major factor of cutting forces, chip formation depend upon the type of cutting, oblique cutting or orthogonal cutting.
- Tool deflection minimize by tool compensation technique, give compensation to tool for that desired shape should be within the tolerance limits.
- In curved geometry the cutting forces vary with each point, so cutting forces should be calculated at each vary geometry in curved surface rather than only same cutting forces in straight or flat surfaces.

2.4 Objective of the Present Work

According to the literature review, it is found that Finite Element Analysis (FEA) is useful for simulation of tool. By using FEA measure the total deflection when forces (radial, tangential, and axial) acts on the tool and by using the bond graph approach modeling of structural model, and compare the result with experimental studies and FEA. The objective of present work is formulated and summary of these objectives are,

- To develop a mathematical model for finding the total deformation and directional deformation.
- Modeling of tool and simulate with the help of FEA for finding the deformation due to forces.
- To devolve a bond graph model of structural analysis.
- Compare the experimental and simulated results.

CHAPTER 3

Finite Element Analysis

3.1 Introduction

Finite element is problem solving technique of engineering and mathematical physics. It's basically used for complex geometry, loading, and material properties, where analytical solution is complex. FEA has so large use in modern days for analyzing the behavior of material, safety purpose, and for optimal design etc. common application of FEA are in mechanical, civil, aerospace engineering. Also the main advantages of FEA are in structural analysis where stress analysis, deformation etc. are easily possible for complex structures like gear, cutters etc.

3.2 Methodology

The technique used for the calculation of deformation of end mill cutter is FEA. By using this technique, the deformation in each direction when force is applied on it is calculated, basic principle of FEA is that discretization of object in small parts, means the end mill cutter is first dividing into an equivalent system of many smaller bodies and says units (finite elements) where two or more than two elements are interconnected with each others called nodes or nodal points. The properties and the governing relationship are assumed over these elements and expressed mathematically in terms of unknown values at specific point in the elements called nodes.

3.2.1 Modeling of End Mill Cutters geometry

The modeling of simulated end mill cutter in modeling software as shown below Fig. 3.1. The extension file of modeling software is .PRT converted into Standardized graphic exchange file format (STEP) or initial graphics exchange specification file format (IGES) so that it allows the digital exchange of information among Computer-aided design (CAD) systems.

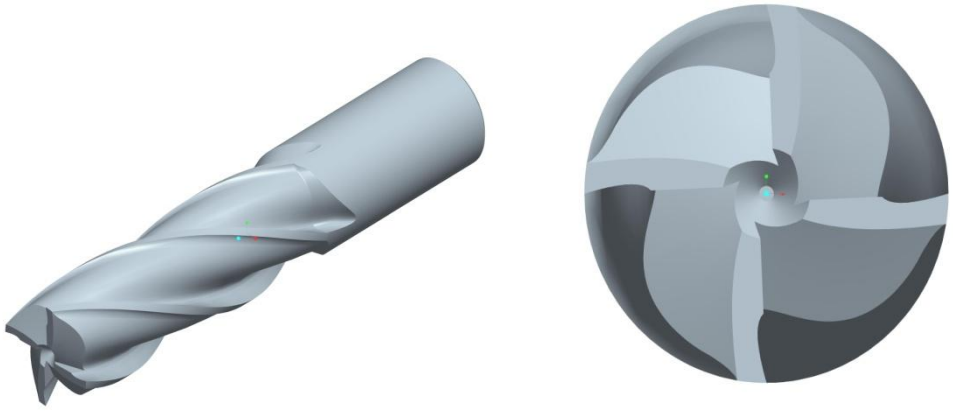

(a) (b)

Fig. 3.1 (a) Isometric view of end mill (b) top view of end mill

The specification of models in given below Table 3.1. The modeling of end mill cutters is based on the actual end mill cutters used in the experimental study.

Table 3.1 Parameters of end mill cutter

Parameter	Tool 1	Tool 2
Overall length of tool (mm)	70	75
Shank diameter (mm)	9.5	12.5
Flute length (mm)	30	40
Flute diameter (mm)	9.5	14
Number of flute	4	4
Helix angle (degree)	30	30

3.2.2 *Interfaces between modeling software and analysis software*

Analysis software conection product help overcomes this problem by directly reading the ‘native’ part files produced by the CAD pakage. The modeling of end mill cutters in the modeling software, and only two ways to import modeling software versioned filet into analysis software is STEP and IGES file. Simply the modeling software file is save in one of both this extension and then import into analysis software.

Modeling is also possible in analysis software but the reason to draw in modeling software is that due to complexity of the tool geometry. Due to less modeling tools in analysis software, modeling is not so powerful as compare to other mechanical modeling software. But still some changes are done in analysis software. The model is slice in small parts to distribute the force in each part equally as shown below in Fig. 3.2, the slicing of model is depend upon the depth of cut that has given in experiment study. increasing the slicing of model will increase the processing time and memory used. So the optimum value is selected for slicing.

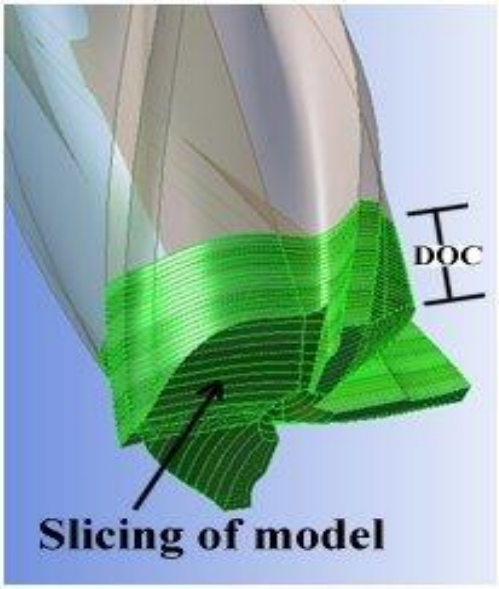

Fig. 3.2 Sliced model of end mill cutter

3.2.3 *Material Properties of End Mill Cutter*

The material properties of end mill cutter taken here is high speed steel due to its mechanical strength, these day carbide tool are much popular but due to the economical and other benefits HSS end mill cutter used. The material properties of HSS end mill cutter as shown below in Table 3.2

Table 3.2 Mechanical properties of HSS

Density	7.972×10^{-006} kg/mm^3
Coefficient of thermal expansion	1.2×10^{-005} /℃
Specific heat	$4.34 \times 10^{+005}$MJ/kg– ℃
Thermal conductivity	6.05×10^{-002}W/kg–°C
Compressive yield strength	250 MPa
Tensile yield strength	320 MPa
Tensile ultimate strength	460 MPa
Reference temperature	22 ℃
Young's modulus	200 GPa
Poisson's ratio	0.3

3.2.4 *Meshing of End Mill Cutter*

Meshing is very important part of finite element modeling. For more accurate result rot the solution domain into an appropriate number of locations. In meshing two considerations are very important detail and refinement**.**

- **Detail**

  In this consideration analyze that how much geometric detail is relevant to the simulation. Including the unnecessary detail can greatly increase the effort required to simulation.

- **Refinement**

  It is also important where in the domain are the most complex. These area required higher densities of mesh elements.

But the greater number of element requires more compute resources like memory and processing time. The quality of mesh is defining on the bases of elements and complexity of the geometry. In areas of high geometric complexity mesh element become destroyed. Poor quality element can lead to poor results or in some cases no results.

In FEA of end mill cutter used a default and automatic mesh because of it complexity but some refinement in the area where boundary condition are applied. The fig shows the comparison between automatic mesh and mesh after refinement. After refinement elements and nodes on the stress area increased and it helps to keep more accurate results.

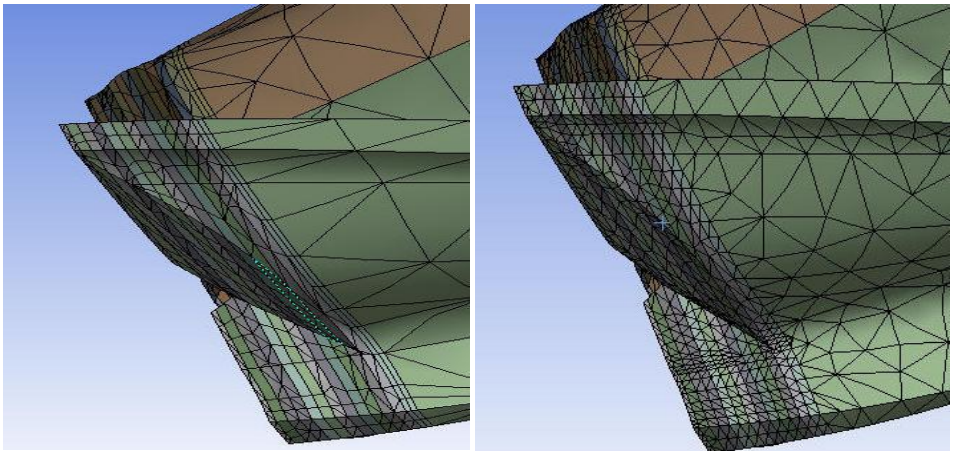

(a) (b)

Fig 3.3 Meshing of the tool (a) before refinement and (b) after refinement

Mesh properties of the tool is shown in Table 3.3.

Table 3.3 Mesh properties of end mill cutter

Object name	Mesh
State	Solved
Defaults	
Physics preference	Mechanical
Relevance	0
Sizing	
Use advanced size function	Off
Relevance center	Fine
Element size	Default
Initial size seed	Active assembly
Smoothing	Medium
Transition	Fast
Span angle center	Fine
Minimum edge length	4.2928×10^{-003} mm
Inflation	
Use automatic inflation	None
Inflation option	Smooth transition
Transition ratio	0.272
Maximum layers	5
Growth rate	1.2
Inflation algorithm	Pre
View advanced options	No

Patch Conforming Options	
Triangle surface mesher	Program controlled
Advanced	
Shape checking	Standard mechanical
Element midside nodes	Program controlled
Straight sided elements	No
Number of Retries	Default (4)
Extra retries for assembly	Yes
Rigid body behavior	Dimensionally reduced
Mesh morphing	Disabled
Defeaturing	
Pinch tolerance	Please define
Generate Pinch on Refresh	No
Automatic mesh based defeaturing	On
Defeaturing tolerance	Default
Statistics	
Nodes	108336
Elements	46342

3.2.5 *Boundary conditions*

Defining boundary condition involves the location of the boundaries on the basis of model. The data required at a boundary depends upon the boundary conditions type and physical model. In this model boundary conditions are forces in axial, radial and tangential direction and fixed support as discussed below.

- **Forces**

In physical model of end mill cutter practically if seen there are three type of forces which has major impact namely axial, radial and tangentially. The effect of cutting forces on the tool only in the half portion.

The forces calculated from experimental results with the help of dynamometer are put in the boundary conditions. Firstly the radial force which is act along the Y axis of the model. The model is sliced so that the forces are equally distributed on each part of the model as shown in Fig. 3.4.

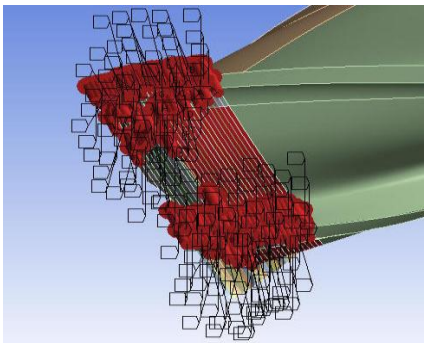

Fig. 3.4 Radial forces

Tangential force which only acts on the tooth of the end mill cutter, the distributed forces as shown in Fig. 3.5.

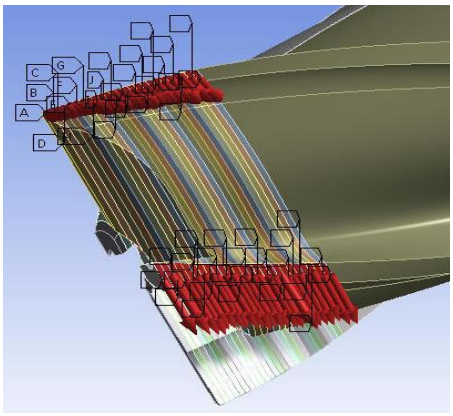

Fig. 3.5 Tangential forces

Axial force is along the axis of the tool known as Z direction as shown in Fig. 3.6.

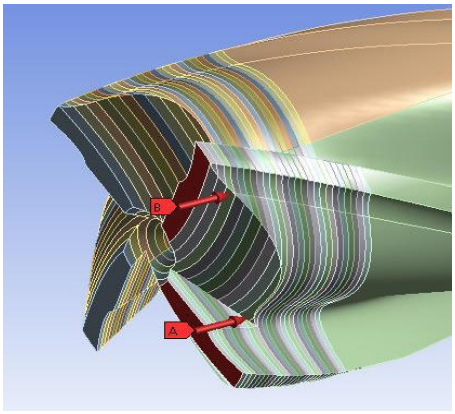

Fig. 3.6 Axial forces

- **Fixed support**

The model is fixed from one end to make it cantilever beam model shown in Fig. 3.7.

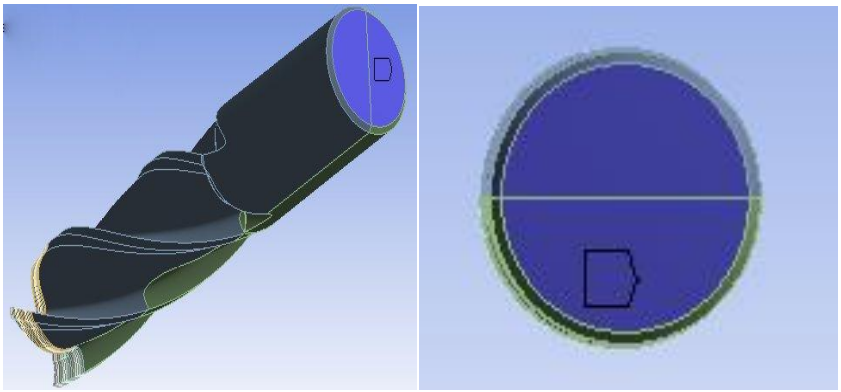

Fig. 3.7 Fixed support of tool

3.2.6 *Simulation*

The next stage of the FEA process is analysis. The FEM conducts a series of computational procedures involving applied forces, and the properties of the elements which produce a model solution. Such a structural analysis allows the determination of effects such as deformations, strains, and stresses which are caused by applied structural loads such as force, pressure and gravity.

3.2.7 *Post processing*

Post processing is the image of results. To identify the boundary condition and identify the effect of these conditions can be studied by using image of results. Representation of data i.e. Numerical and graphical helps to identified the failure and prediction of results.

3.3 Result and Analysis

The graphical and simulation results of FEA for each experimental condition as shown below.

3.3.1 *Deflection due to radial force*

- **Radial deflection due to depth of cut**

Table 3.4 Radial deflection due to depth of cut

(constant Cutting speed = 250 rpm and constant feed = 20 mm/min)

DOC (mm)	Radial deflection (microns)	
	For 9.5mm tool	For 14 mm tool
2	270	194
3	441.8	393
4	507	398

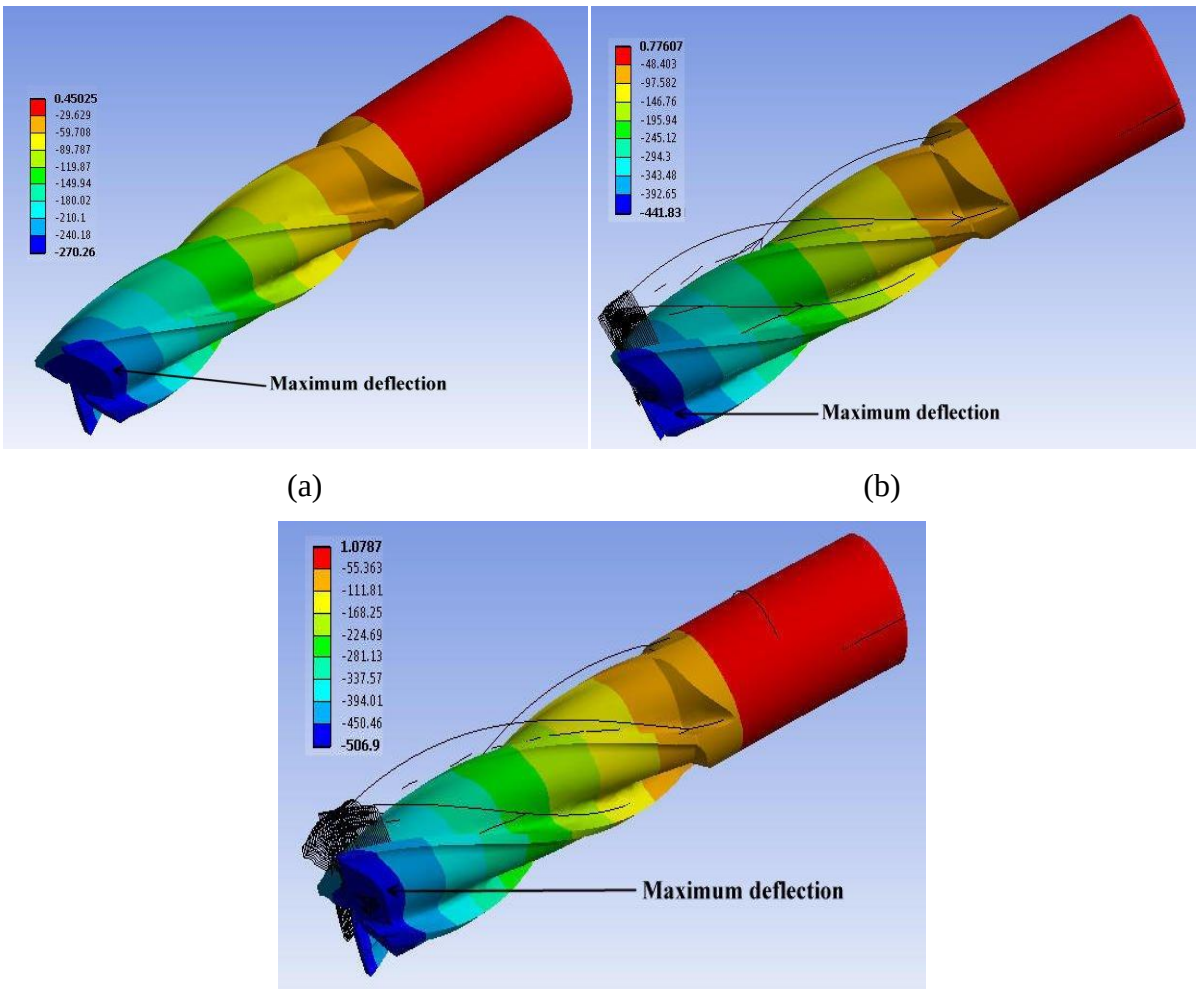

(a) (b)

(c)

Fig. 3.8 Simulation results by FEA for radial deflection due to DOC for 9.5mm diameter tool, (a) DOC 2 mm, (b) DOC 3 mm, (c) DOC 4 mm
(constant Cutting speed = 250 rpm and constant feed = 20 mm/min)

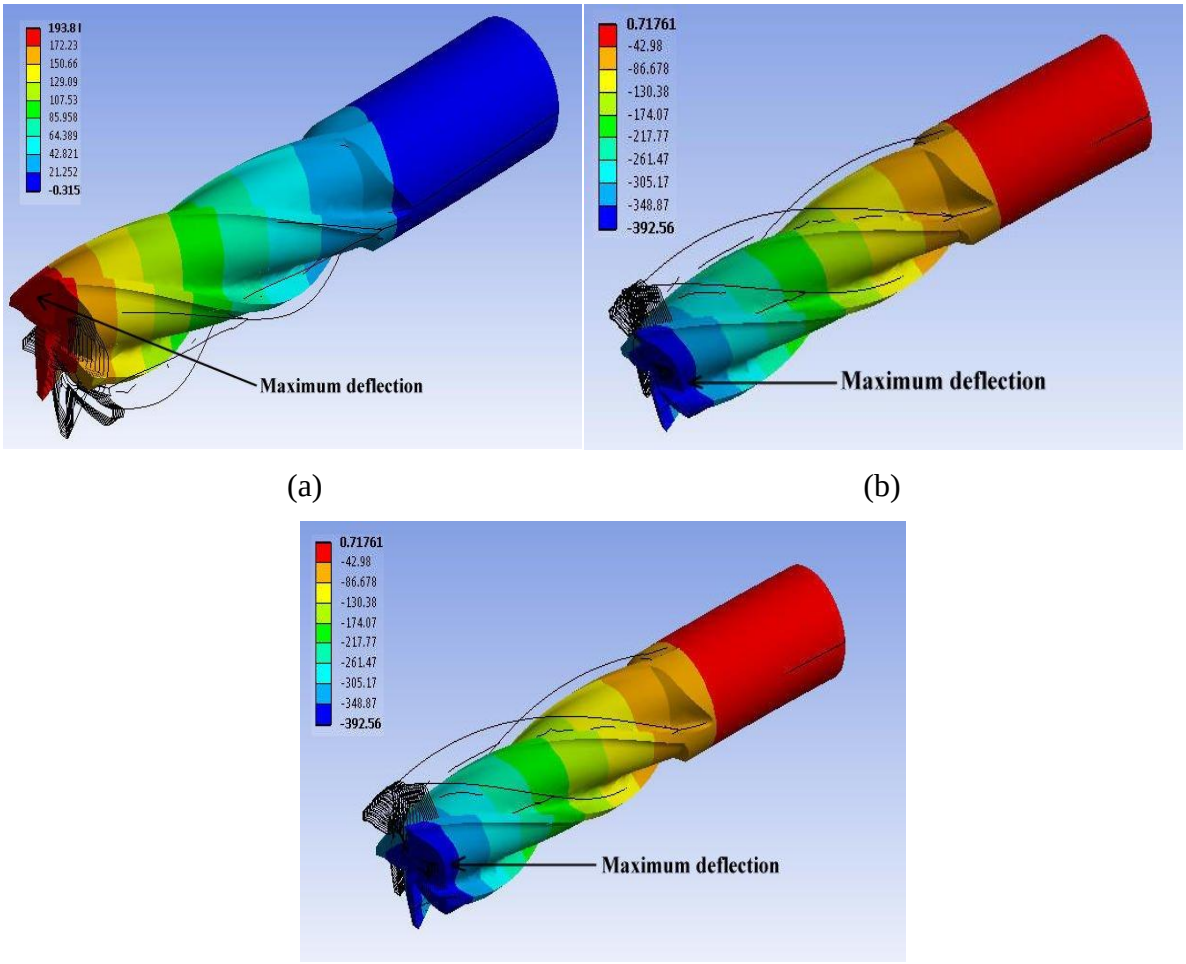

Fig. 3.9 Simulation results by FEA for radial deflection due to DOC for 14 mm diameter tool, (a) DOC 2 mm, (b) DOC 3 mm, (c) DOC 4 mm
(constant Cutting speed = 250 rpm and constant feed = 20 mm/min)

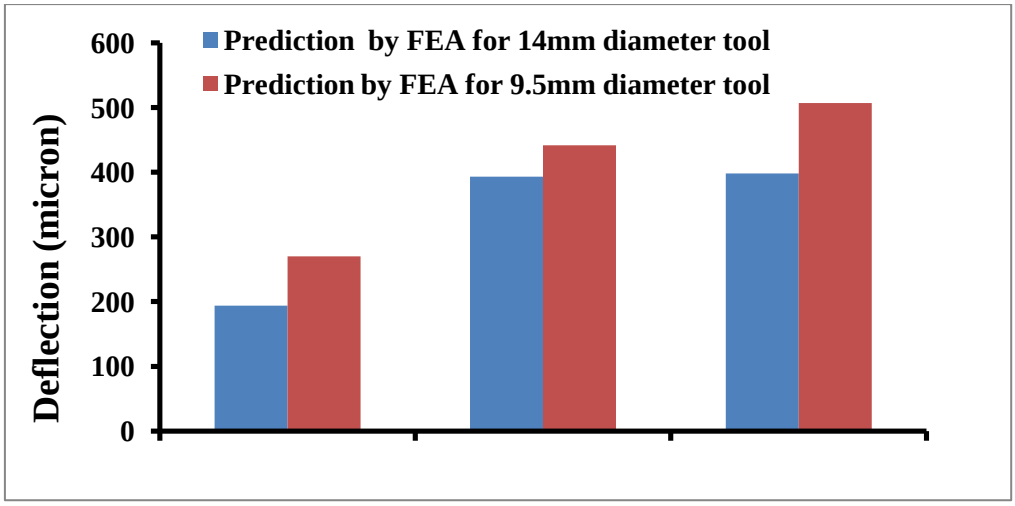

Fig. 3.10 Graphical representation of radial deflection due to depth of cut by FEA
(constant Cutting speed = 250 rpm and constant feed = 20 mm/min)

- **Radial deflection due to feed**

Table 3.5 Radial deflections due to feed
(constant Cutting speed = 350 rpm and constant DOC = 2 mm)

Feed (mm/min)	Radial deflection (microns)	
	For 9.5 mm tool	For 14 mm tool
15	215	191
25	297	145
35	270	235

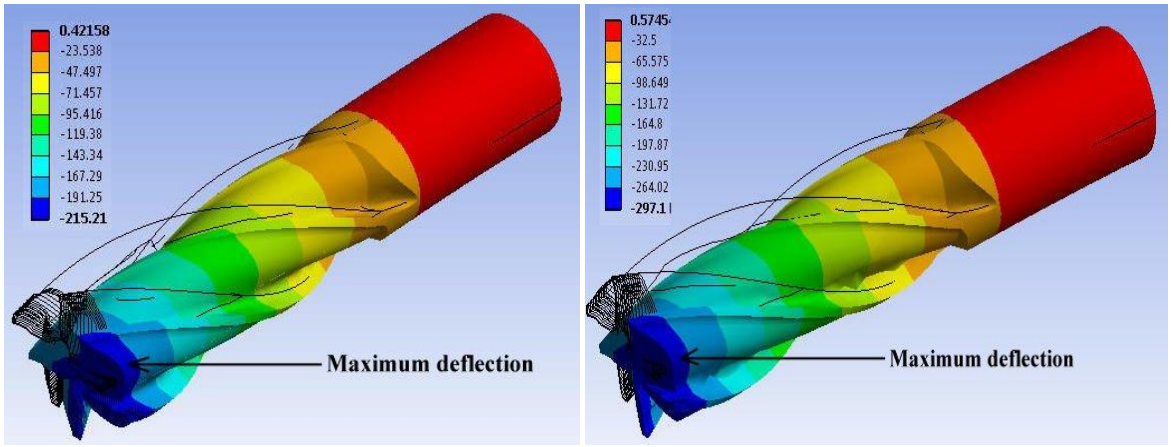

(a) (b)

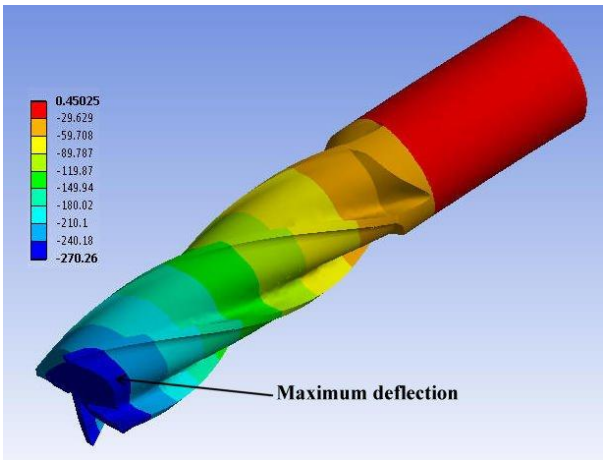

(c)

Fig. 3.11 Simulation results by FEA for radial deflection due to feed for 9.5 mm diameter tool, (a) Feed 15 mm/min, (b) Feed 25 mm/min, (c) Feed 35 mm/min
(constant Cutting speed = 350 rpm and constant DOC = 2 mm)

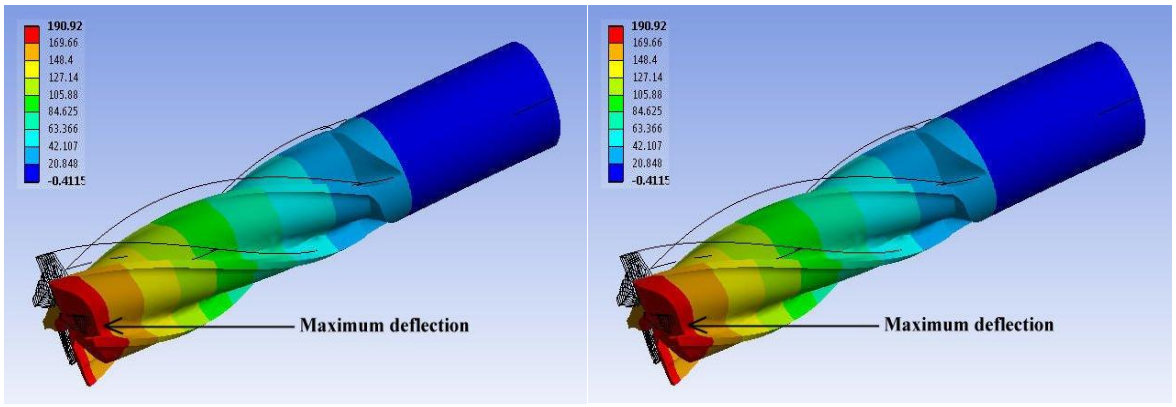

(a) (b)

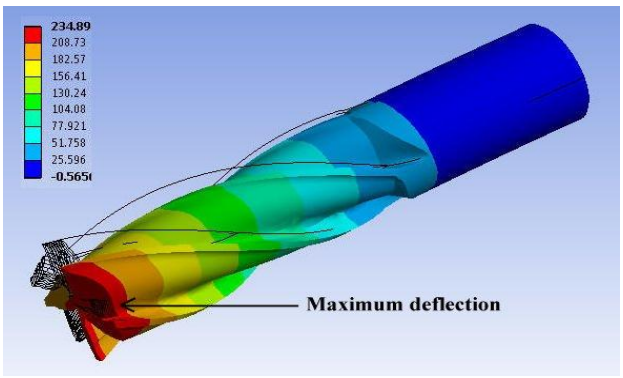

(c)

Fig. 3.12 Simulation results by FEA for radial deflection due to feed for 14 mm diameter, (a) Feed 15 mm/min, (b) Feed 25 mm/min, (c) Feed 35 mm/min (constant Cutting speed = 350 rpm and constant DOC = 2 mm)

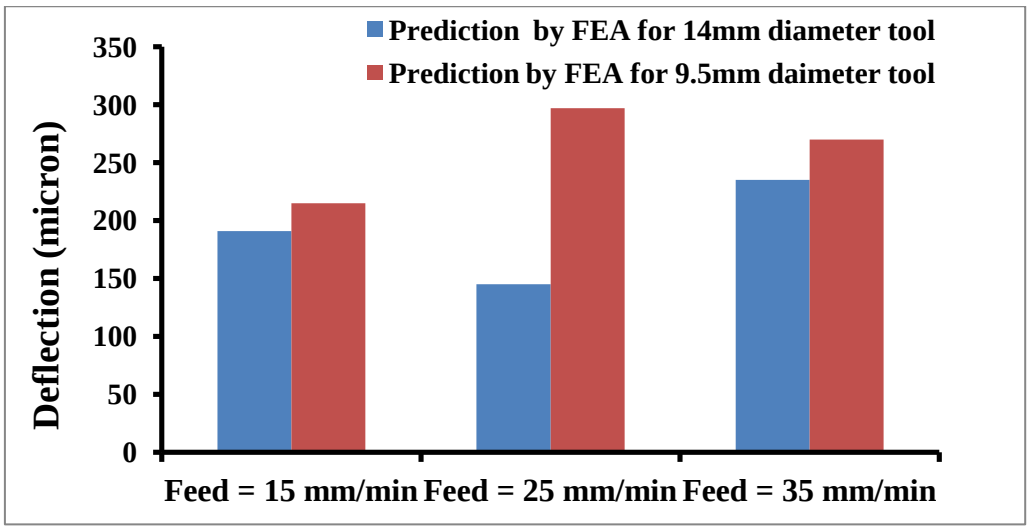

Fig. 3.13 Graphical representation of radial deflection due to feed by FEA (constant Cutting speed = 350 rpm and constant DOC = 2 mm)

- **Radial deflection due to cutting speed**

Table 3.6 Radial deflections due to cutting speed
(constant feed = 35 mm/min and constant DOC = 4 mm)

Cutting speed (RPM)	Radial deflection (microns)	
	For 9.5 mm tool	For 14 mm tool
350	578	410
500	444	494
600	359	430

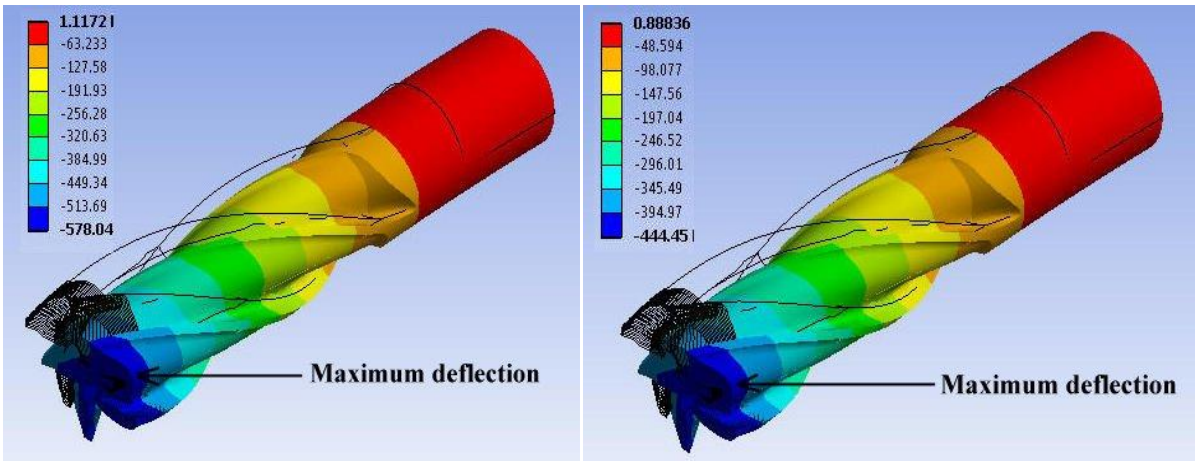

(a) (b)

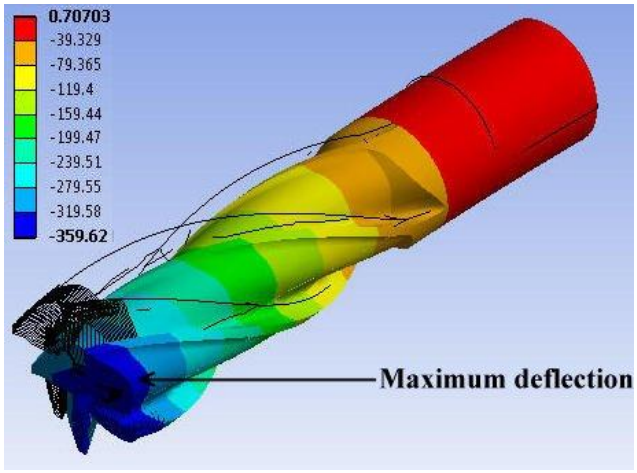

(c)

Fig. 3.14 Simulation results by FEA for radial deflection due to speed for 9.5mm diameter tool, (a) Cutting speed 350 RPM, (b) Cutting speed 500RPM, (c) Cutting speed 600RPM (constant feed = 35 mm/min and constant DOC = 4 mm)

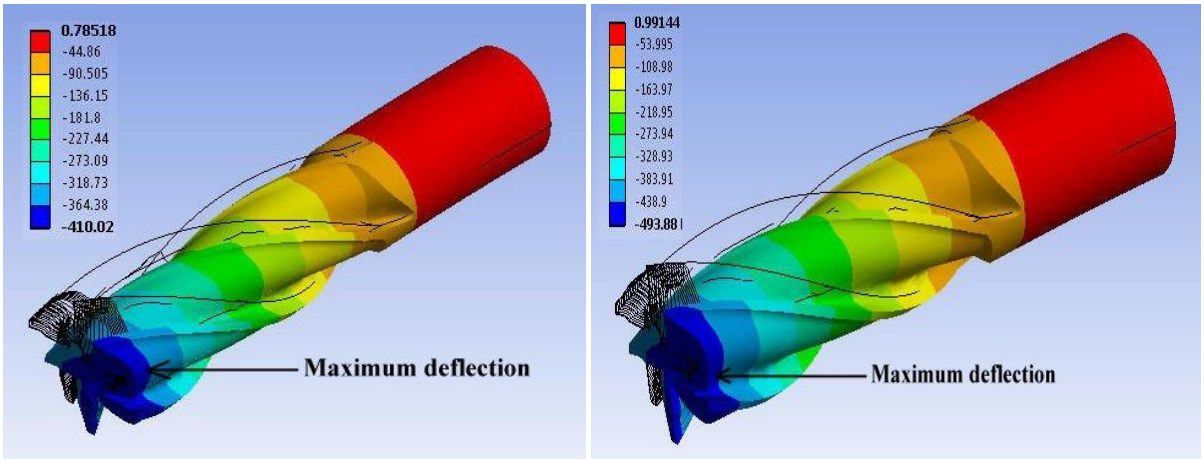

(a) (b)

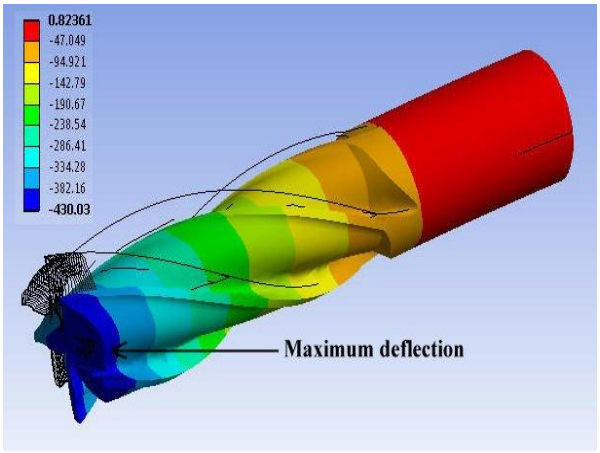

(c)

Fig. 3.15 Simulation results by FEA for radial deflection due to speed for 14 mm diameter tool, (a) Cutting speed 350 RPM, (b) Cutting speed 500RPM, (c) Cutting speed 600RPM (constant feed = 35 mm/min and constant DOC = 4 mm)

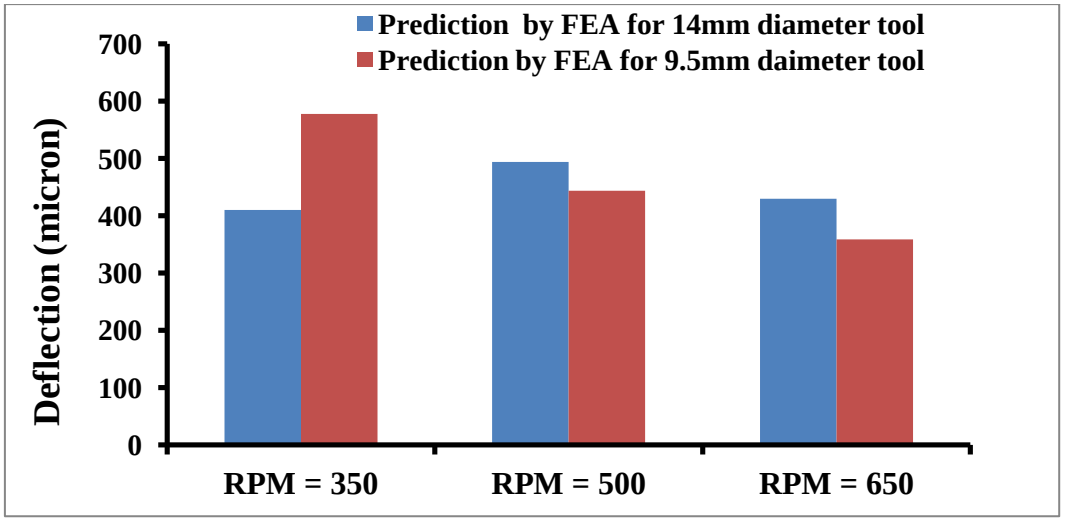

Fig. 3.16 Graphical representation of radial deflection due to cutting speed by FEA (constant feed = 35 mm/min and constant DOC = 4 mm)

3.3.2 Deflection due to tangential force

There is no option to find directy the tangential force by analysis software, but here first calculate deflection in both the direction *i.e.* X direction and Y direction, then by finding the magnitude of both directional forces is equal to the tangential force. So that force in X direction for each experimental condition shown below, and in y diection already shown above in radial deflections.

- **Tangential deflection due to depth of cut**

Table 3.7 Tangential deflections due to depth of cut
(constant Cutting speed = 250 rpm and constant feed = 20 mm/min)

DOC (mm)	Tangential deflection (microns)	
	For 9.5mm tool	For 14 mm tool
2	258.7	254
3	412.4	445
4	529	557

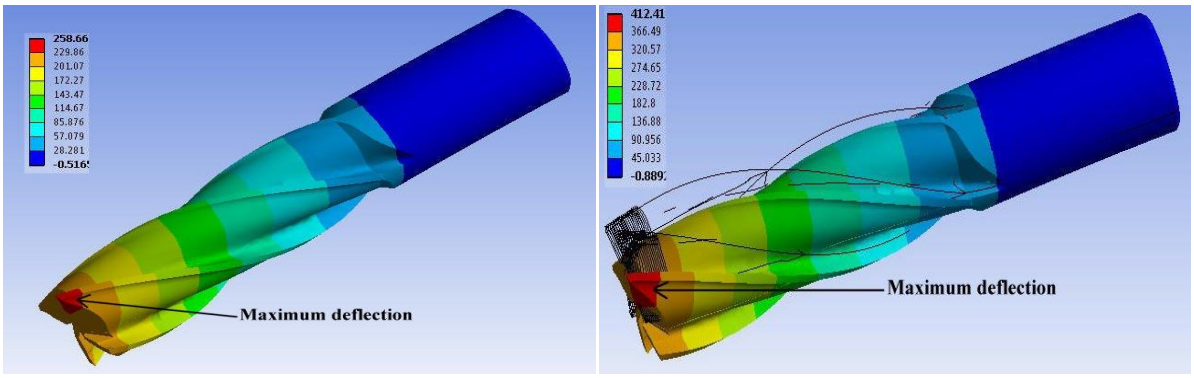

(a) (b)

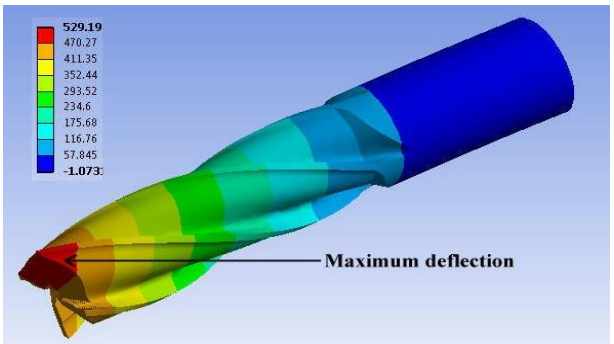

(c)

Fig. 3.17 Simulation results for deflection in X direction due to DOC for 9.5mm diameter tool, (a) DOC 2 mm, (b) DOC 3 mm, (c) DOC 4 mm
(constant Cutting speed = 250 rpm and constant feed = 20 mm/min)

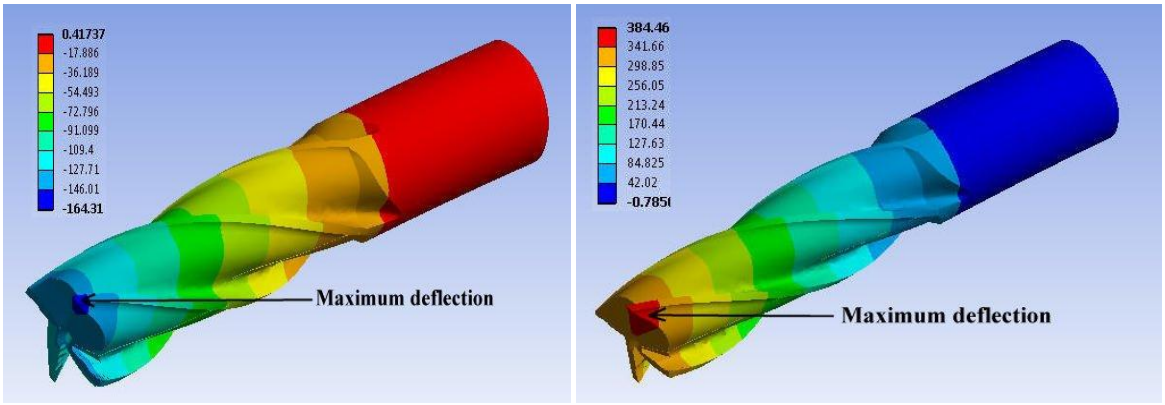

(a) (b)

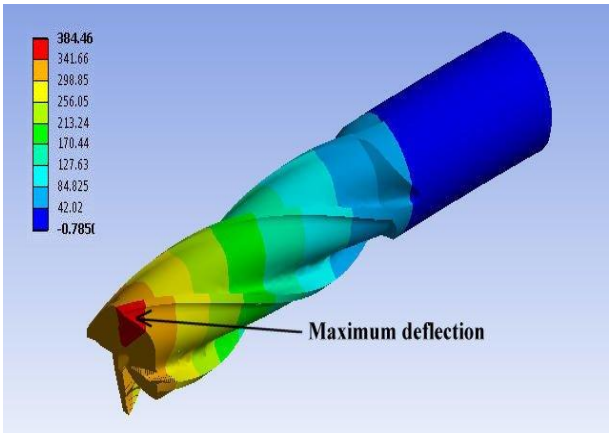

(c)

Fig. 3.18 Simulation results for deflection in X direction due to DOC for 14 mm diameter, (a) DOC 2 mm, (b) DOC 3 mm, (c) DOC 4 mm
(constant Cutting speed = 250 rpm and constant feed = 20 mm/min)

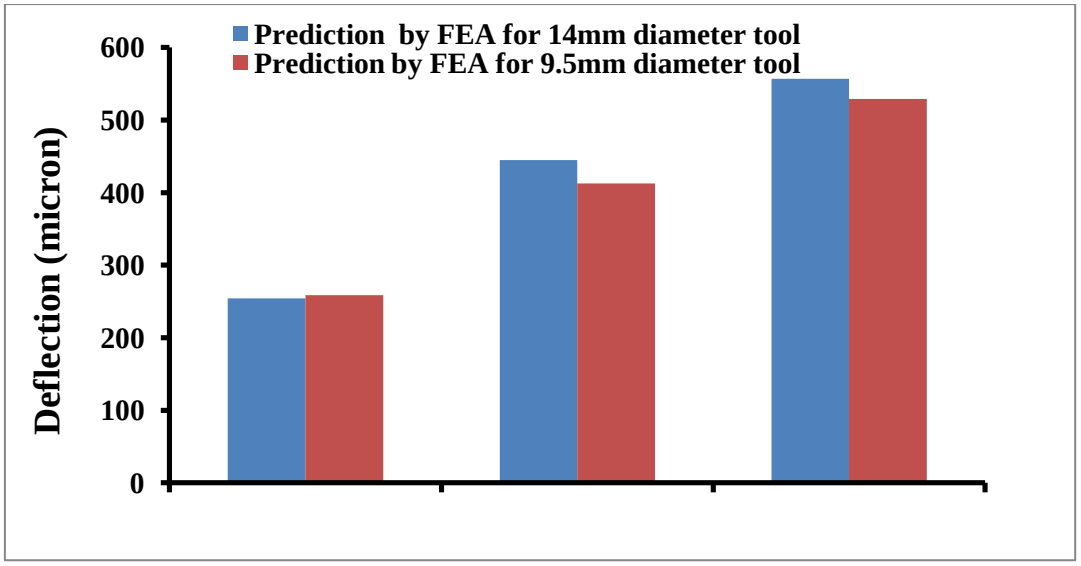

Fig. 3.19 Graphical representation of tangential deflection due to depth of cut by FEA
(constant Cutting speed = 250 rpm and constant feed = 20 mm/min)

- **Tangential deflection due to feed**

Table 3.8 Tangential deflections due to feed
(constant Cutting speed = 350 rpm and constant DOC = 2 mm)

Feed (mm/min)	Tangential deflection (microns)	
	For 9.5mm tool	For 14 mm tool
15	237	294
25	313.7	217
35	258	379

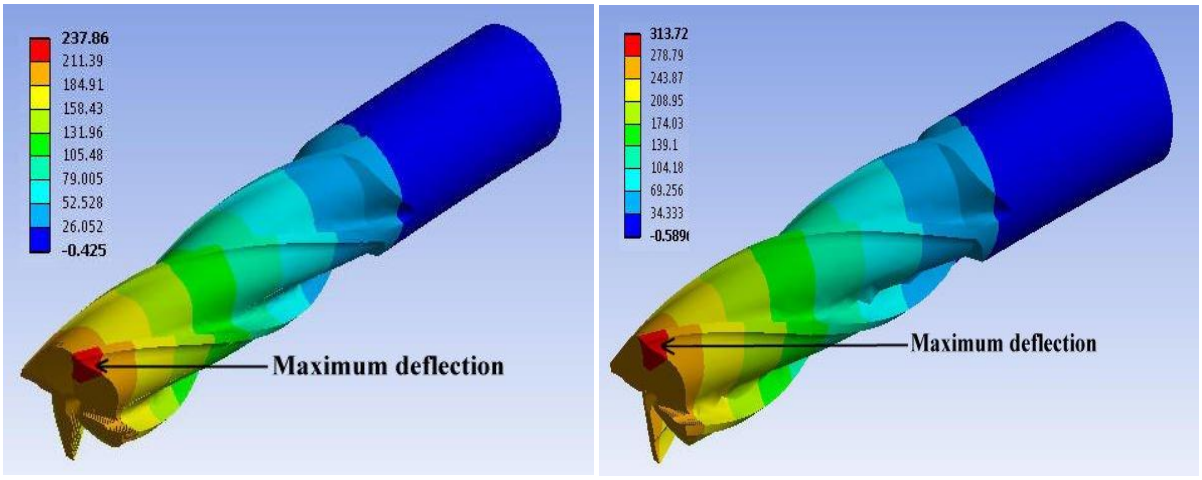

(a) (b)

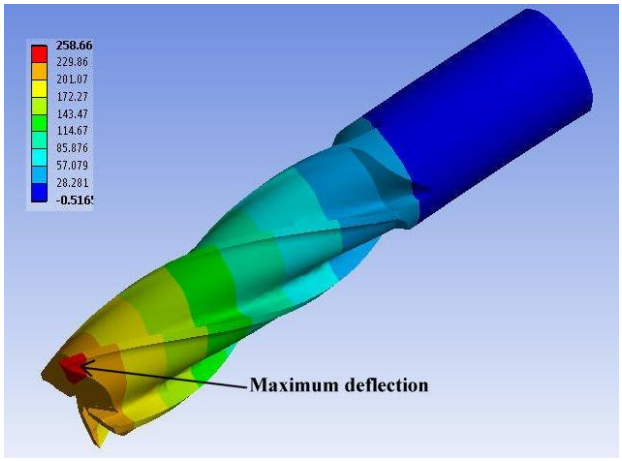

(c)

Fig. 3.20 Simulation results by FEA for radial deflection in X direction due to feed for 9.5mm diameter tool, (a) Feed 15 mm/min, (b) Feed 25 mm/min, (c) Feed 35 mm/min (constant Cutting speed = 350 rpm and constant DOC = 2 mm)

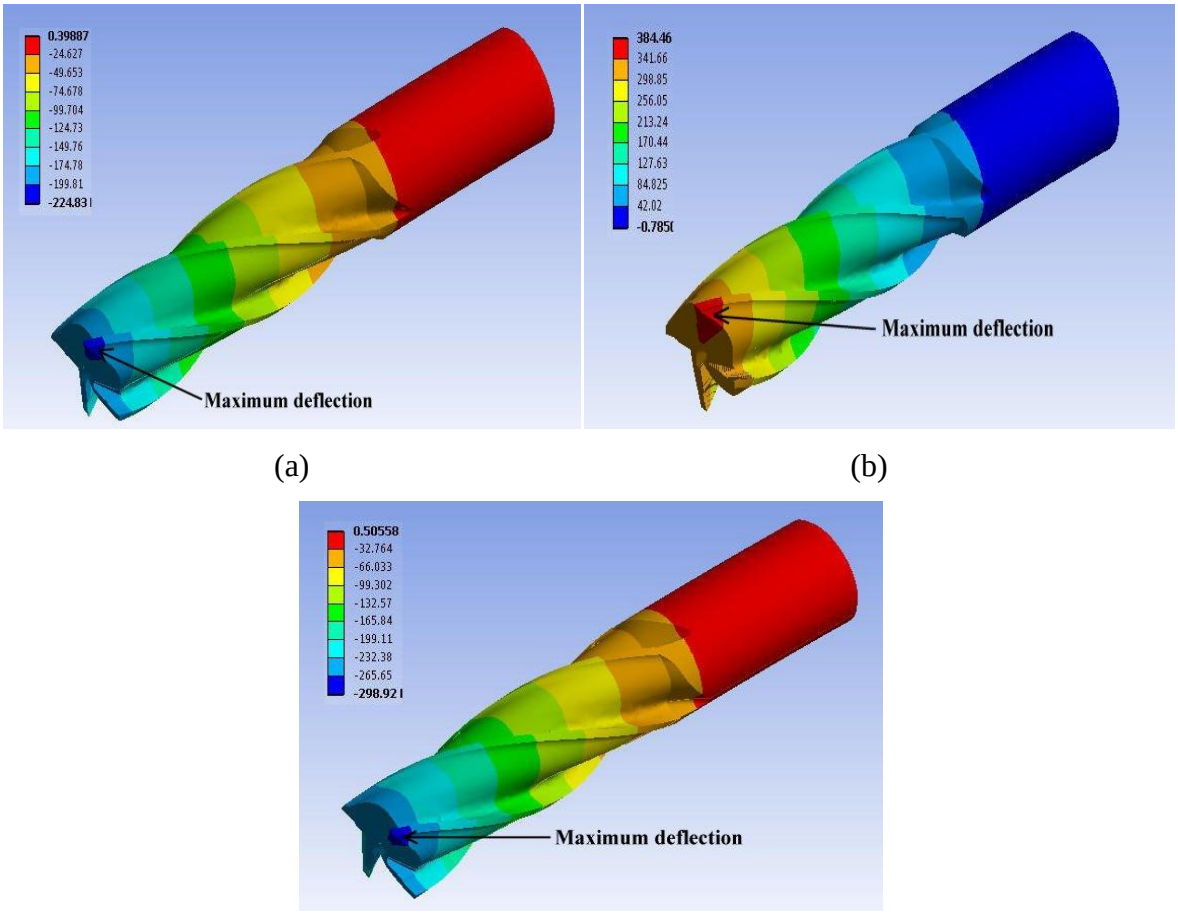

(a) (b)

(c)

Fig. 3.21 Simulation results for deflection in X direction due to feed for 14 mm diameter tool, (a) Feed 15 mm/min, (b) Feed 25 mm/min, (c) Feed 35 mm/min (constant Cutting speed = 350 rpm and constant DOC = 2 mm)

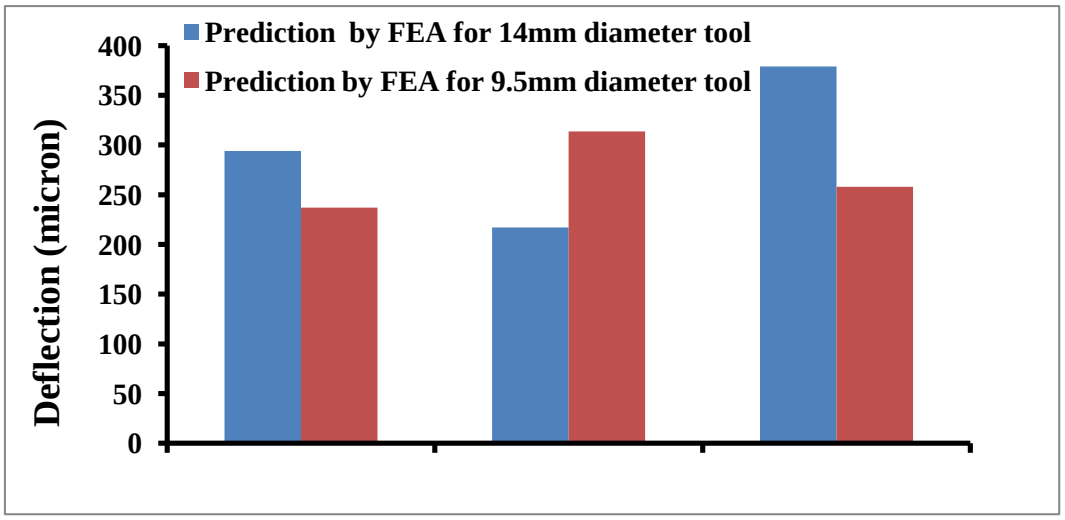

Fig. 3.22 Graphical representation of tangential deflection due to feed by FEA (constant Cutting speed = 350 rpm and constant DOC = 2 mm)

- **Tangential deflection due to cutting speed**

Table 3.9 Tangential deflections due to speed
(constant feed = 35 mm/min and constant DOC = 4 mm)

Cutting speed (RPM)	Tangential deflection (microns)	
	For 9.5mm tool	For 14 mm tool
350	559.9	587
500	444.72	723
600	367	615

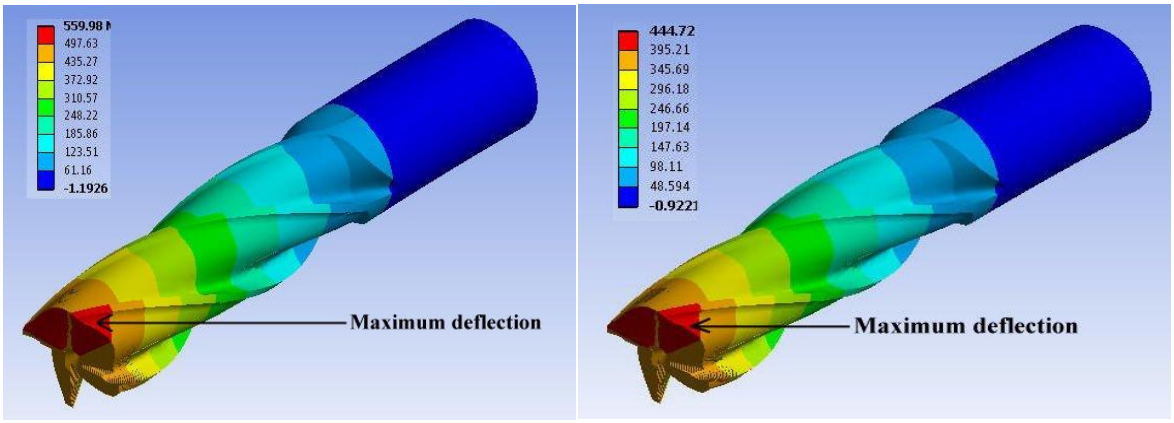

(a) (b)

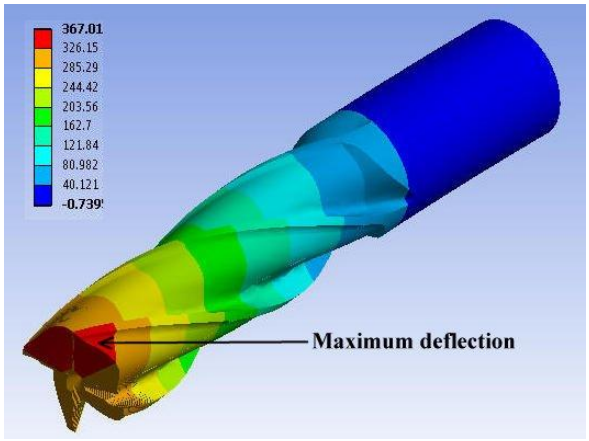

(c)

Fig. 3.23 Simulation results for deflection in X direction due to speed for 9.5mm diameter tool, (a) Cutting speed 350 RPM, (b) Cutting speed 500RPM, (c) Cutting speed 600RPM (constant feed = 35 mm/min and constant DOC = 4 mm)

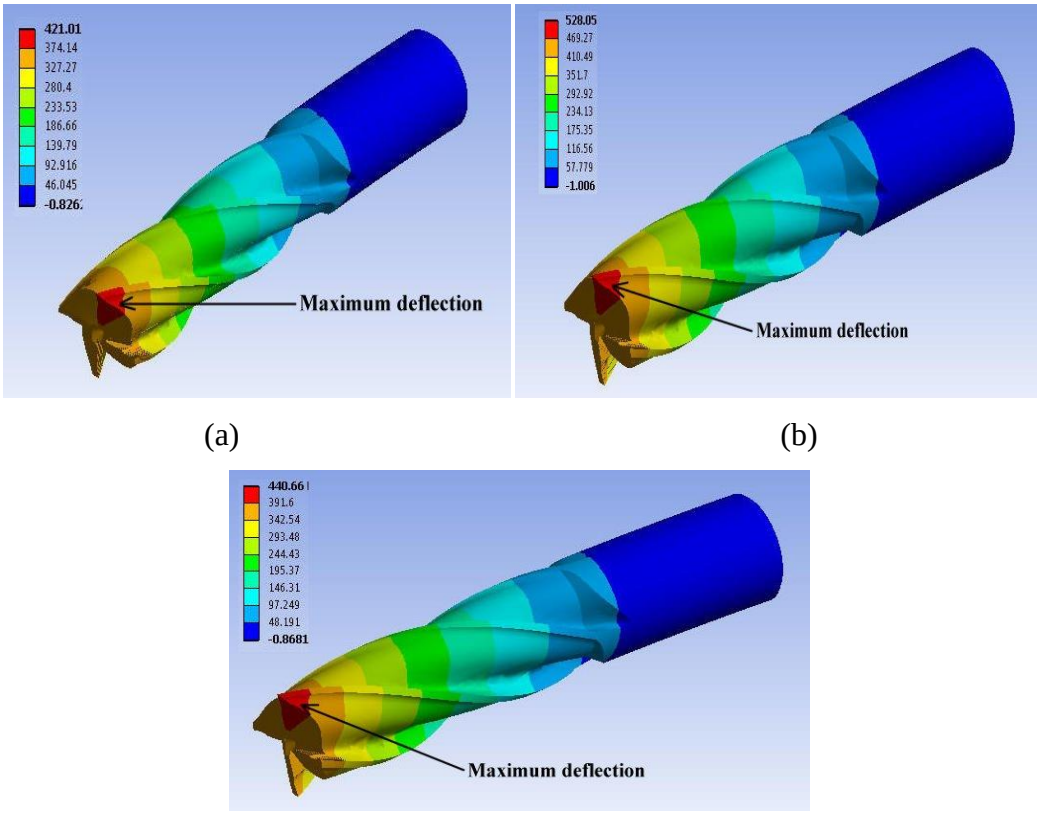

(a) (b)

(c)

Fig. 3.24 Simulation results for deflection in X direction due to speed for 14 mm diameter, (a) Cutting speed 350 RPM, (b) Cutting speed 500RPM, (c) Cutting speed 600RPM (constant feed = 35 mm/min and constant DOC = 4 mm)

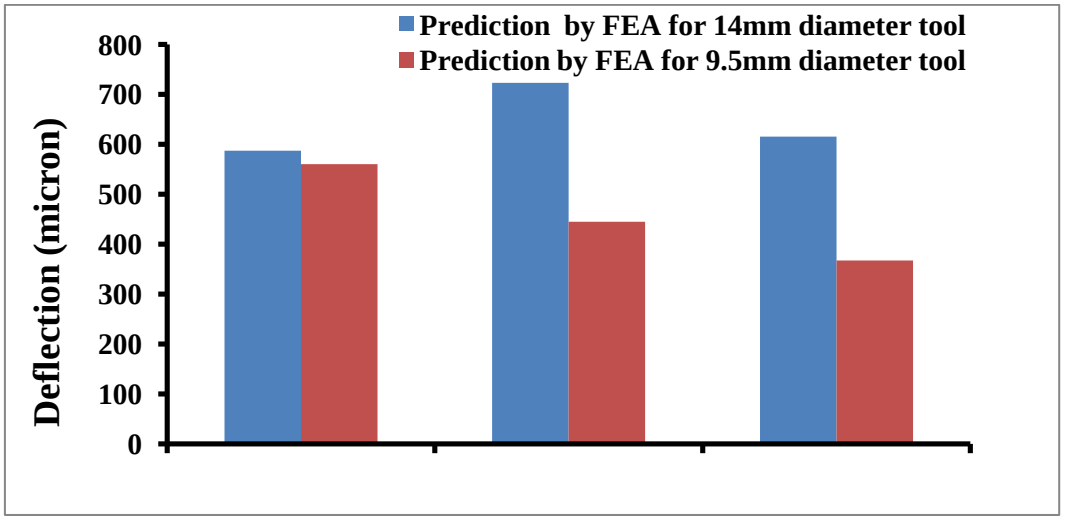

Fig. 3.25 Graphical representation of tangential deflection due to cutting speed by FEA (constant feed = 35 mm/min and constant DOC = 4 mm)

3.3.3 Deflection due to axial force

- **Axial deflection due to depth of cut**

Table 3.10 Axial deflections due to depth of cut
(constant Cutting speed = 250 rpm and constant feed = 20 mm/min)

DOC (mm)	Axial deflection (microns)	
	For 9.5mm tool	For 14 mm tool
2	0.37	0.25
3	0.55	0.25
4	0.83	0.36

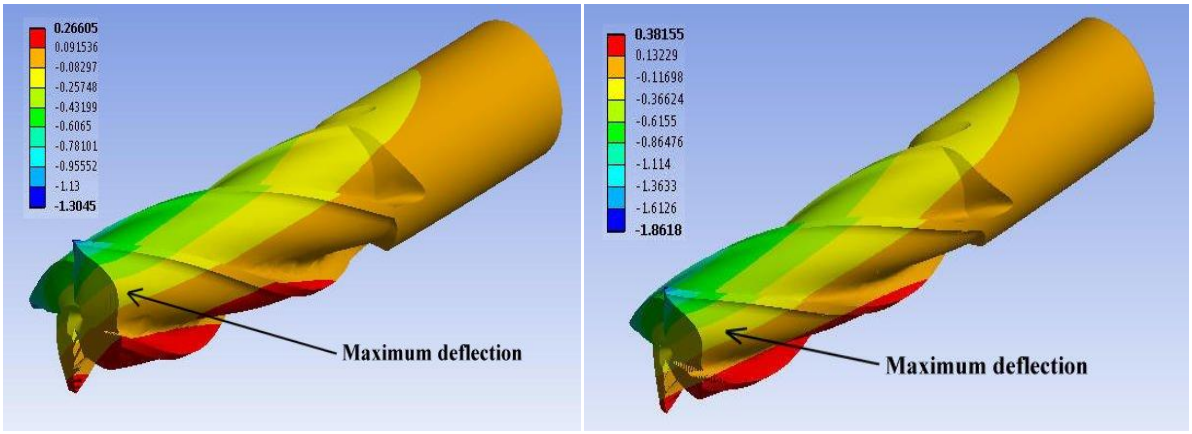

(a) (b)

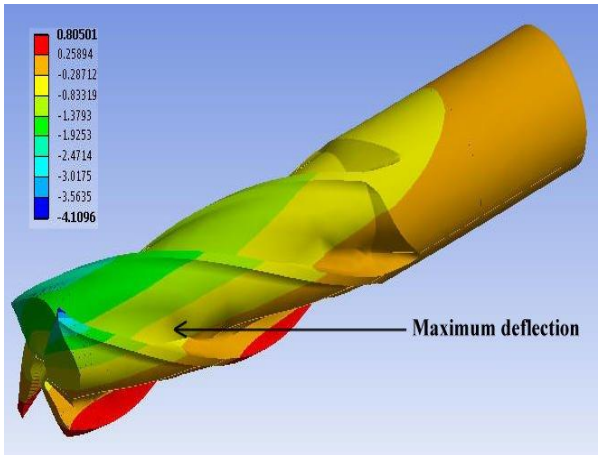

Fig. 3.26 Simulation results for axial deflection due to DOC for 9.5mm diameter tool, (a) DOC 2 mm, (b) DOC 3 mm, (c) DOC 4 mm
(constant Cutting speed = 250 rpm and constant feed = 20 mm/min)

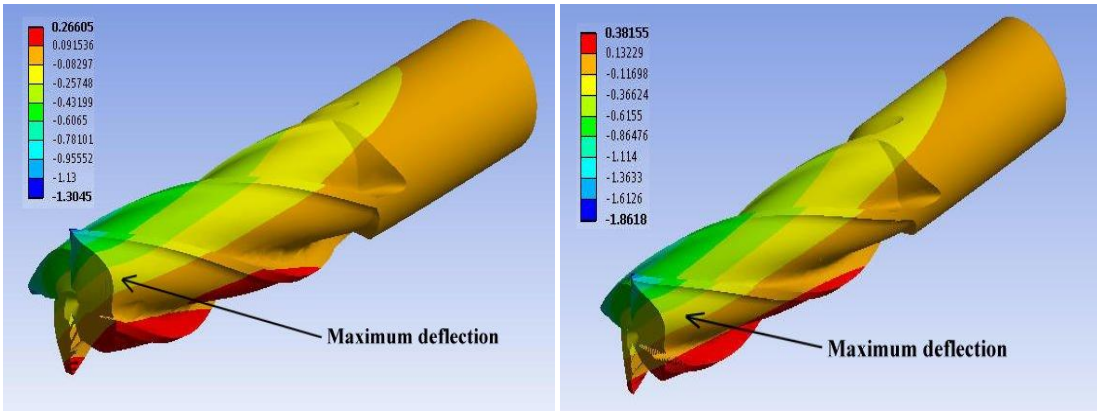

(a) (b)

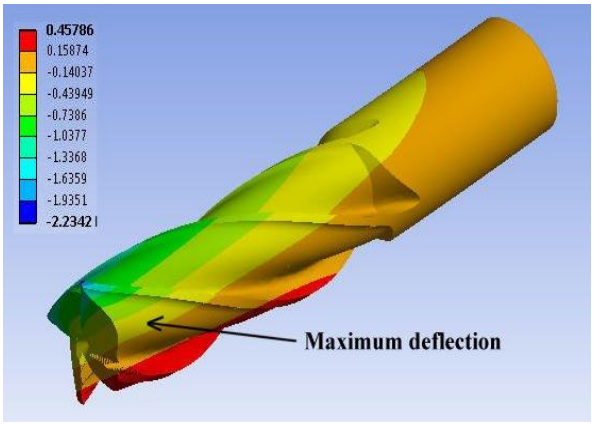

(c)

Fig. 3.27 Simulation results for axial deflection due to DOC for 14 mm diameter tool, (a) DOC 2 mm, (b) DOC 3 mm, (c) DOC 4 mm
(constant Cutting speed = 250 rpm and constant feed = 20 mm/min)

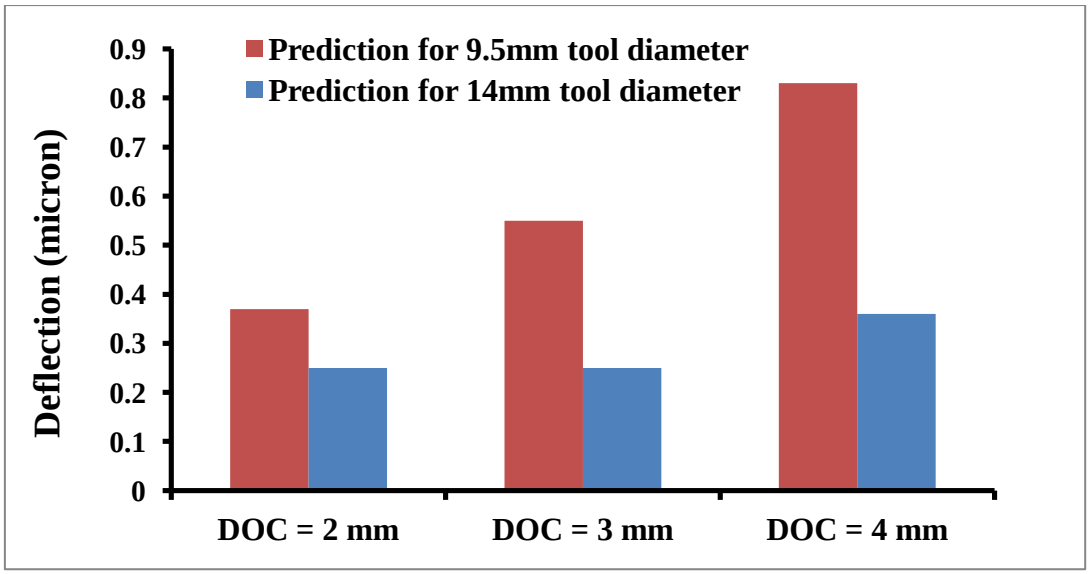

Fig. 3.28 Graphical representation of axial deflection due to depth of cut by FEA
(constant Cutting speed = 250 rpm and constant feed = 20 mm/min)

- **Axial deflection due to feed**

Table 3.11 Axial deflections due to feed
(constant Cutting speed = 350 rpm and constant DOC = 2 mm)

Feed (mm/min)	Axial deflection (microns)	
	For 9.5mm tool	For 14 mm tool
15	0.37	0.36
25	0.37	0.36
35	0.37	0.36

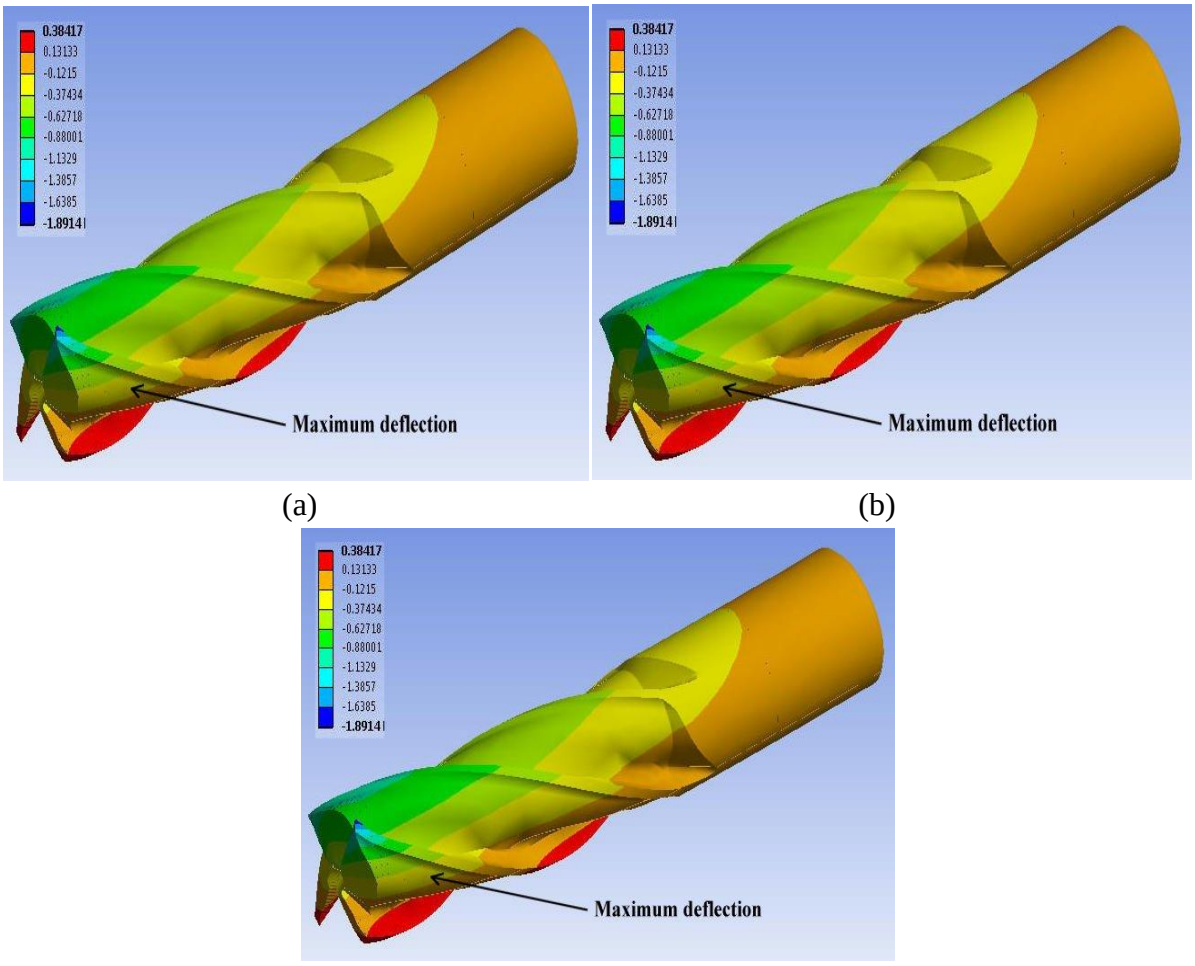

Fig. 3.29 Simulation results for axial deflection due to feed for 9.5mm diameter tool, (a) Feed 15 mm/min, (b) Feed 25 mm/min, (c) Feed 35 mm/min
(constant Cutting speed = 350 rpm and constant DOC = 2 mm)

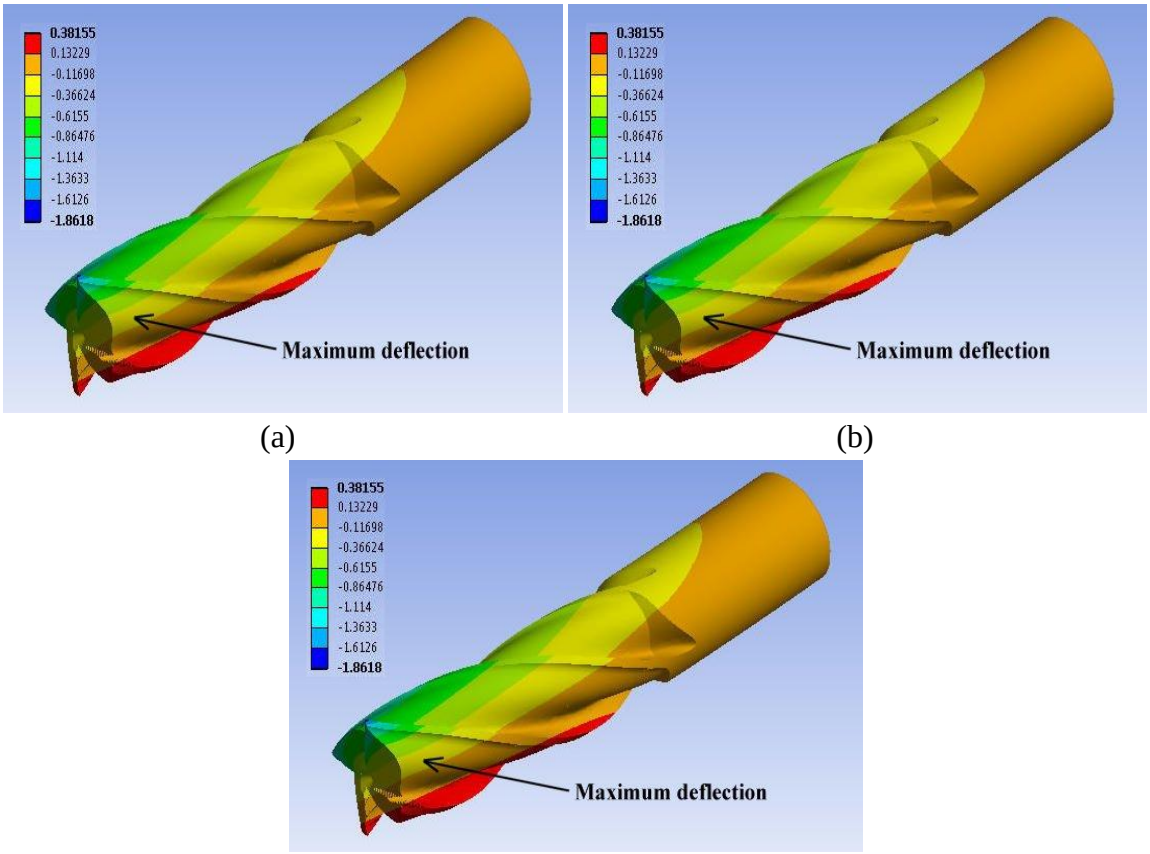

Fig. 3.30 Simulation results for axial deflection due to feed for 14 mm diameter tool, (a) Feed 15 mm/min, (b) Feed 25 mm/min, (c) Feed 35 mm/min (constant Cutting speed = 350 rpm and constant DOC = 2 mm)

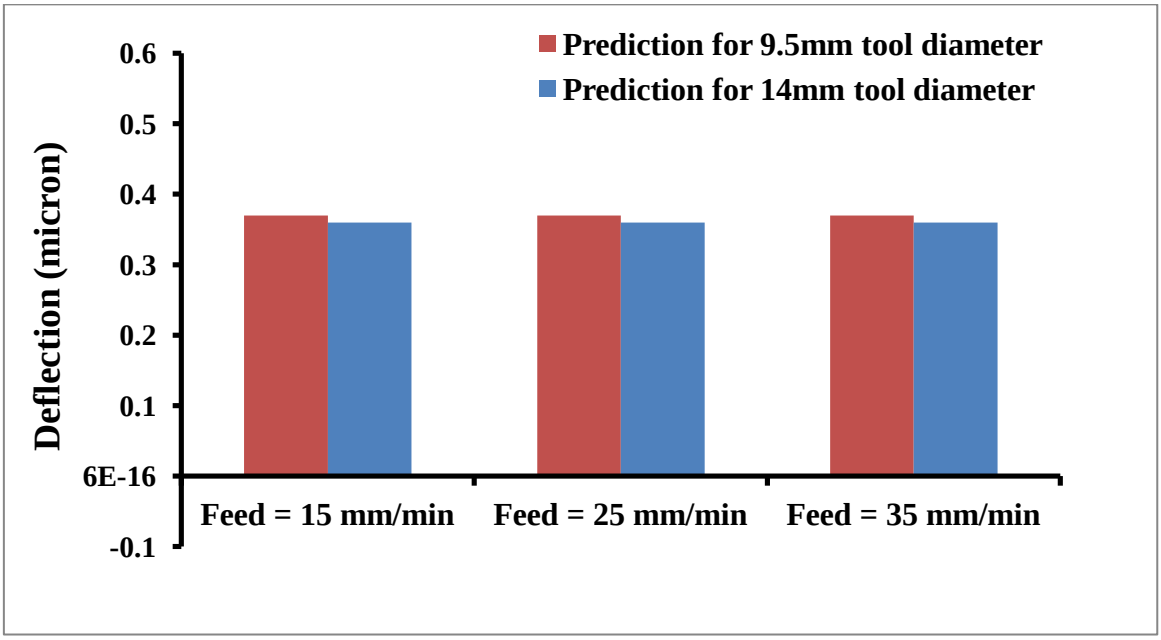

Fig. 3.31 Graphical representation of axial deflection due to feed by FEA (constant Cutting speed = 350 rpm and constant DOC = 2 mm)

- **Axial deflection due to cutting speed**

Table 3.12 Axial deflections due to cutting speed
(constant feed = 35 mm/min and constant DOC = 4 mm)

Cutting speed (RPM)	Axial deflection (microns)	
	For 9.5mm tool	For 14 mm tool
350	0.55	0.38
500	0.83	0.56
600	0.37	0.68

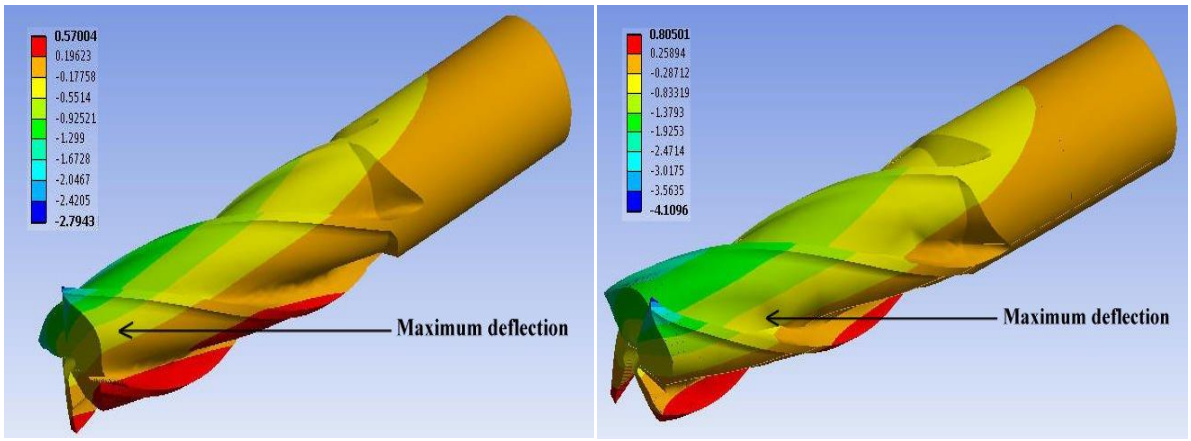

(a) (b)

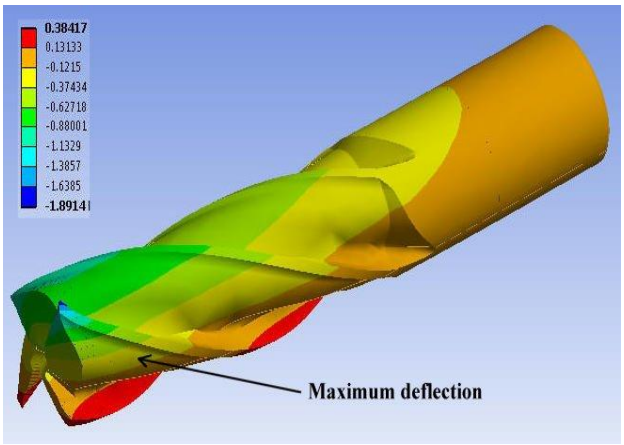

(c)

Fig. 3.32 Simulation results by FEA for axial deflection due to speed for 9.5mm diameter tool, (a) Cutting speed 350 RPM, (b) Cutting speed 500RPM, (c) Cutting speed 600RPM (constant feed = 35 mm/min and constant DOC = 4 mm)

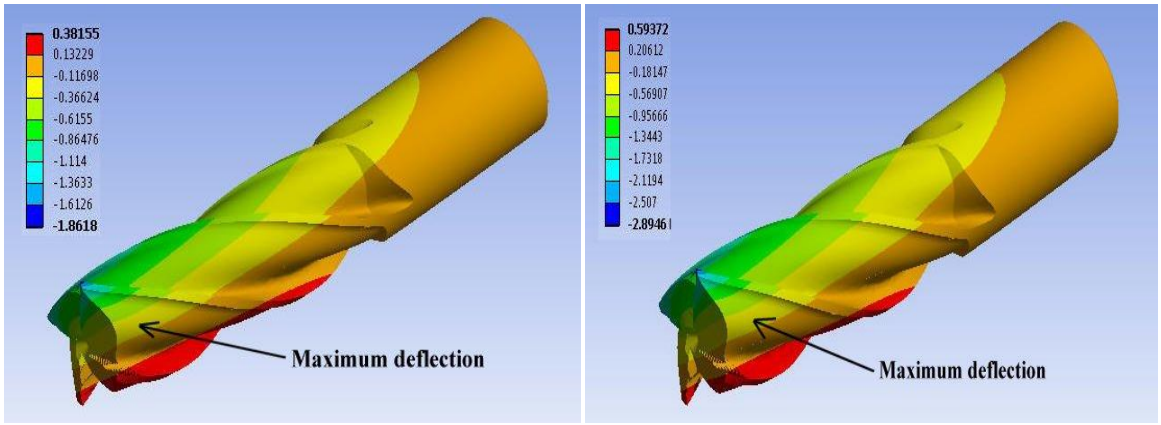

(a) (b)

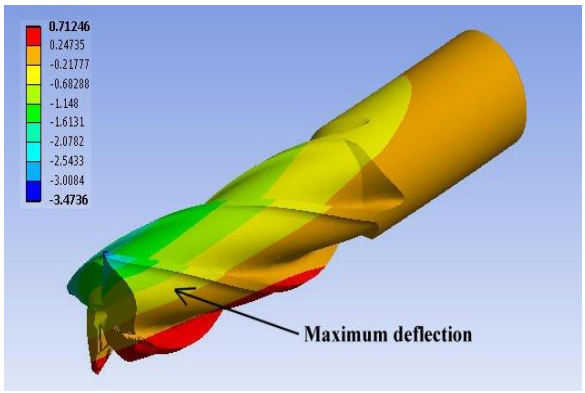

(c)

Fig. 3.33 Simulation results by FEA for axial deflection due to speed for 14 mm diameter tool, (a) Cutting speed 350 RPM, (b) Cutting speed 500RPM, (c) Cutting speed 600RPM (constant feed = 35 mm/min and constant DOC = 4 mm)

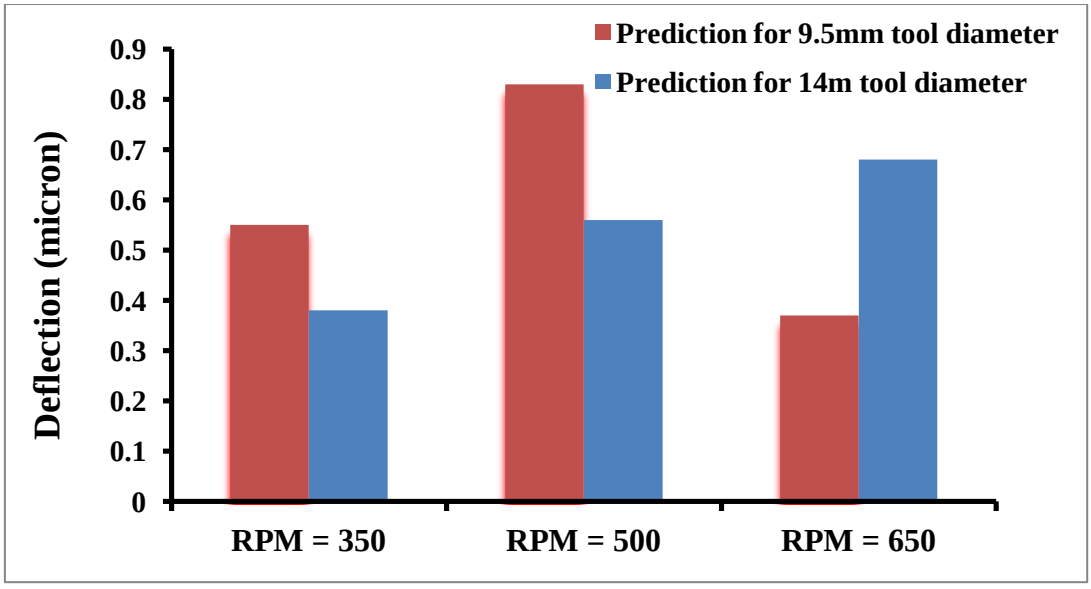

Fig. 3.34 Graphical representation of axial deflection due to cutting speed by FEA (constant feed = 35 mm/min and constant DOC = 4 mm)

Chapter 4

Bond Graph Modeling Of Cutter Deflection

4.1 Introduction

A bond graph is known as a graphical representation of a physical dynamic system. The difference is that the arcs represent the bi- directional exchange of physical energy while unidirectional represent by those in block diagram and signal-flow graphs..

In terms of structural members bond graph is extremely used, some cases there are problems in system modeling where lumping of inertia and compliance, with which comfortable in rigid body dynamics, fails to catch the essential dynamics of the system. For example in modeling an E.O.T crane, while the carriage can be represented by a rigid body, it will be improper to treat the grider in a similar way.

4.2 Modeling of Cutter Deflection

When external forces are applied to a beam or structure the structure distorts. The external forces perform work and the energy is stored in the structure in the form stress and elastic deformation. In conformance with the law of conservation of energy the work done in the small movements of the external forces (*W*) must be equal to the potential energy (*U*) stored in the structure.

External work done (*W*) = Internal energy stored (*U*)

4.2.1 Strain Energy under Axial Load

Consider a member of constant cross sectional area (*A*), subjected to axial load (*P*) as shown in Fig. 4.1 , let the (*E*) be a Young's modulus of material. Now, the applied load (*P*) is resist by uniformly distributed internal stresses given by average stress *i.e.*

$$\sigma = \frac{P}{A} \tag{4.1}$$

The incremental elongation du of small element of length of (*dx*) beam is given by,

$$du = \varepsilon dx \tag{4.2}$$

$$du = \frac{\sigma}{E} dx \tag{4.3}$$

$$du = \frac{P}{AE} dx \tag{4.4}$$

Now the total elongation of the member of length (L) may be obtained by integration.

$$u = \int_0^L \frac{P}{AE} dx \tag{4.5}$$

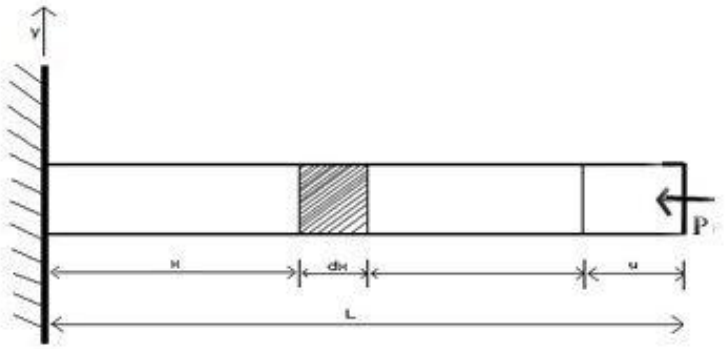

Fig. 4.1 Strain Energy due to Axial Deformation

Now the work done by external loads, $W = \frac{1}{2} Pu$

In conservative system, the external work done is stored as the internal strain energy. Hence strain energy stored in axial deformation is

$$U = \frac{1}{2} Pu \tag{4.6}$$

Now, substituting the Eq. 4.5 in Eq. 4.6

$$U = \int_0^L \frac{P^2}{2AE} dx \tag{4.7}$$

The required equation is net strain energy stored in axial deformation **[Srinath 2009]**.

4.2.2 Strain Energy Due to Bending

Consider a small segment of beam of length (*dx*) subjected to bending moment a shown in Fig 4.2. Now one cross section rotates about another cross section by a small amount ($d\emptyset$), then

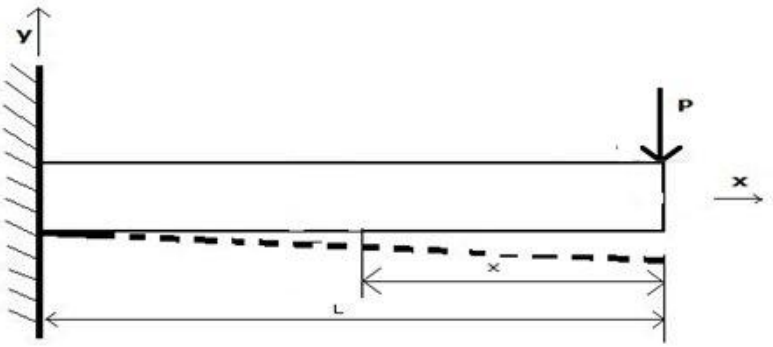

Fig. 4.2 Scheme of deflection for a cantilever under point load P at end

$$d\theta = \frac{1}{R} dx = \frac{M}{EI} dx \tag{4.8}$$

Hence,

$$dU = \frac{1}{2} d\theta \tag{4.9}$$

Substituting $(d\theta)$ in equation,

$$dU = \frac{1}{2}\frac{M^2}{EI}dx \tag{4.10}$$

Now, the energy stored in the complete beam of the span (L) may be obtained by integrating equation. Thus,

$$U = \int_0^L \frac{M^2}{2EI}dx \tag{4.11}$$

The required equation is net strain energy stored in bending deformation **[Srinath 2009]**.

4.2.3 Strain Energy Due to Shearing

The shear stress on a cross section of beam of rectangular cross section found out by the relation

$$\tau = \frac{VQ}{bI_{zz}} \tag{4.12}$$

The shear stress across the cross section may be taken as,

$$\tau = k\frac{V}{A} \tag{4.13}$$

Where A is the area of cross section and k is the form factor which is dependent on the shape of cross section, the deformation (*du*) write as,

$$du = \Delta\gamma\, dx \tag{4.14}$$

Where $\Delta\gamma$ is the shear strain and is given by

$$\Delta\gamma = \frac{\tau}{G} = k\frac{V}{AG} \tag{4.15}$$

Hence, total deformation of the beam due to action of shear force is

$$u = \int_0^L k\frac{V}{AG}dx \tag{4.16}$$

Now the strain energy stored in the beam due to action of transverse shear force is given by,

$$U = \frac{1}{2}Vu = \int_0^L \frac{kV^2}{2AG}dx \tag{4.17}$$

Eq. 4.17 gives the strain energy stored in the beam due to action of shear force **[Srinath 2009]**.

4.2.4 Strain Energy Due to Torsion

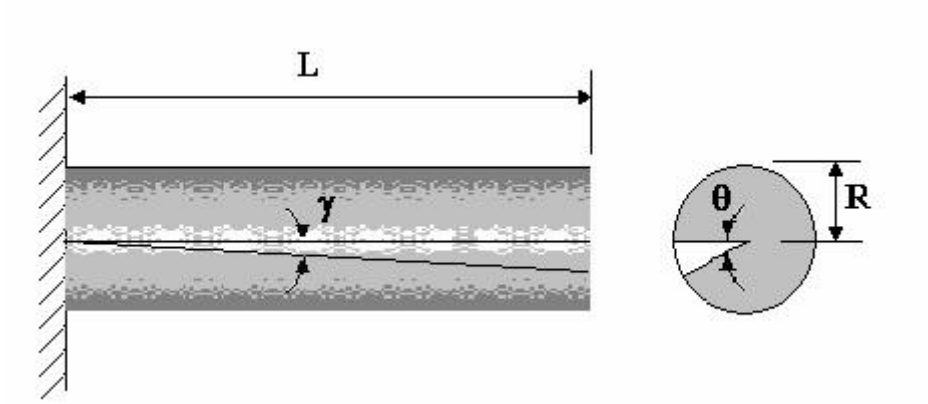

Fig. 4.4 Strain Energy due to torsional deformation **[www.freestudy.co.uk]**

Consider a circular shaft of length (L) radius (R), subjected to a torque (T)at one end. Under the action of torque one end of the shaft rotates with respect to the fixed end by an angle (θ) . Hence the strain energy stored in the shaft is,

$$U = \frac{1}{2}T\theta \tag{4.18}$$

Consider an elemental length dx of the shaft. Let the one end rotates by a small amount $(d\theta)$ with respect to another end. Now the strain energy stored in the elemental length is,

$$dU = \frac{1}{2}Td\theta \tag{4.19}$$

therfore,

$$d\theta = \frac{Tdx}{GJ} \tag{4.20}$$

Where, G is the shear modulus of the shaft material and J is the polar moment of area. Therefore substituting the value of dθ

$$dU = \frac{T^2}{2GJ}dx \tag{4.21}$$

Now, the total strain energy stored in the beam obtained by integrating the above equation.

$$U = \int_0^L \frac{T^2}{2GJ}dx \tag{4.22}$$

The required equation is net strain energy stored in torsional deformation **[Srinath 2009]**.

4.2.5 Modeling of End Milling Cutter for Deformation

For the general purpose a force based model for cutter deformation analysis would be developed by considering the cutter as cantilever beam and also considering the forces and moments as shown in Fig. 4.5, for the calculation of tool deflection measured force components radial force, tangential force, and vertical force are used by using castigliano's theorem. When forces act on elastic systems subject to small displacements, the displacement corresponding to any force collinear with the force is equal of the partial derivative to the total strain energy with respect to that force.

The sign of the displacement is positive, if the displacement is in the same direction as the force Mathematically Catigliano's theorem is stated as follows.

$$\delta_{\mathrm{i}} = \frac{\partial U}{\partial F} \tag{4.23}$$

δ_1 is the deflection in the direction of that force, the total strain energy is calculated as.

$$U = U_1 + U_2 + U_3 + U_4$$

$$\mathrm{U} = \int_0^{\mathrm{L}} \text{axial force } \mathrm{F_z} + \int_0^{\mathrm{L}} \text{bending force} \mathrm{F_r} + \int_0^{\mathrm{L}} \text{tangential force } \mathrm{F_t} + \int_0^{\mathrm{L}} \text{shear force}$$

$$U = \int_0^L \frac{F_z^2}{2AE}\,dx + \int_0^L \frac{M^2}{2EI}\,dx + \int_0^L \frac{T^2}{2GJ}\,dx + \int_0^L \frac{F^2}{2AG}\,dx \tag{4.24}$$

$$U = \frac{F_z^2 L}{2AE} + \frac{F_t^2 L^3}{6EI} + \frac{F_r^2 L^3}{6EI} + \frac{F_t^2 L^3}{6GJ} + \frac{F_t^2 L}{2AG} + \frac{F_r^2 L}{2AG} \tag{4.25}$$

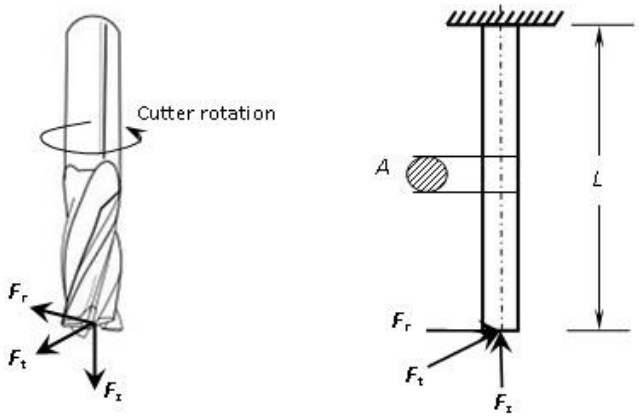

(a) Force exerted by tool on work piece (b) Schema of forces on tool

Fig. 4.5 Force system in end milling to calculate cutter deflection

Therefore by using castigliano's theorem, the deflection in the direction of axial (δ_1), radial (δ_2), and tangential force (δ_3) obtained as.

$$\delta_1 = \frac{\partial u}{\partial F_z} = \frac{F_z L}{AE} \tag{4.26}$$

$$\delta_2 = \frac{\partial U}{\partial F_r} = \frac{F_r L^3}{3EI} + \frac{F_r L}{AG} \tag{4.27}$$

$$\delta_3 = \frac{\partial U}{\partial F_t} = \frac{F_t L^3}{3EI} + \frac{F_t L}{AG} \tag{4.28}$$

Here, L and A are length and cross sectional area of the tool, respectively. E is Young's modulus of tool shank material, and G is modulus of rigidity.

4.3 Basic Steps and Elements in Bond Graph Modeling

The basic variables are the effort (e), the flow (f), time integral of effort (p) and time integral of flow (Q). In a bond graph, the assignment of power directions may be as arbitrary as fixing the co-ordinate systems in classical analysis. The reference power direction is shown by a half -arrow at one end of the bond. The assignment of bond numbers fixes the names of the elements or junctions.

4.3.1 Junction

In bond graph, there are two kinds of junction *i.e.*, 0 junction and 1 junction.

- In 0 junctions, sum of flows are zero and efforts are same. According to this junction, All the forces are equal in all the electrical and mechanical or any other systems.

- In 1 junction, sum of efforts are zero and flows are equal. It corresponds to the Electrical loop, or in mechanical system force is bilinear at a mass.

4.3.2 Causality

Bond graph has a notion of causality and bond determines the instantaneous effort and instantaneous flow. Causality defines the effort and causes relationship between two factors of power. If the system is energetically closed, the notion of causatiuon is used to define the predictive relation in the form of differential or integration equation or in the combination of both. The physical system model is limited in such a way that greater part of universe remains outside its boundaries from which it imparts power or reject to it.

The notion of causality defines in all aspects *i.e.*, integration with exterior, storage or constraints. The flow of information *i.e.*, input and effort information *i.e.*, output of physical system are determined by causal stroke which is shown by the small transverse line at the end of bond in bond graph. The generalized effort and generalized flow signals are directed towards the causal stroke at the end of bond.

4.3.3 Activation

In bond graph, bond gives the exchange of power and information to the flow or effort. Some bond in bond graph gives only exchange of information. This type of bond is also called an activated bond. There are two types of activated bonds: flow activated bond and effort activated bond. These bonds are not power bonds, which mean that these types of bonds do not interact with the system. This type of bond represents the velocity, force information, acceleration, displacement and any type of motion in the system and in the bond represent a force sensor and information of flow must be masked. In the causal stroke, a full arrow shows that some information is passed and some information is masked (Refers to Table 4.2) **[Singh, 2013]**.

Table 4.1 Definition of single bond

Name	Type	Symbol
Single Bond	Effort	
	Flow	

4.4 Rayleigh Beam Model

Rayleigh beam model is an improvement over Euler Bernoulli model in that it accounts for rotary inertia of beam through shear deformation is neglected. Create the Rayleigh beam model from a different consideration rather than the difference form of governing equations. By this model create a bond graph model of cantilever beam model which is used to find the deformation of end mill cutter when forces acts on it, in each direction the deformation will be measured namely axial, radial and tangentially which is discussed below.

4.4.1 Rayleigh Beam Model for Axial Deformation

The bond graph model of axial deformation of milling cutter by using eq. (4.26). The shank and flute of the tool are modeled in the left and right of the Fig. 4.6. The shank and the flute of the tool are discretized into 10 elements each in which the slice of model from depth of ut region with lower thickness. One end of the shank is fixed, where source flow is zero and it is connected at the 0-junction. The stiffness is denoted by the C connected at same junction and mass is represented by inertial element I connected at 1-junction. All the reticules of the flute portion are modeled in a similar way except the free end reticule. The axial force is represented by Se element which is connected at the 1-junction of the free end reticule of the flute. The flow sensor (Df) connected at the same 1-junction measures the axial deflection of the cutter due to axial force.

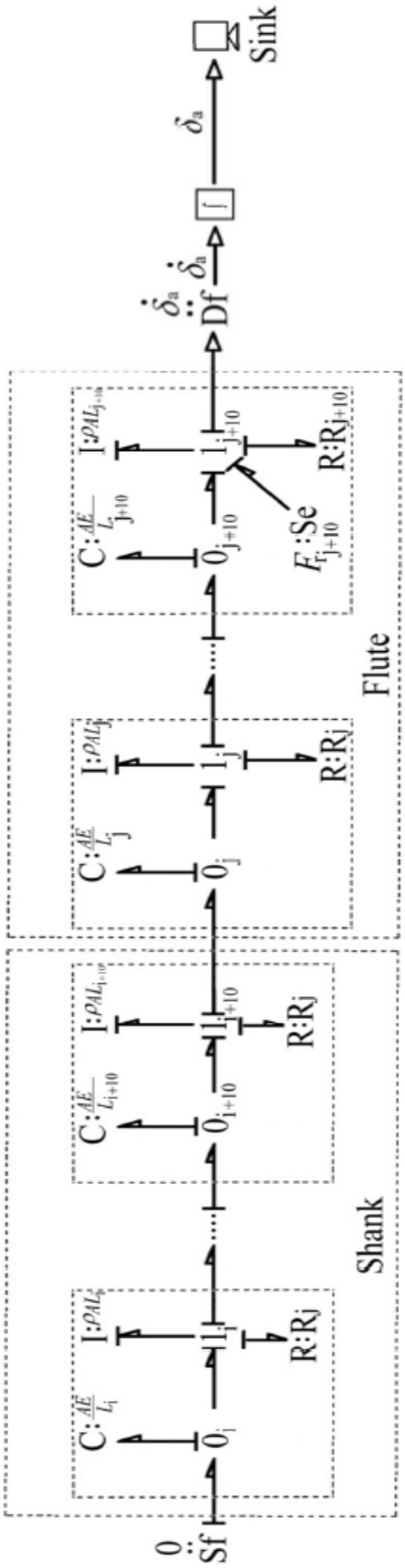

Fig. 4.6 Raleigh beam model for axial deformation

4.4.2 Rayleigh Beam Model for Radial Deformation

The bond graph model for modeling radial deformation of the milling cutter using Eq. (4.27) is shown in Fig. 4.7. Rayleigh beam model may be applied for modeling radial deformation. Rayleigh beam model is an improvement over Euler Bernoulli model as it accounts for rotary inertia of the cutter but it does not account for shear deformation. As in this present work shear deformation ($\frac{F_r L}{AG}$) *which* is the first part of Eq.(4.27) is considered, the bond graph model of Rayleigh beam model is modified. The lower part of Fig. 4.7 is the model for shear deformation and this model is almost similar to the model for axial deformation that is already described.

The Rayleigh beam model is presented in the top part of Fig. 2(a). As the end of the tool is fixed, two zero sources of flow are connected at the two 1-junctions which are the linear and rotary ports. The cutter is subjected to both shear forces and moments and hence, stiffness matrix relates generalized forces with the generalized displacements. The flow sensor (Df) connected at the free end linear 1-junction measures the radial deflection δ_{r_1} of the cutter due to radial force. The total radial deflection is the summation of $\delta_{r_1}$and δ_{r_2}. The torsional moment due to tangential force is not considered in calculating the tangential deflection and hence, Eq. (4.27) is similar to Eq. (4.28). Only the radial force is to be substituted by the tangential force. So, the bond graph model for the tangential deflection would be similar to the model for radial deflection as shown in Fig. 4.7.

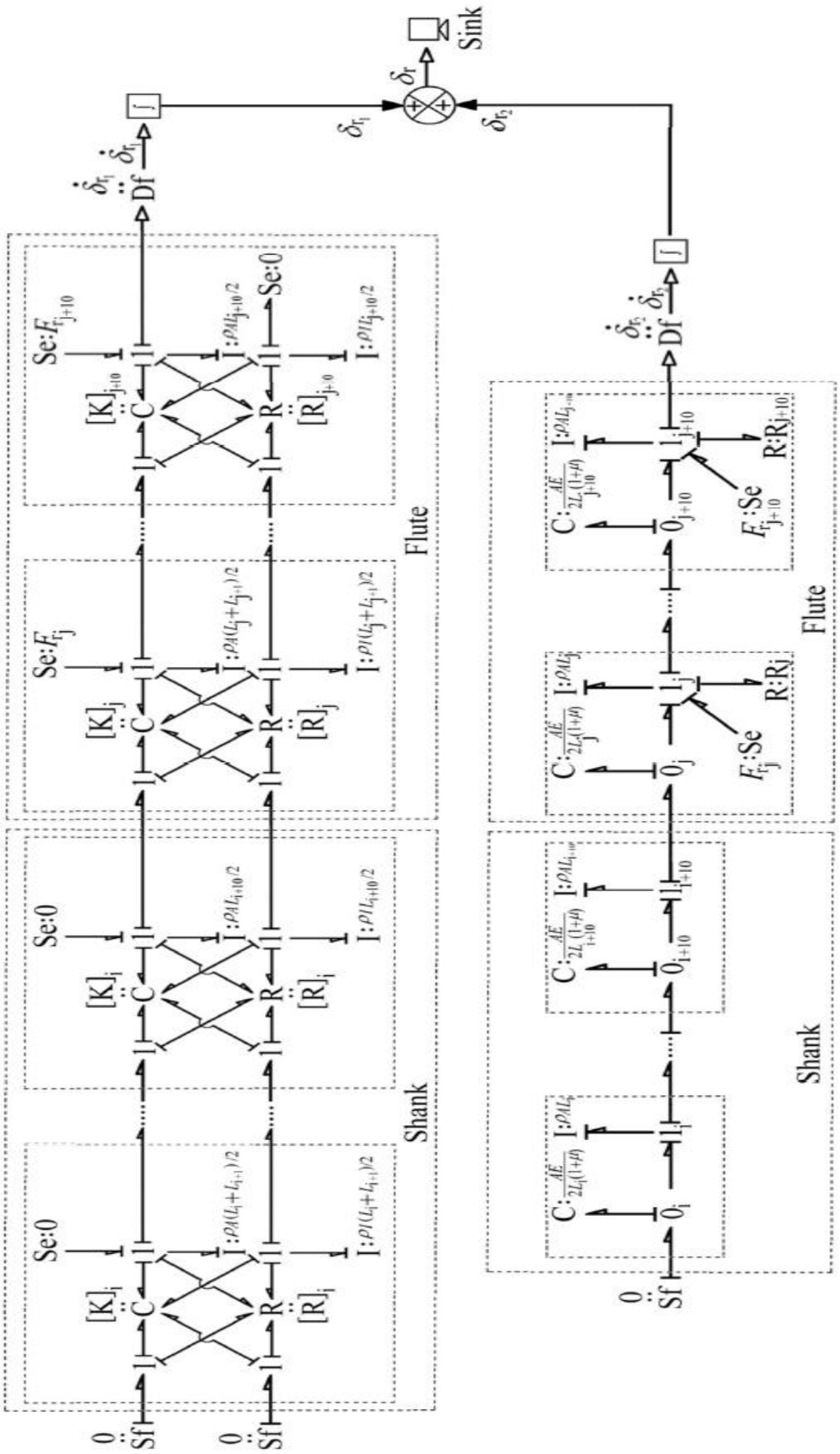

Fig. 4.7 Raleigh beam model for radial deformation

4.5 Simulation Results and Analysis

The simulation result of bond graph on each experimental condition is shown below graphically.

4.5.1 Deflection due to radial force

- **Radial deflection due to depth of cut**

`Table 4.2 Radial deflections due to depth of cut
(constant Cutting speed = 250 rpm and constant feed = 20 mm/min)

DOC (mm)	Radial deflection (microns)	
	For 9.5mm tool	For 14 mm tool
2	247	305.9
3	421.5	485.8
4	493.5	503.8

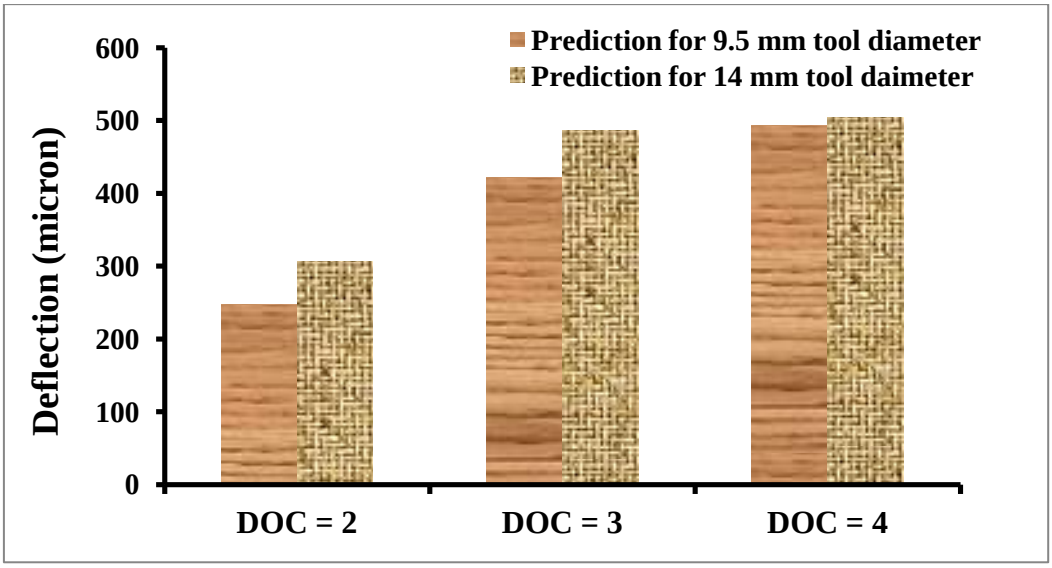

Fig. 4.8 Graphical representation of radial deflection due to depth of cut by bond graph
(constant Cutting speed = 250 rpm and constant feed = 20 mm/min)

- **Radial deflection due to feed**

Table 4.3 Radial deflections due to feed
(constant Cutting speed = 350 rpm and constant DOC = 2 mm)

Feed (mm/min)	Radial deflection (microns)	
	For 9.5mm tool	For 14 mm tool
15	211.5	269.9
25	279.7	197.9
35	247	341.9

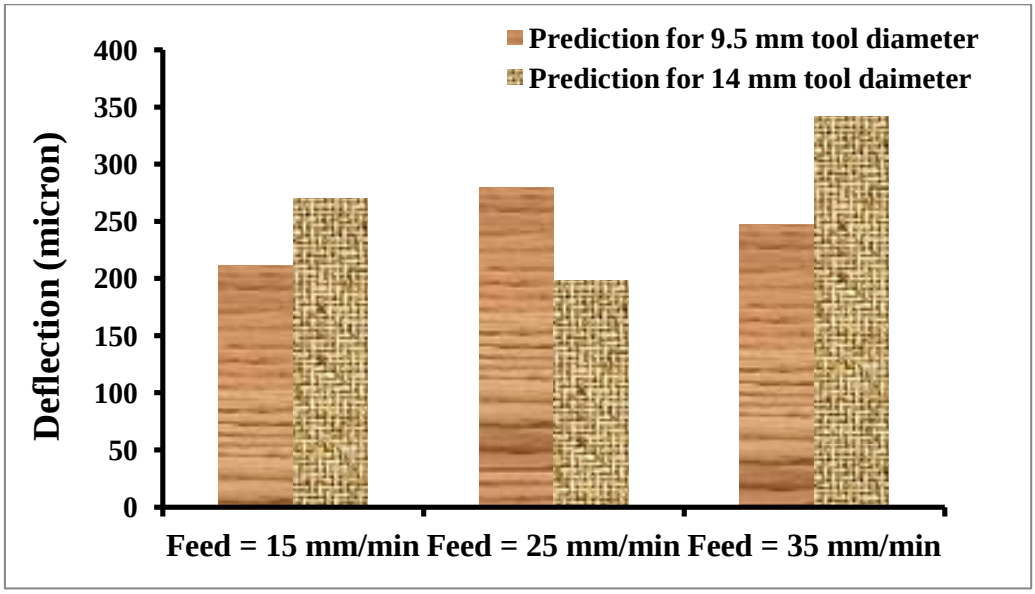

Fig. 4.9 Graphical representation of radial deflection due to feed by bond graph

- **Radial deflection due to cutting speed**

Table 4.4 Radial deflections due to cutting speed
(constant feed = 35 mm/min and constant DOC = 4 mm)

Cutting speed (RPM)	Radial deflection (microns)	
	For 9.5mm tool	For 14 mm tool
350	579	521.8
500	452	629.8
600	371	539.8

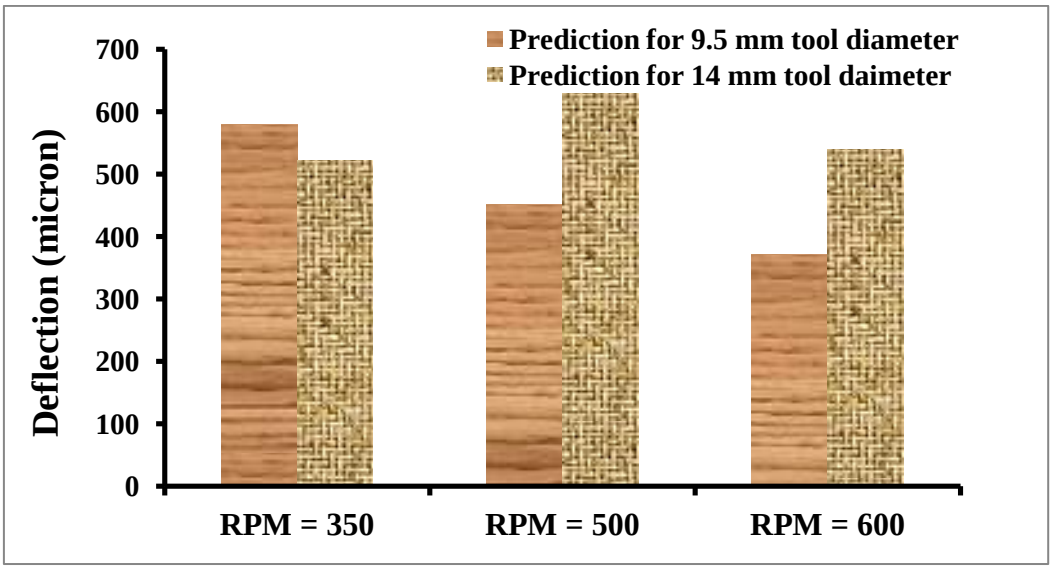

Fig. 4.10 Graphical representation of radial deflection due to speed by bond graph
(constant feed = 35 mm/min and constant DOC = 4 mm)

4.5.2 Deflection due to tangential force

- **Tangential deflection due to depth of cut**

Table 4.5 Tangential deflections due to depth of cut
(constant Cutting speed = 250 rpm and constant feed = 20 mm/min)

DOC (mm)	Tangential deflection (microns)	
	For 9.5mm tool	For 14 mm tool
2	249.5	354.1
3	386.5	477.9
4	543	534.8

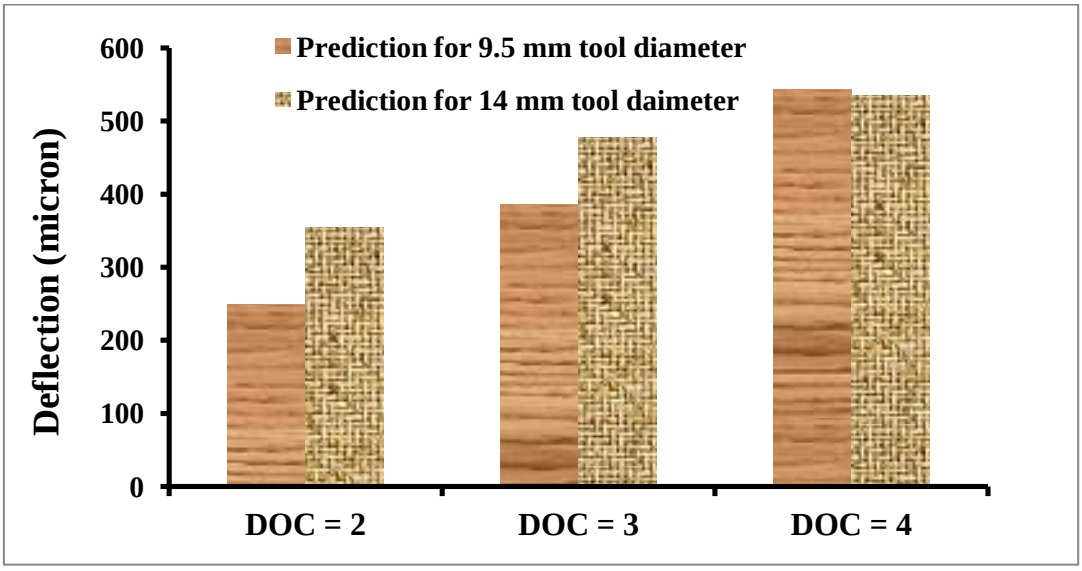

Fig. 4.11 Graphical representation of tangential deflection due to depth of cut by bond graph
(constant Cutting speed = 250 rpm and constant feed = 20 mm/min)

- **Tangential deflection due to feed**

Table 4.6 Tangential deflections due to feed
(constant Cutting speed = 350 rpm and constant DOC = 2 mm)

Feed (mm/min)	Tangential deflection (microns)	
	For 9.5mm tool	For 14 mm tool
15	214.5	279.2
25	281.8	199.7
35	252.3	370.7

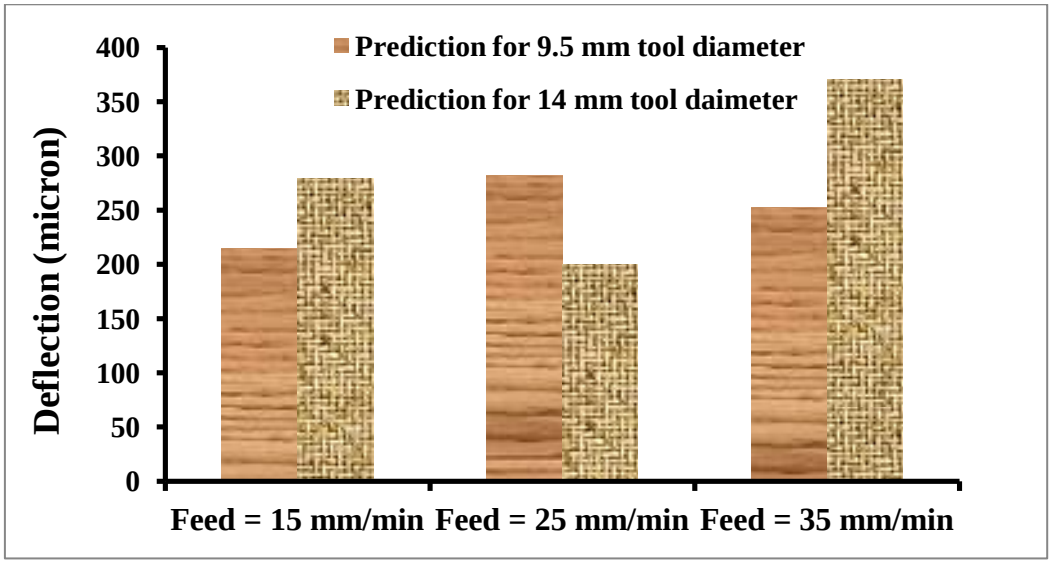

Fig. 4.12 Graphical representation of tangential deflection due to feed by bond graph
(constant Cutting speed = 350 rpm and constant DOC = 2 mm)

- **Tangential deflection due to cutting speed**

Table 4.7 Tangential deflections due to cutting speed
(constant feed = 35 mm/min and constant DOC = 4 mm)

Cutting speed (RPM)	Tangential deflection (microns)	
	For 9.5mm tool	For 14 mm tool
350	492.2	522.9
500	388	655
600	378	547

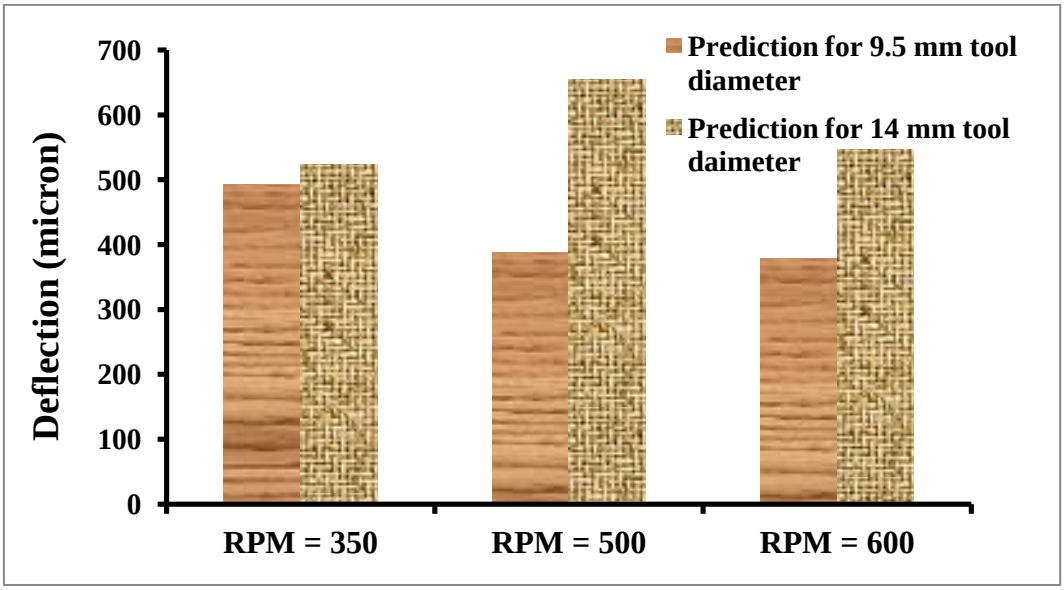

Fig. 4.13 Graphical representation of tangential deflection due to speed by bond graph
(constant feed = 35 mm/min and constant DOC = 4 mm)

4.5.3 Deflection due to axial force

- **Axial deflection due to depth of cut**

Table 4.8 Axial deflections due to depth of cut
(constant Cutting speed = 250 rpm and constant feed = 20 mm/min)

DOC (mm)	Axial deflection (microns)	
	For 9.5mm tool	For 14 mm tool
2	0.24	0.25
3	0.35	0.25
4	0.52	0.36

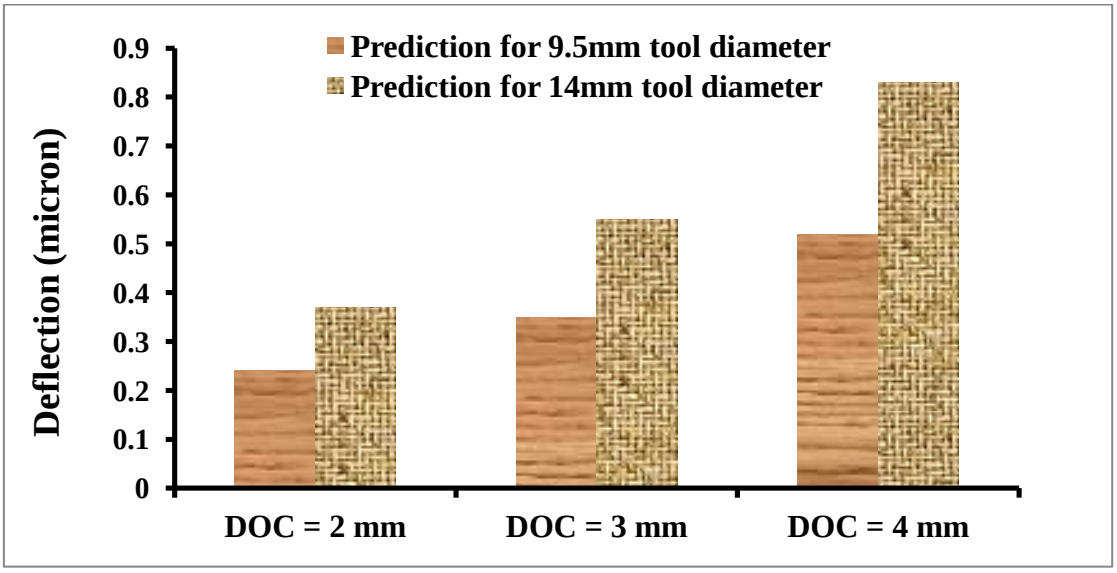

Fig. 4.14 Graphical representation of axial deflection due to depth of cut by bond graph
(constant Cutting speed = 250 rpm and constant feed = 20 mm/min)

- **Axial deflection due to feed**

Table 4.9 Axial deflections due to feed
(constant Cutting speed = 350 rpm and constant DOC = 2 mm)

Feed (mm/min)	Axial deflection (microns)	
	For 9.5mm tool	For 14 mm tool
15	0.24	0.38
25	0.27	0.38
35	0.24	0.38

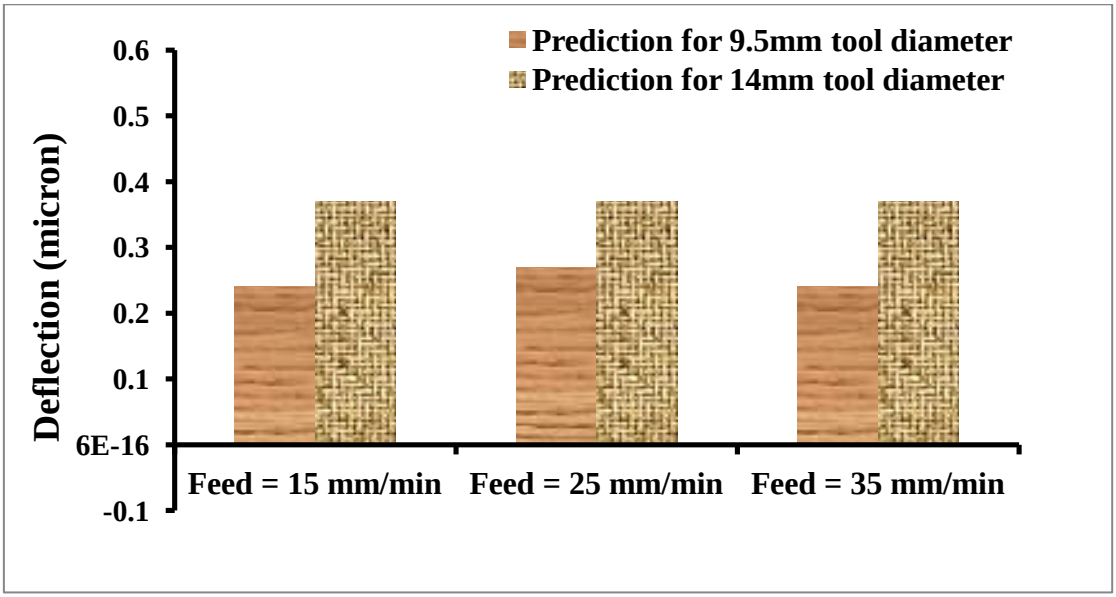

Fig. 4.15 Graphical representation of axial deflection due to feed by bond graph
(constant Cutting speed = 350 rpm and constant DOC = 2 mm)

- **Axial deflection due to cutting speed**

Table 4.10 Axial deflections due to cutting speed
(constant feed = 35 mm/min and constant DOC = 4 mm)

Cutting speed (RPM)	Axial deflection (microns)	
	For 9.5mm tool	For 14 mm tool
350	0.35	0.38
500	0.52	0.56
600	0.24	0.68

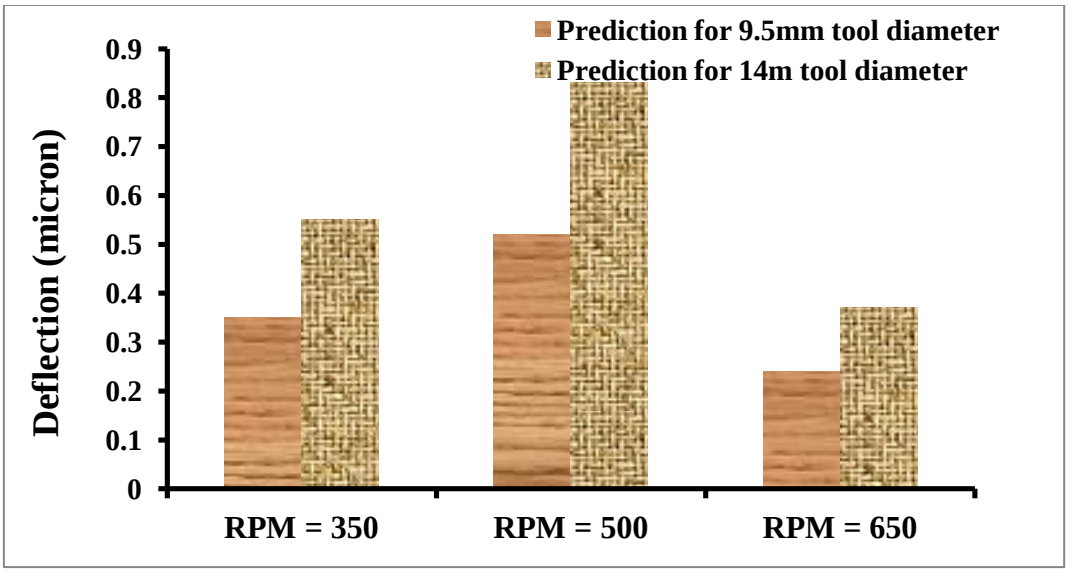

Fig. 4.16 Graphical representation of axial deflection due to cutting speed by bond graph
(constant feed = 35 mm/min and constant DOC = 4 mm)

CHAPTER 5

Experimental Study

5.1 Introduction

This chapter includes the experimental study of cutting forces and deflection of end mill cutter due to these forces. These chapter discuses about the forces measured during cutting with the help of kistler dynamometer on each direction, which is mounted on the vertical milling CNC machine by varying the parameter namely feed rate, spindle speed and depth of cut with two different size of end mill cutter. As deflection cannot measured directly, so after cutting on each pair of set the deflection is measured on coordinate measuring machine and compare the actual variation with ideal cutting.

5.2 Experimental Setup

Present experimental work has been carried out using the apparatus listed below:

5.2.1 Machine

- **Vertical milling machine**

The Chandra machining center is 3 axis numerical controlled machine tool equipped with automatic tool changer. This machine is capable of doing such operation tapping, threading, drilling, etc.

Fig. 5.1 Vertical milling CNC

The vertical milling machine has 3 axis coordinate machine travelled in three axis *X*, *Y* and *Z* as shown in Fig. 5.2.

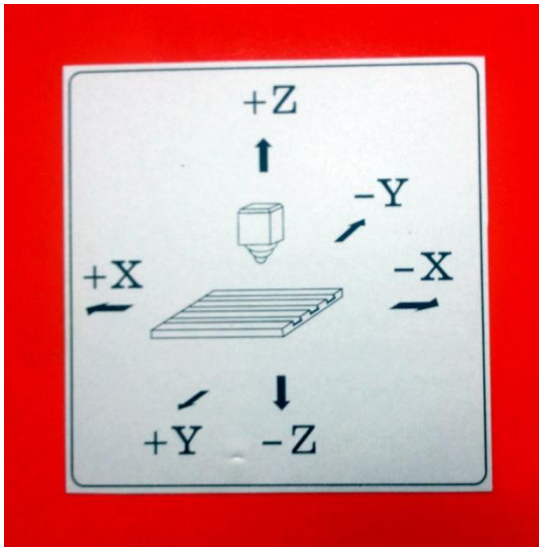

Fig. 5.2 Coordinate system of CNC

Controlled axis and movement of bed and spindle with sign convention as show below in Table 5.1.

Table 5.1 Table movement direction

Controlled axis and Table movement direction		
Axis	Movement direction	+ (plus), - (minus)
X	Table, left and right	Left movement + (as viewed from front of machine)
Y	Saddle, back and forth	Forward movement (+)
Z	Spindle, up and down	Up movement(+)

Machine programming is based on the *G* codes called geometry code which is basically define the cutting geometry like operation of cutting, transverse technique and *M*-code called is machine codes which control the machine like spindle ON/OFF, coolant ON/OFF etc.

- **Coordinate Measuring Machine**

The accurate coordinate measuring machine is 3 axis machine used to measure the physical geometrical characteristics of an object. The machine has both manual and computer numerical controlled system and corporate with accuracy. The measurement of the required geometry with the help of stylus which is attached with probe system on *Z* axis of the

machine as shown in Fig 5.3. The stylus carried ball made of ruby, and it may be laser, optical, or mechanical.

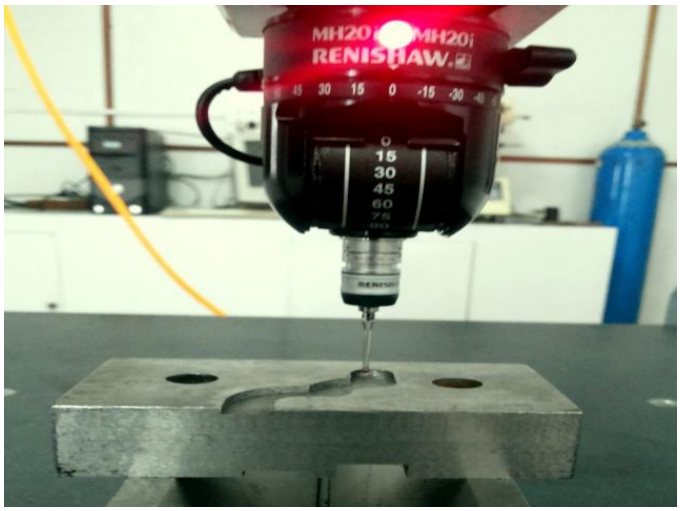

Fig. 5.3 Probing system of CMM

This machine is also used to predict the accurate geometry for manufacturing by measuring the coordinate and then transform these coordinate into 3-dimensional modeling.

Fig. 5.4 Coordinate measuring machine

This machine includes the three main components.

- Measured data are collected by using desktop and application software. It's a part of machine controller. Where each direction coordinate of machine and object coordinate are seen. The software used in this machine is TANGRAM.

- The main structure of the machine is its frame on which the machine is moved. It's made up of granite.
- Probing system which is very important part of the machine used to measure the coordinate in each direction from its origin, the probe system is shown above in Fig. 5.3

5.2.2 Kistler Piezoelectric Dynamometer

A dynamometer is device used to measure the cutting force, torque and power for various purposes, In this experimental study purpose of using kistler piezoelectric dynamometer is to measure the cutting force during milling at different condition discussed below.

(a) (b)

Fig. 5.5 (a) Kistler piezoelectric dynamometer (b) desktop and application software

Fig. 5.5 (b) shows desktop and application software for the measurement of forces, the collected in both graphically and binary format, which directly browse in excel. The unit of measuring force by default in Newton.

Dynamometer is mounted in bed with the help of T-bolt as shown above and the work piece hold over the dynamometer with the help of Allen bolts.

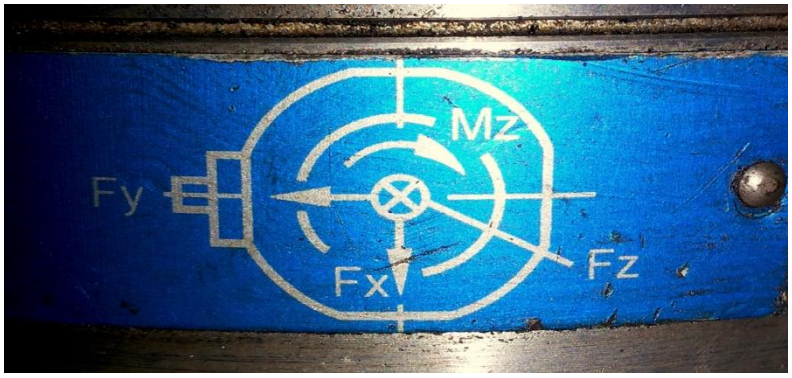

Fig. 5.6 Directions of cutting forces in dynamometer

The direction of force in each direction *X*, *Y* and *Z* is shown in Fig. 5.6.

- F_y defines the force in *Y* direction, where as the force perpendicular to the F_y is F_x in *X* direction.
- The force along the axis of rotation is F_z as shown above.
- M_z denotes torque.

5.2.3 End Mill Cutters

In this experimental study two different standard tools are used as shown in Fig. 5.7 and the dimensions of tools are shown in Table 5.2.


Fig. 5.7 End mill cutters

Table 5.2 Dimensions of end mill cutters

Tool No.	Diameter of the tool	Cutting Length	Sleeve length
Tool 1	9.5	30	40
Tool 2	14	40	45

5.2.4 Work piece material

In this experimental study the work piece material machined is medium carbon steel AISI 1045 with 0.4 % carbon as shown in fig 5.8. In terms of machining AISI 1045 has good machinability in normalized condition, These types of steels are also known as structural steel. The physical properties of these steels are high, also manganese and carbon levels are generally high. Medium carbon steels have a good balance of ductility and strength.

Fig. 5.8 Work piece material

Typical applications are rails and rail products, couplings, crankshafts, axles, bolts, rods, gears, forgings, tubes, plates and constructional steels. The chemical composition and mechanical properties of AISI 1045 is shown in Table 5.3 and 5.4.

Table 5.3 Chemical composition of AISI 1045

Element	Content
Carbon	0.4 – 0.5 %
Iron	98.51 - 98.98 %
Manganese	0.60 - 0.90 %
Sulfur	≤0.050 %
Phosphorus	≤0.040 %

Table 5.4 Mechanical properties of steel

Density	7.7×10^3 kg m^{-3}
Hardness	170 HB
Elastic modulus	190–210 GPa
yield strength	480 MPa
Tensile strength	585 MPa
Elongation	12 %
Poisson ratio	0.27–0.3

5.3 Result and analysis

By using the precise apparatus for measuring coordinate system called CMM is used to find the deflection of the end mill cutter, the principle behind is that if the give slot length during cutting in vertical milling CNC, then that cutting slot is measured in the CMM precisely, so that the due to deflection the actual length of cut is not equal to desired length of cut after measurement, some where it is less then actual length of cut.

5.3.1 *Cutting forces*

Behind all theory the cutting forces is the only responsible for deflection, control over cutting forces means desired geometry is very close to actual geometry. The cutting forces depend upon many factors, like tool angles, cutting speed, depth of cut, feed etc. The cutting forces are measured by dynamometer by varying the variables depth of cut, feed, and cutting speed as shown graphically below.

- **Cutting force for 9.5mm tool diameter**

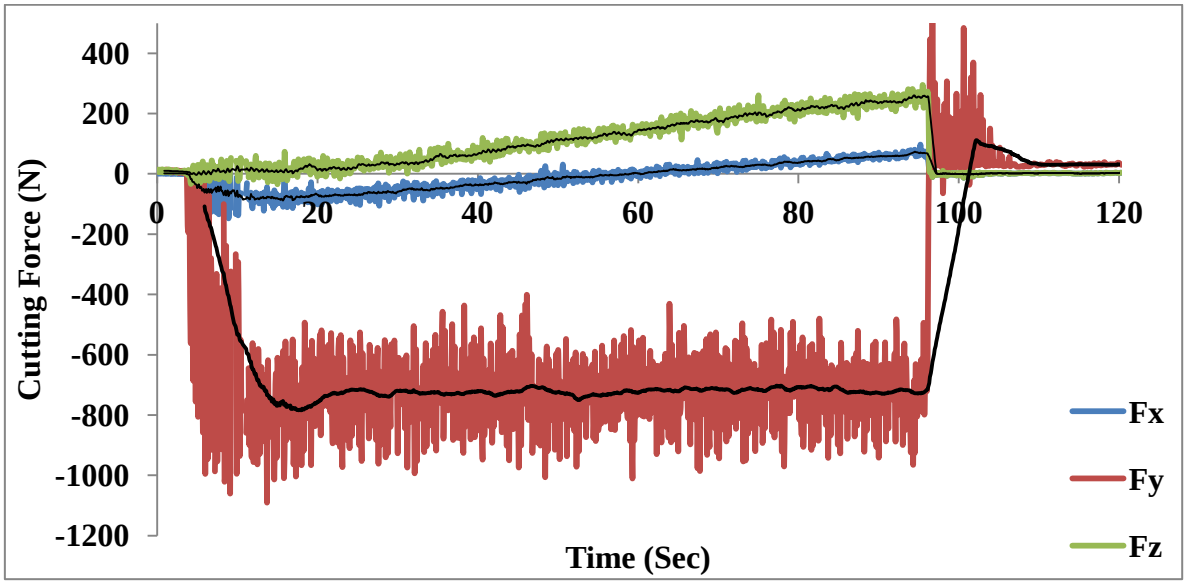

Fig. 5.9 Graphical representation of cutting forces
(cutting speed = 250 rpm, DOC = 2 mm, feed = 20 mm/min)

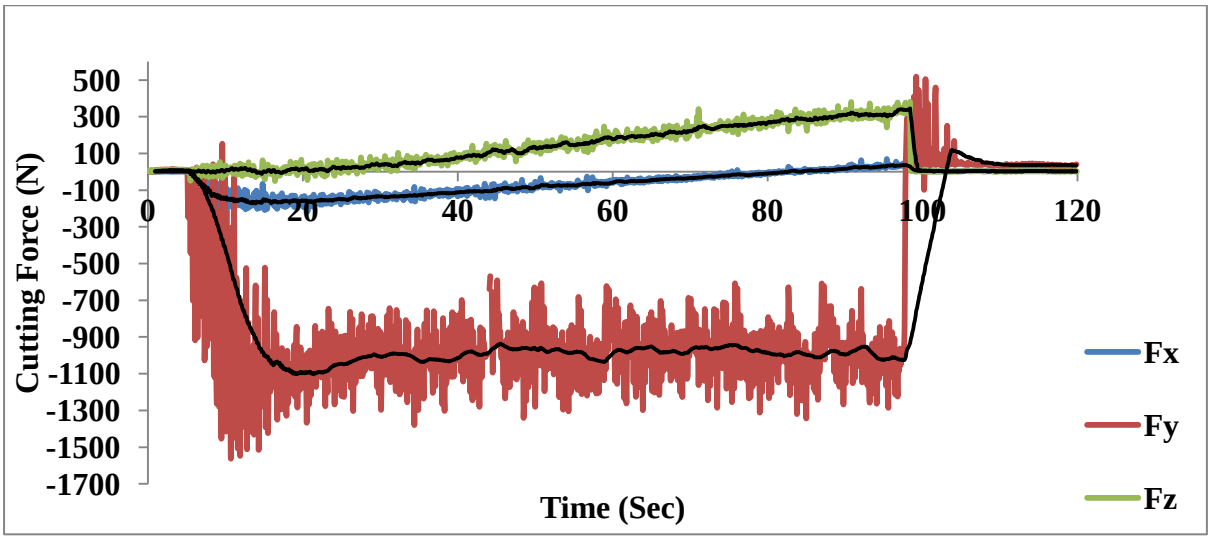

Fig. 5.10 Graphical representation of cutting forces
(cutting speed = 250 rpm, DOC = 3 mm, feed = 20 mm/min)

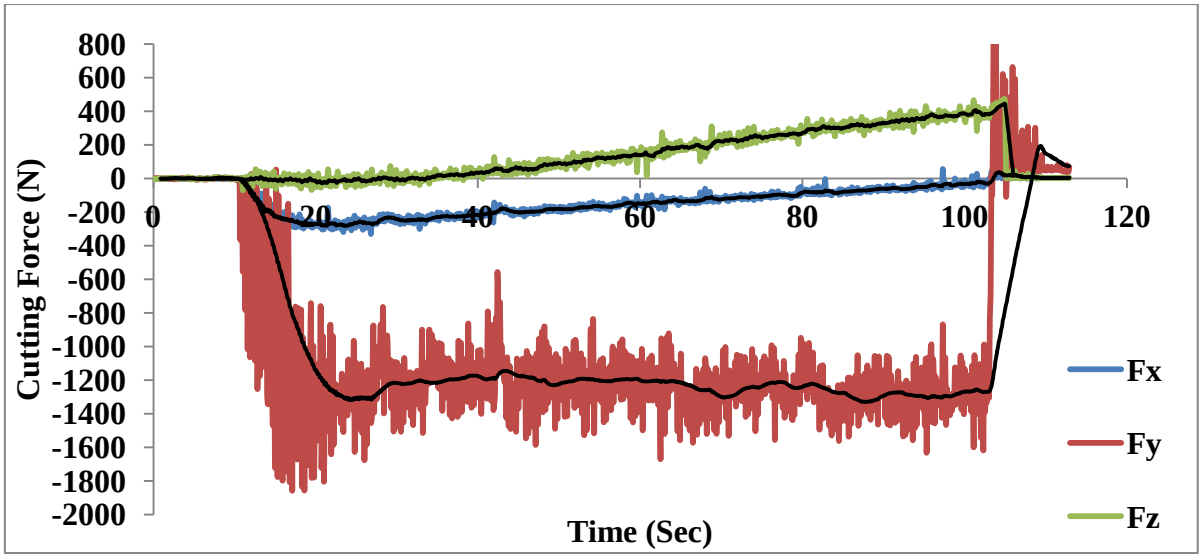

Fig. 5.11 Graphical representation of cutting forces
(cutting speed = 250 rpm, DOC = 3 mm, feed = 20 mm/min)

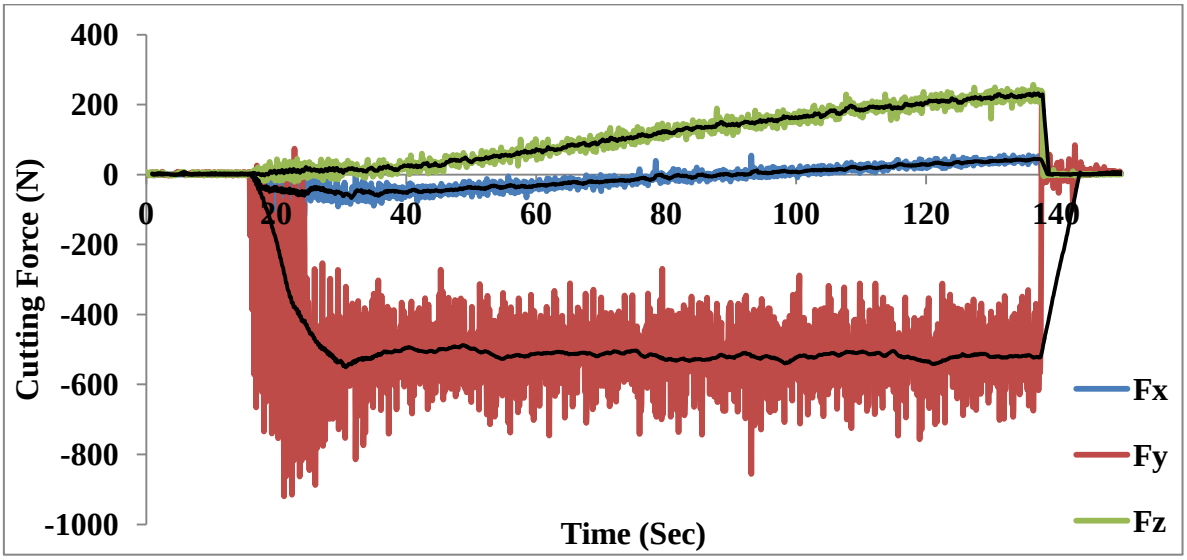

Fig. 5.12 Graphical representation of cutting forces
(cutting speed = 350 rpm, DOC = 2 mm, feed = 15 mm/min)

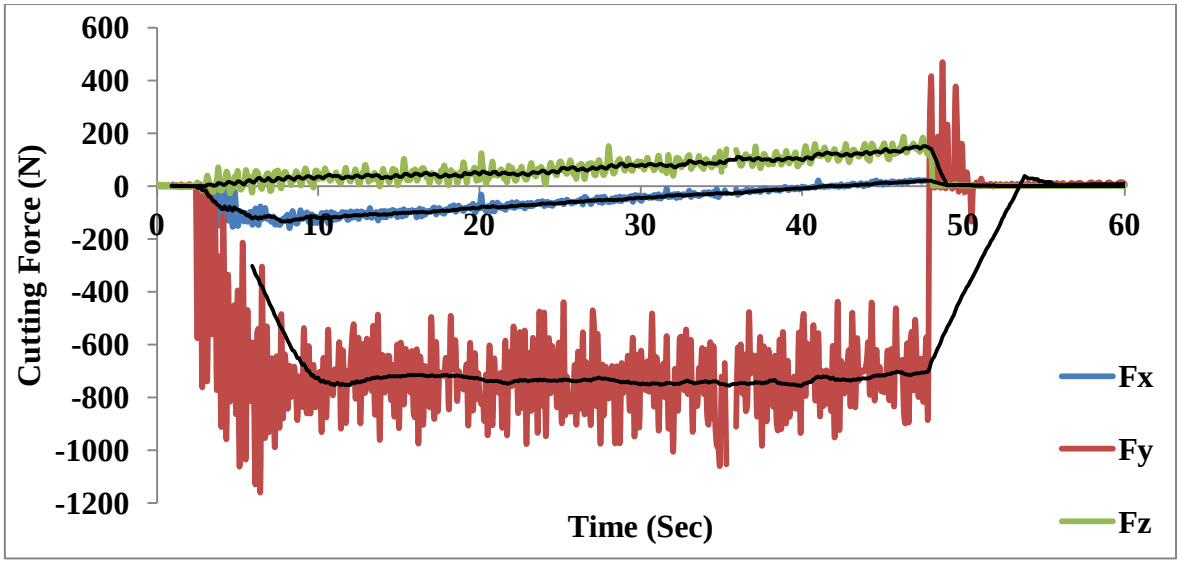

Fig. 5.13 Graphical representation of cutting forces
(cutting speed = 350 rpm, DOC = 2 mm, feed = 25 mm/min)

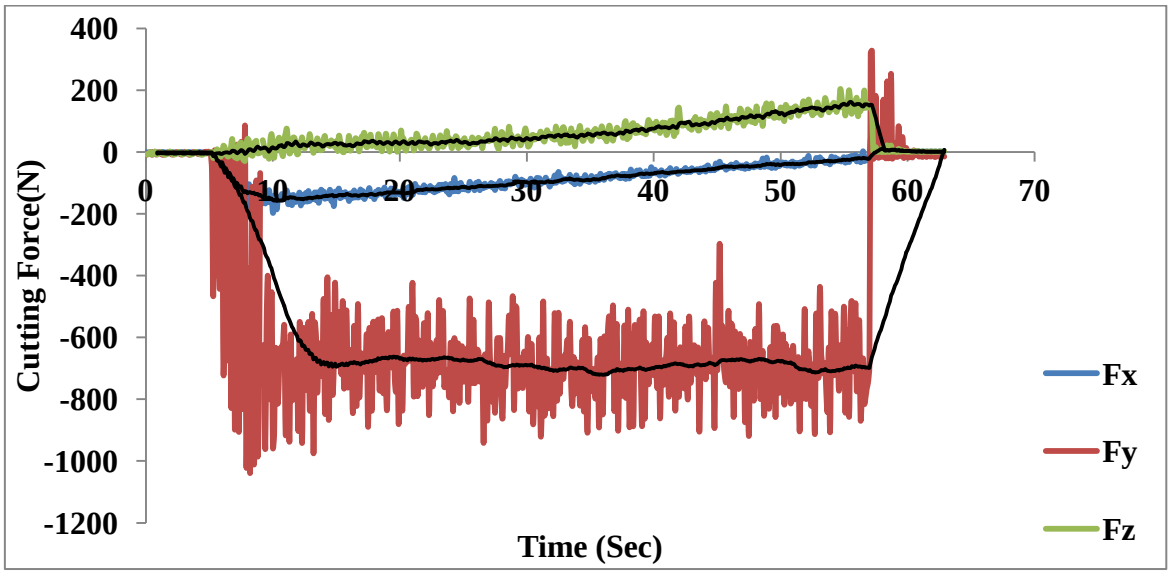

Fig. 5.14 Graphical representation of cutting forces
(cutting speed = 350 rpm, DOC = 2 mm, feed = 35 mm/min)

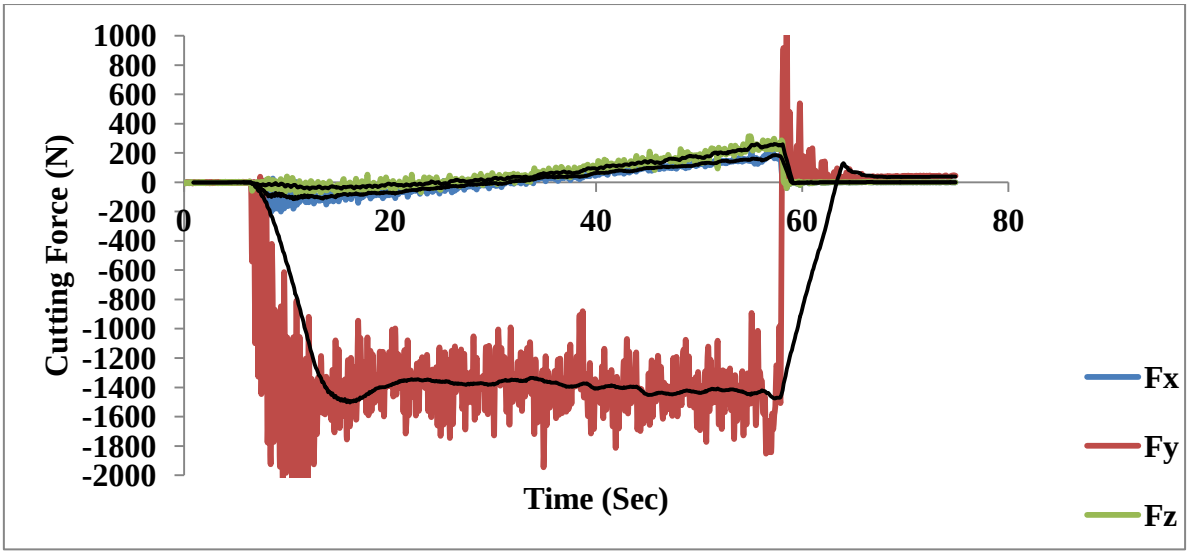

Fig. 5.15 Graphical representation of cutting forces
(cutting speed = 350 rpm, DOC = 4 mm, feed = 35 mm/min)

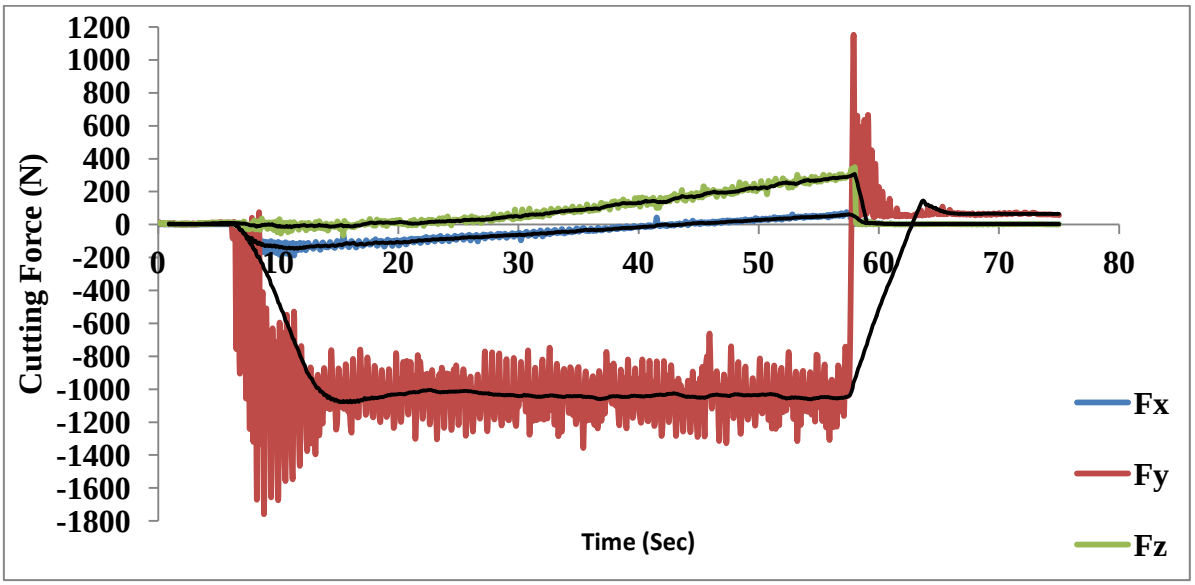

Fig. 5.16 Graphical representation of cutting forces
(cutting speed = 500 rpm, DOC = 4 mm, feed = 35 mm/min)

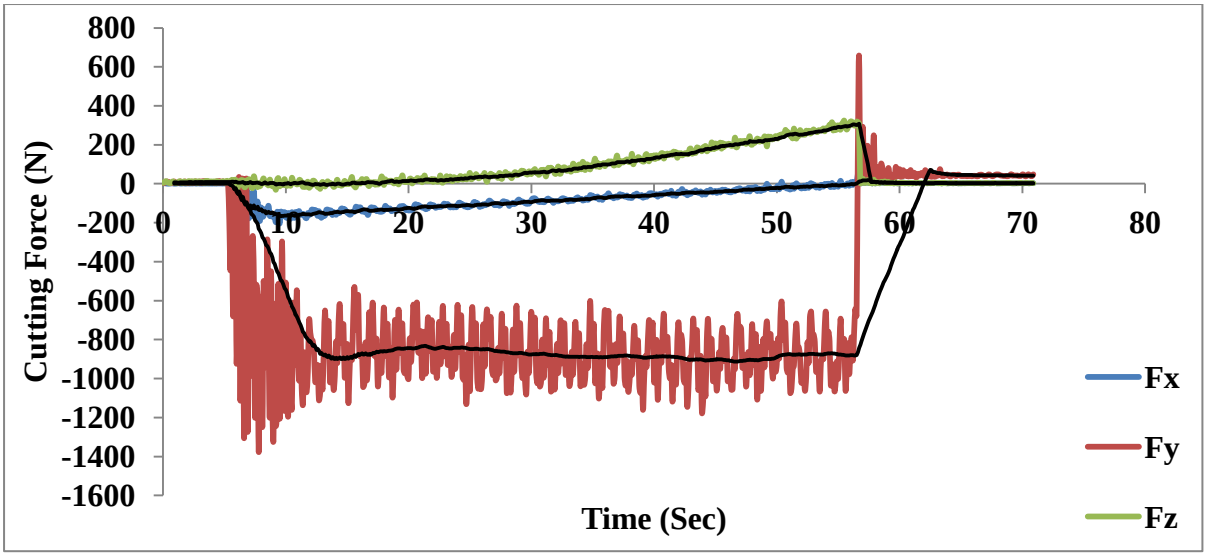

Fig. 5.17 Graphical representation of cutting forces
(cutting speed = 650 rpm, DOC = 4 mm, feed = 35 mm/min)

- **Cutting force for 14 mm tool diameter**

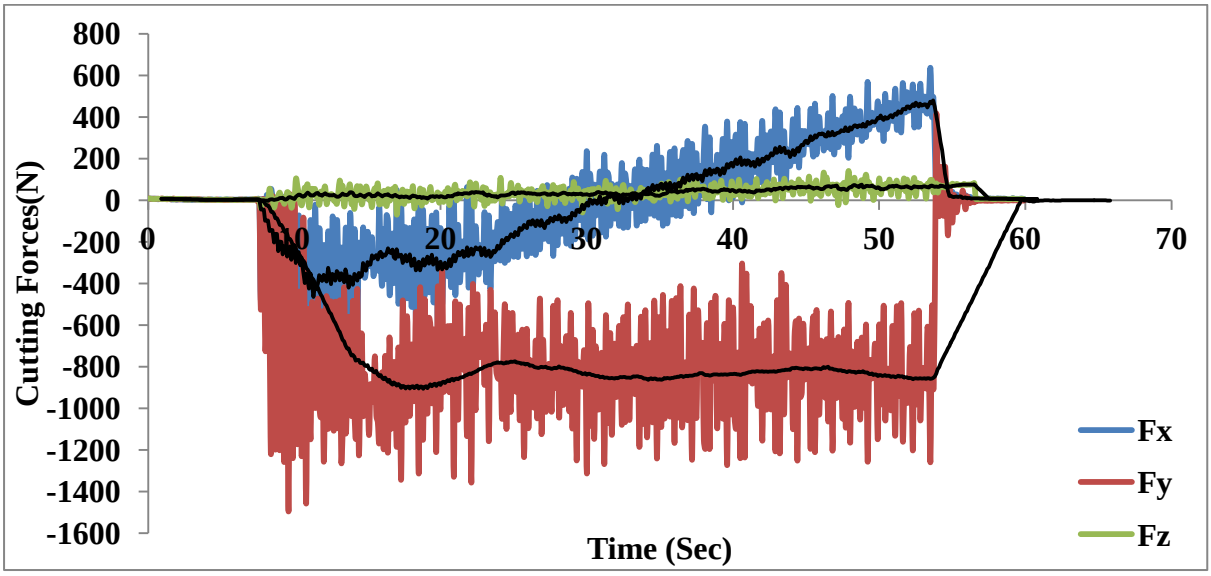

Fig. 5.18 Graphical representation of cutting forces
(cutting speed = 250 rpm, DOC = 2 mm, feed = 20 mm/min)

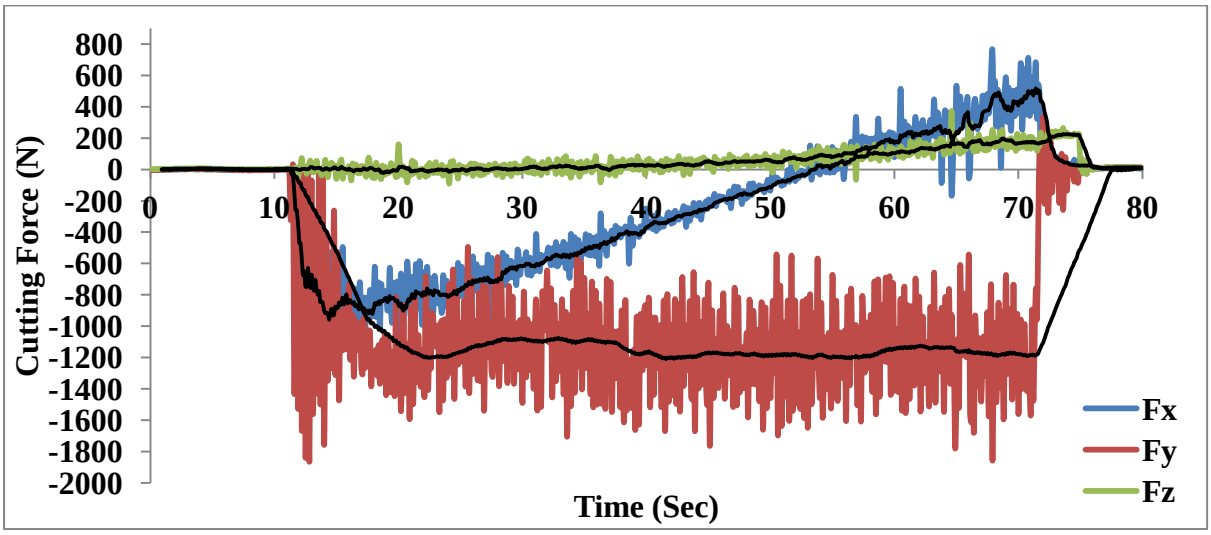

Fig. 5.19 Graphical representation of cutting forces
(cutting speed = 250 rpm, DOC = 3 mm, feed = 20 mm/min)

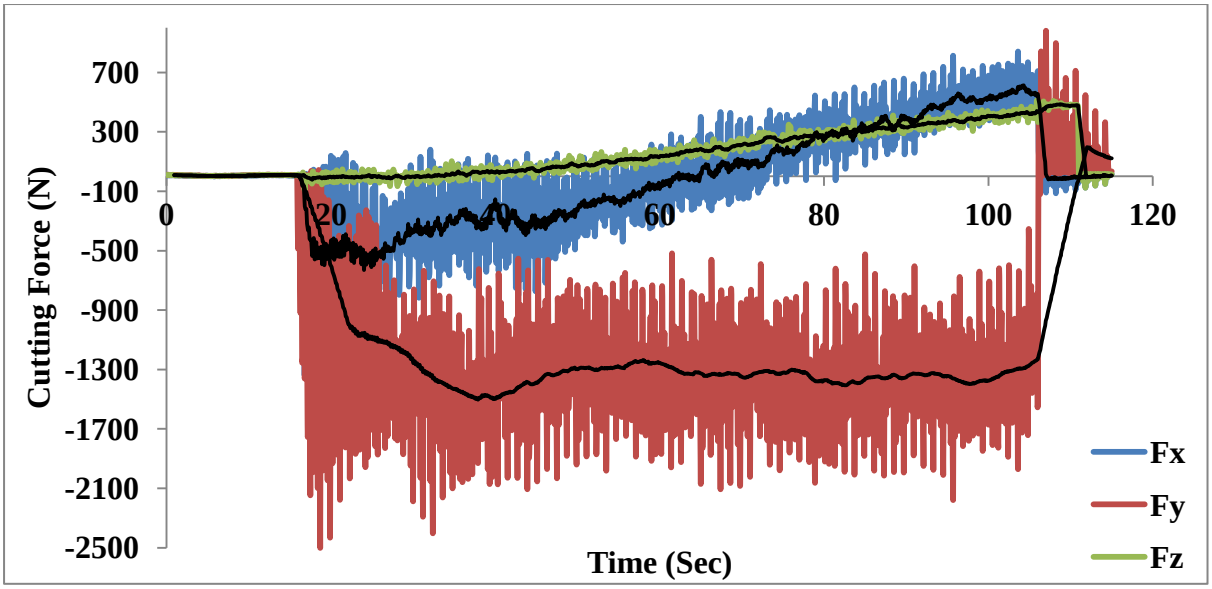

Fig. 5.20 Graphical representation of cutting forces
(cutting speed = 250 rpm, DOC = 4 mm, feed = 20 mm/min)

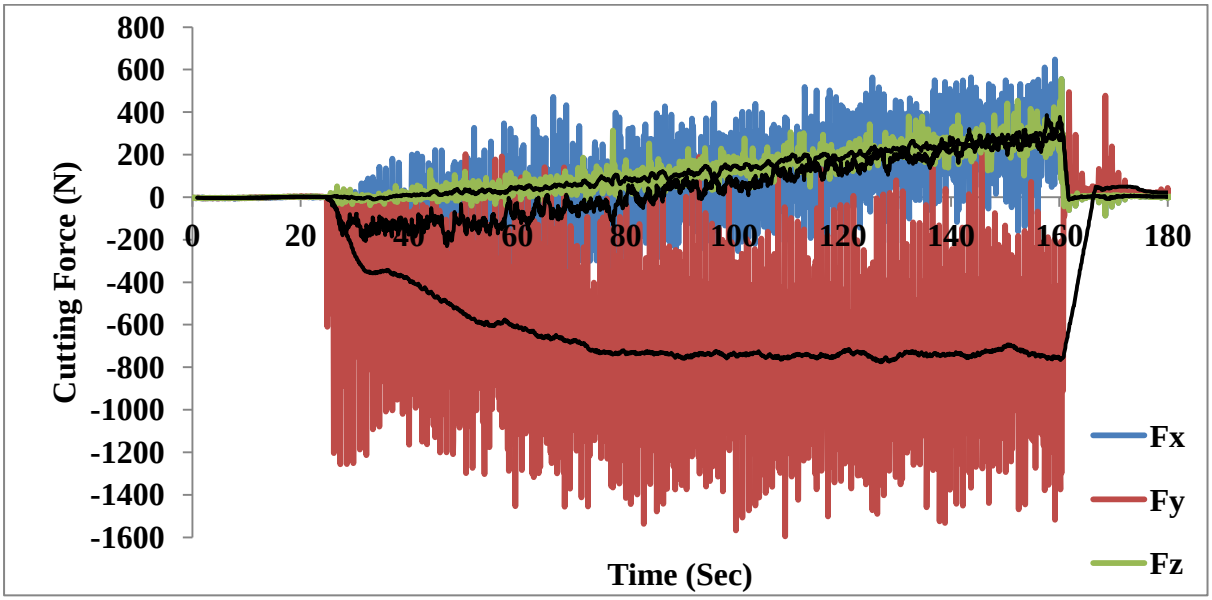

Fig. 5.21 Graphical representation of cutting forces
(cutting speed = 350 rpm, DOC = 2 mm, feed = 15 mm/min)

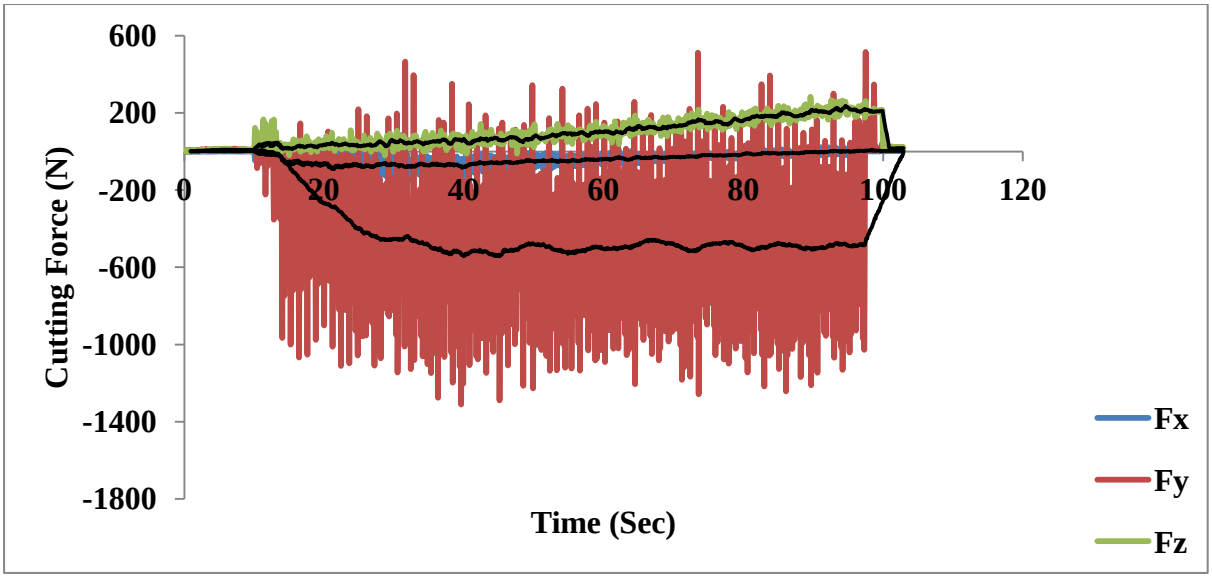

Fig. 5.22 Graphical representation of cutting forces
(cutting speed = 350 rpm, DOC = 2 mm, feed = 25 mm/min)

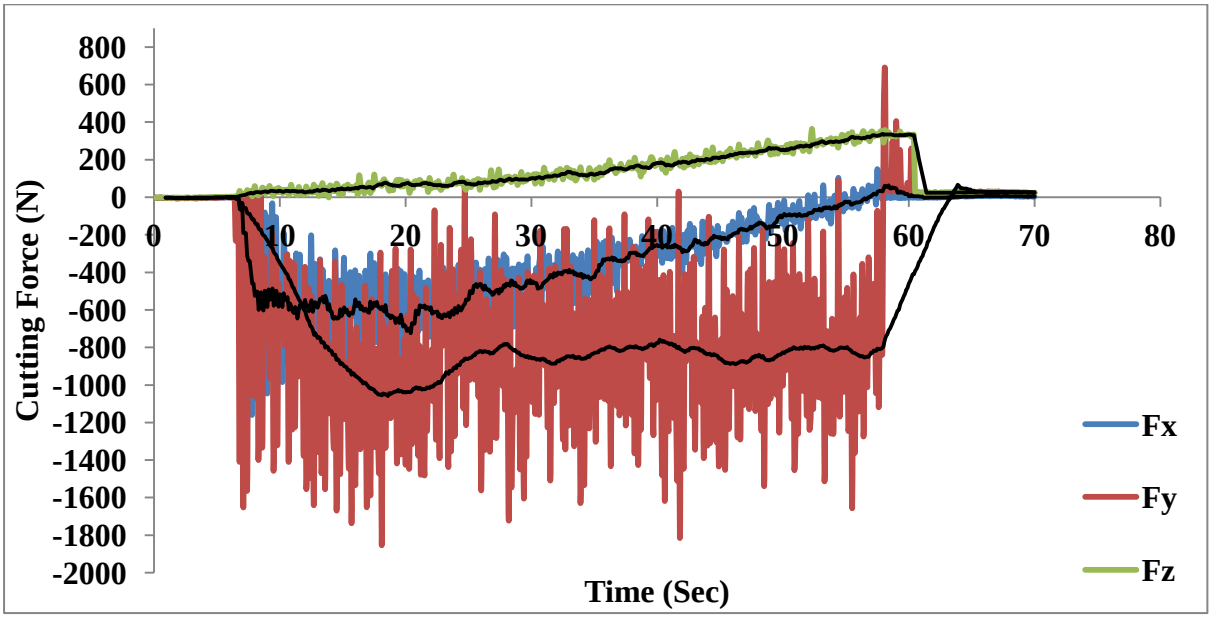

Fig. 5.23 Graphical representation of cutting forces
(cutting speed = 350 rpm, DOC = 2 mm, feed = 35 mm/min)

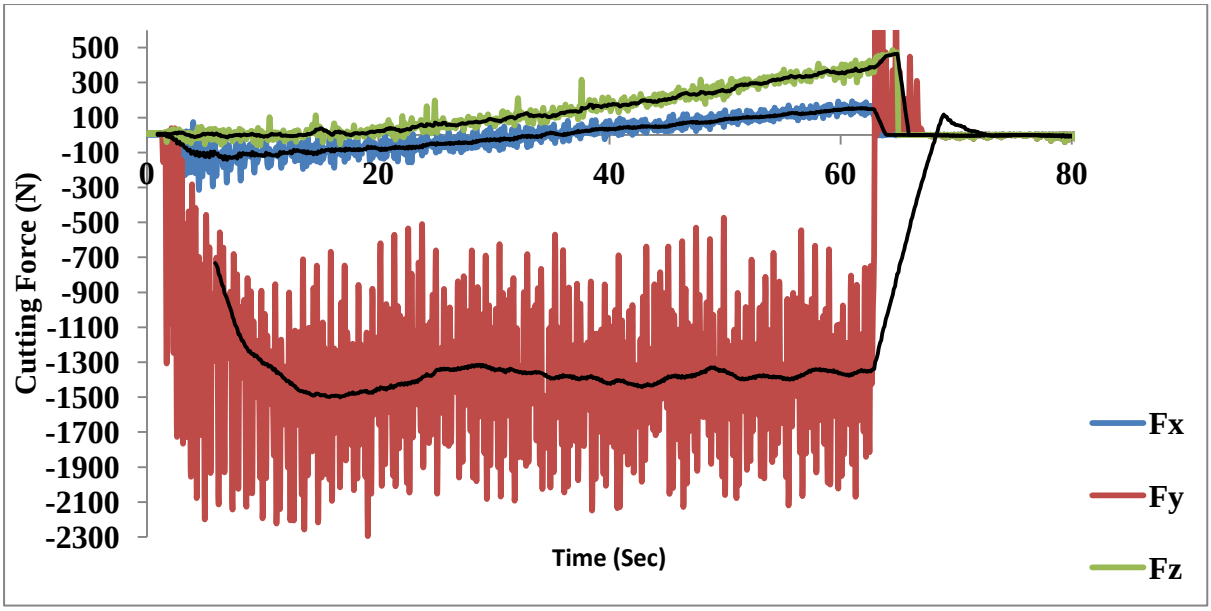

Fig. 5.24 Graphical representation of cutting forces
(cutting speed = 350 rpm, DOC = 4 mm, feed = 35 mm/min)

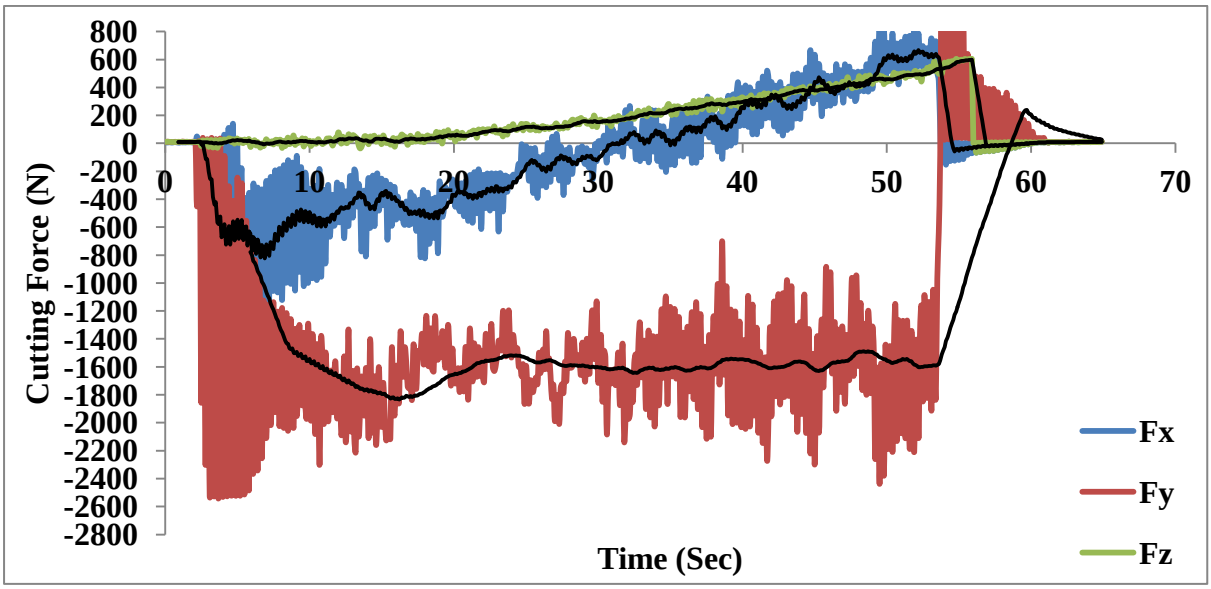

Fig. 5.25 Graphical representation of cutting forces
(cutting speed = 500 rpm, DOC = 4 mm, feed = 35 mm/min)

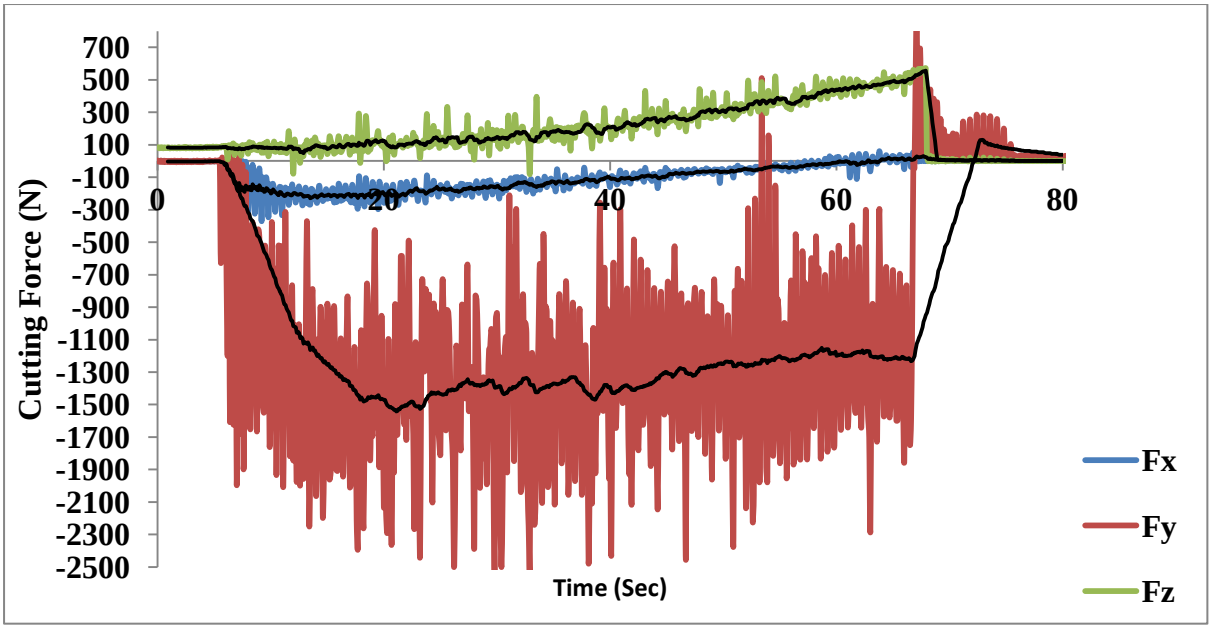

Fig. 5.26 Graphical representation of cutting forces
(cutting speed = 650 rpm, DOC = 4 mm, feed = 35 mm/min)

5.3.2 *Deflection of Cutter and Geometric Accuracy of Machine Slot*

The measurement of cutting slot in CMM machine and compare it with actual measurement. By CMM machine coordinate of each profile is taken and import into excel sheet, so that easily get a desired profile and compare with actual profile. The profile of each experimental condition systematically is shown below in table 5.14.

Table 5.5 Comparison between actual (measured) and desired (ideal) geometry for 9.5mm and 14 mm diameter tool

Experimental condition (cutting speed, DOC, feed)	Comparison between actual and desired profile	
	For 9.5mm cutter	For 14 mm cutter
250 rpm, 10mm, 20 mm/min	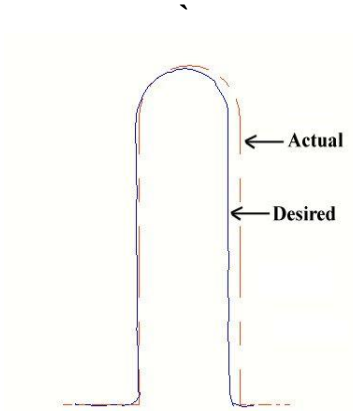	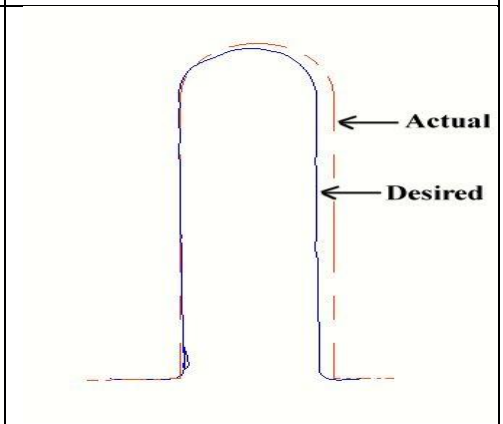
250 rpm, 3mm, 20 mm/min	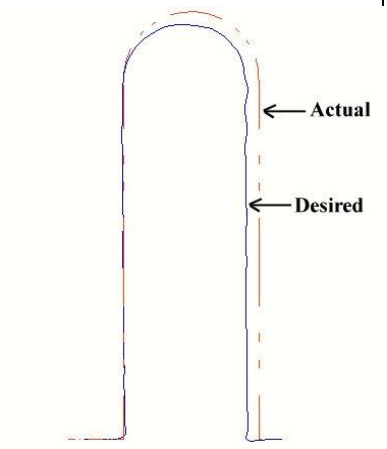	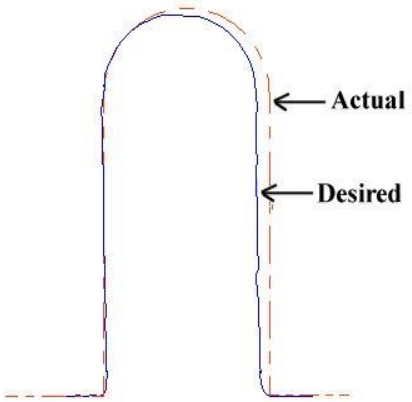

250 rpm, 4mm, 20 mm/min	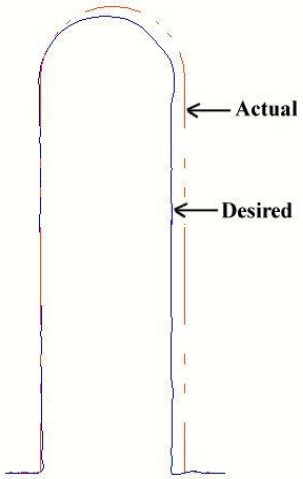	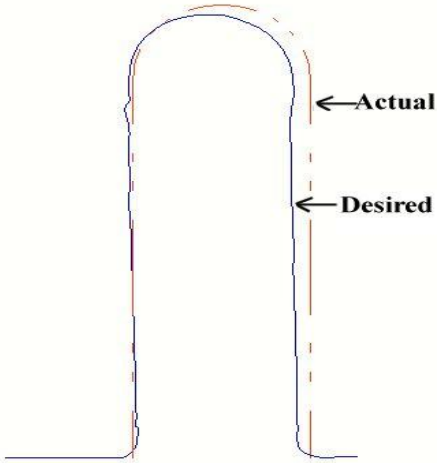
350 rpm, 2 mm, 15 mm/min	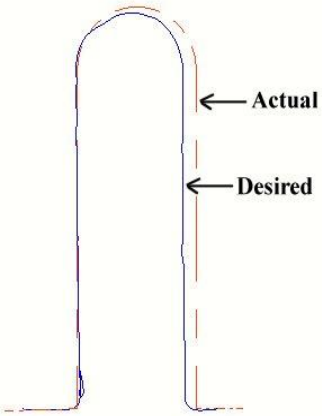	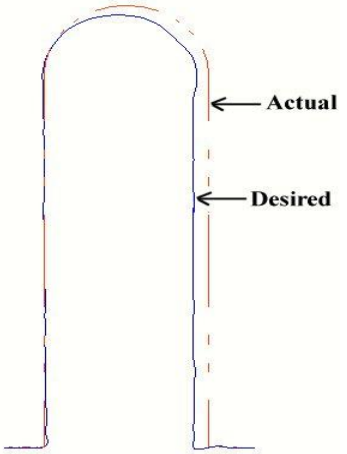
350 rpm, 2 mm, 25 mm/min	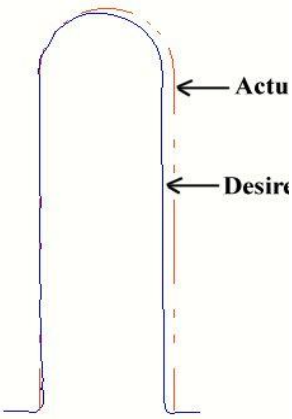	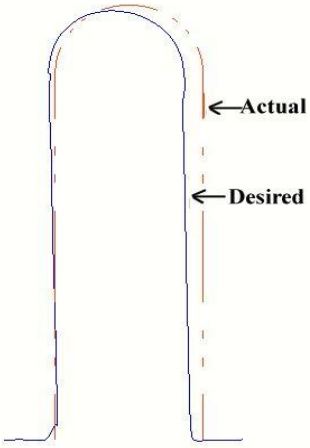

350 rpm, 2 mm, 35 mm/min	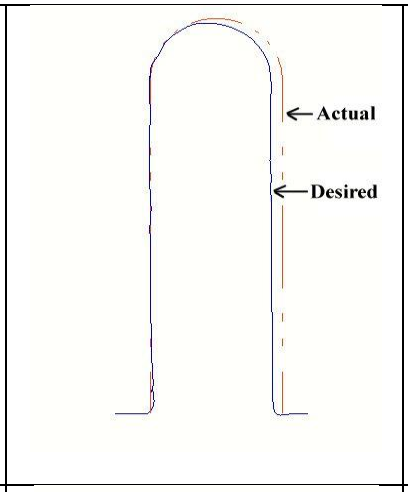	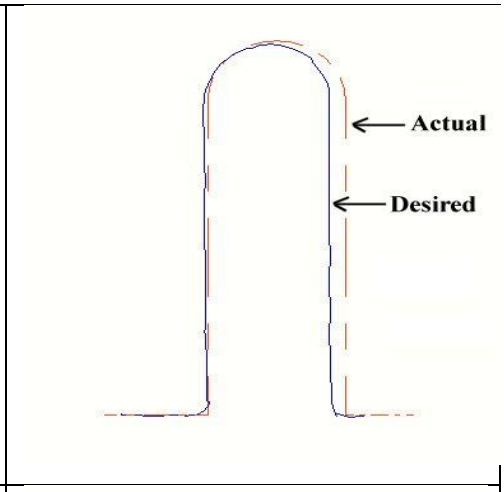
350 rpm, 4 mm, 35 mm/min	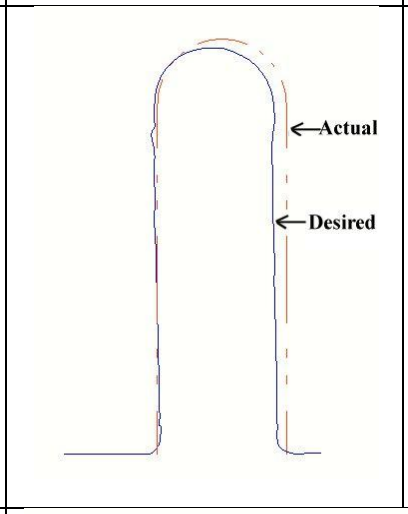	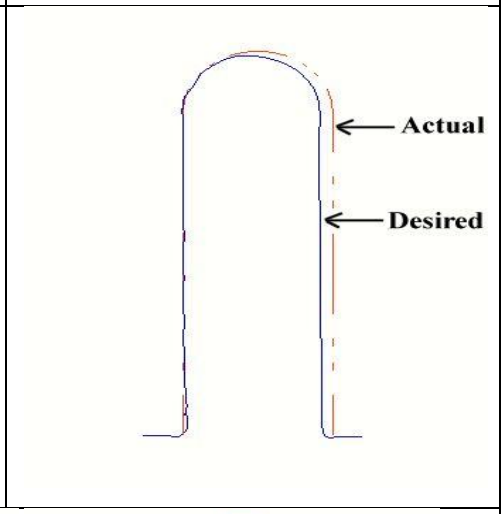
500 rpm, 4 mm, 35 mm/min	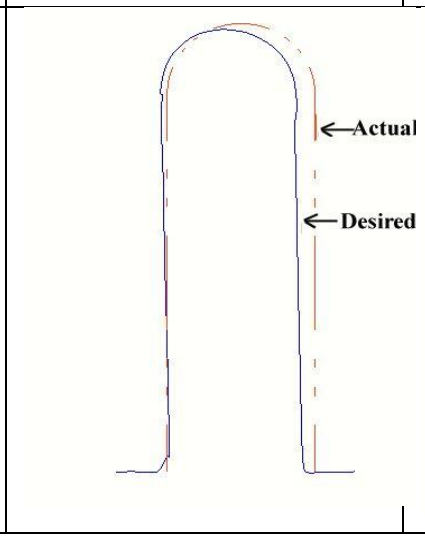	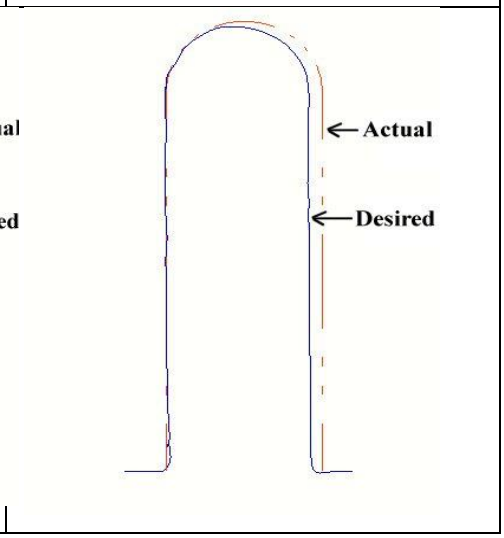

650 rpm, 4 mm, 35 mm/min	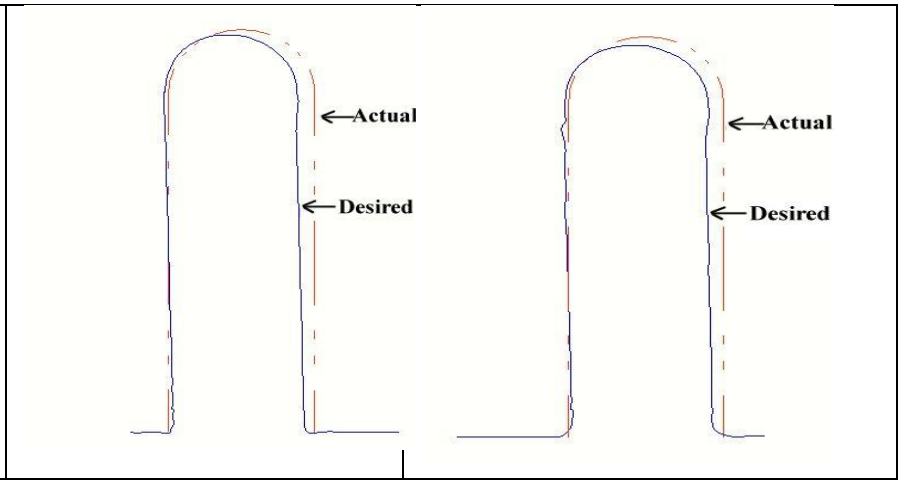

5.4 Comparison and Validation of Results

5.4.1 *For 9.5mm tool diameter*

- **Radial deflection due to depth of Cut**

Table 5.6 Radial deflection due to depth of cut
(constant Cutting speed = 250 rpm and constant feed = 20 mm/min)

	Radial Deflection		
	Bond Graph	FEA	Experimental
DOC = 2 mm	247	270	272
DOC = 3 mm	421.5	441.8	504
DOC = 4 mm	493.5	512	573

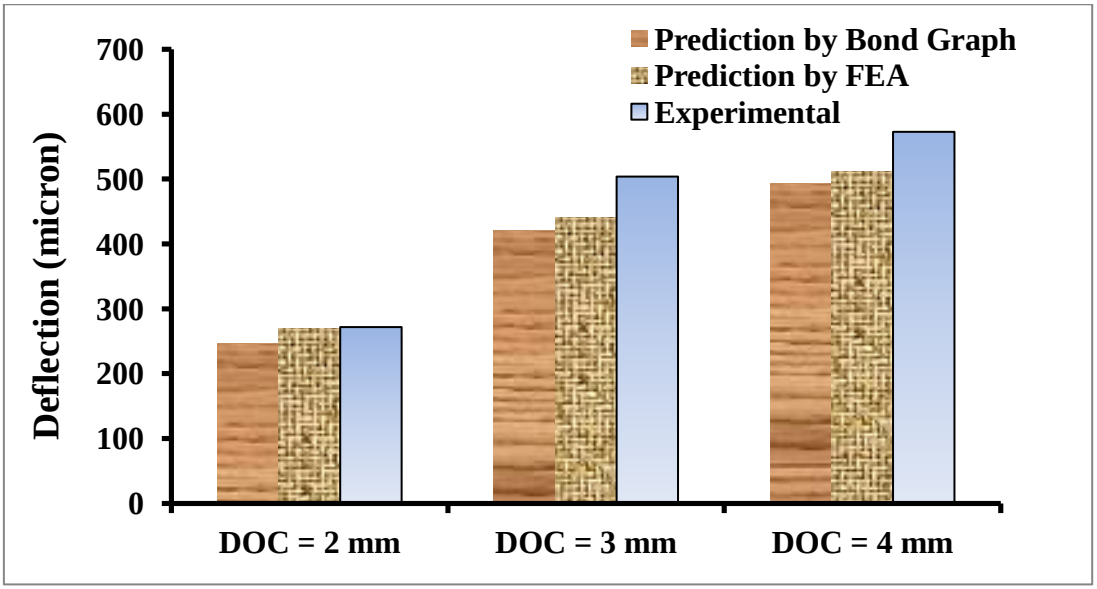

Fig. 5.27 Graphical representation of radial deflection due to depth of cut by bond graph, FEA and experimental study for 9.5mm diameter tool
(constant Cutting speed = 250 rpm and constant feed = 20 mm/min)

- **Tangential deflection due to depth of cut**

Table 5.7 Tangential deflection due to depth of cut
(constant Cutting speed = 250 rpm and constant feed = 20 mm/min)

	Tangential Deflection		
	Bond Graph	FEA	Experimental
DOC = 2 mm	249.5	258.7	282
DOC = 3 mm	386.5	412.4	523
DOC = 4 mm	543	529	545

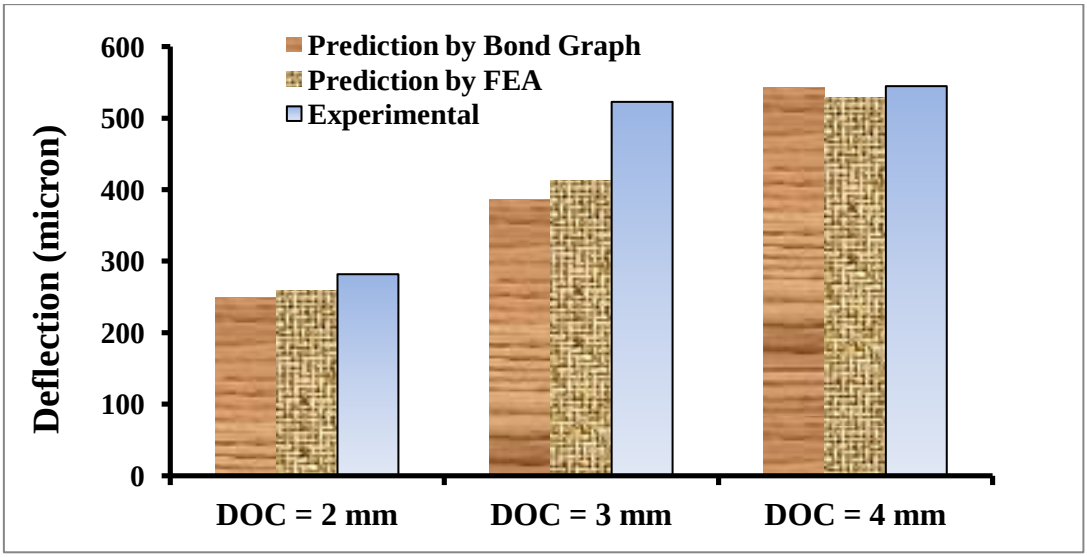

Fig. 5.28 Graphical representation of tangential deflection due to depth of cut by bond graph, FEA and experimental study for 9.5mm diameter tool
(constant Cutting speed = 250 rpm and constant feed = 20 mm/min)

- **Axial deflection due to depth of cut**

Table 5.8 Axial deflection due to depth of cut
(constant Cutting speed = 250 rpm and constant feed = 20 mm/min)

	Axial Deflection		
	Bond Graph	FEA	Experimental
DOC = 2 mm	0.24	0.37	2
DOC = 3 mm	0.35	0.55	5
DOC = 4 mm	0.52	0.83	6

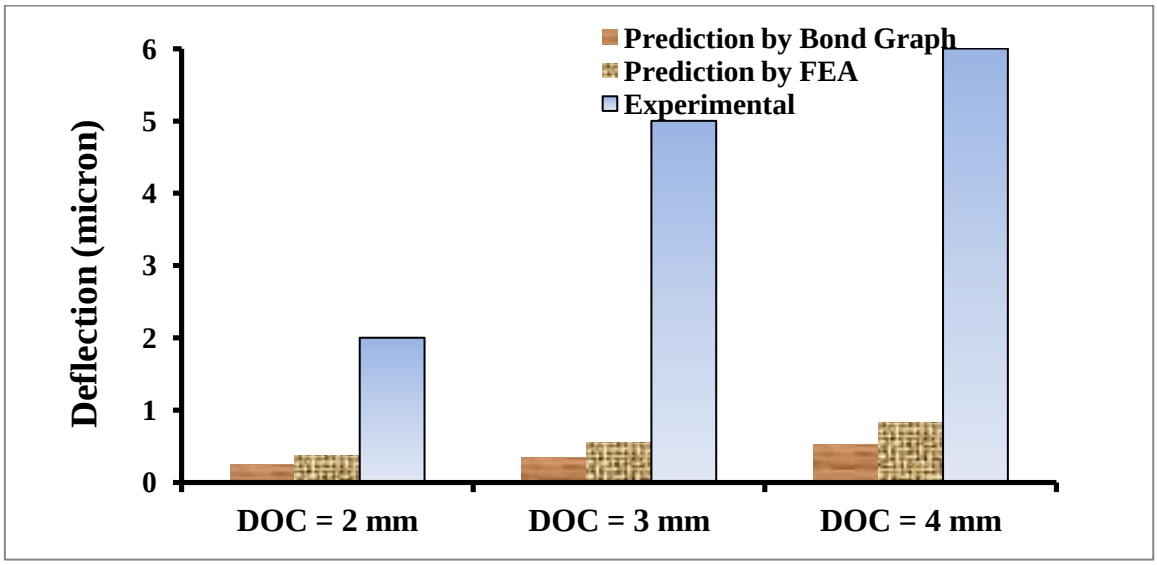

Fig. 5.29 Graphical representation of axial deflection due to depth of cut by bond graph, FEA and experimental study for 9.5mm diameter tool
(constant Cutting speed = 250 rpm and constant feed = 20 mm/min)

- **Radial deflection due to feed**

Table 5.9 Radial deflection due to feed
(constant Cutting speed = 350 rpm and constant DOC = 2 mm)

	Radial Deflection		
	Bond Graph	FEA	Experimental
Feed = 15 mm/min	211.5	215	282.5
Feed = 25 mm/min	279.7	297	259.5
Feed = 35 mm/min	247	270	319.8

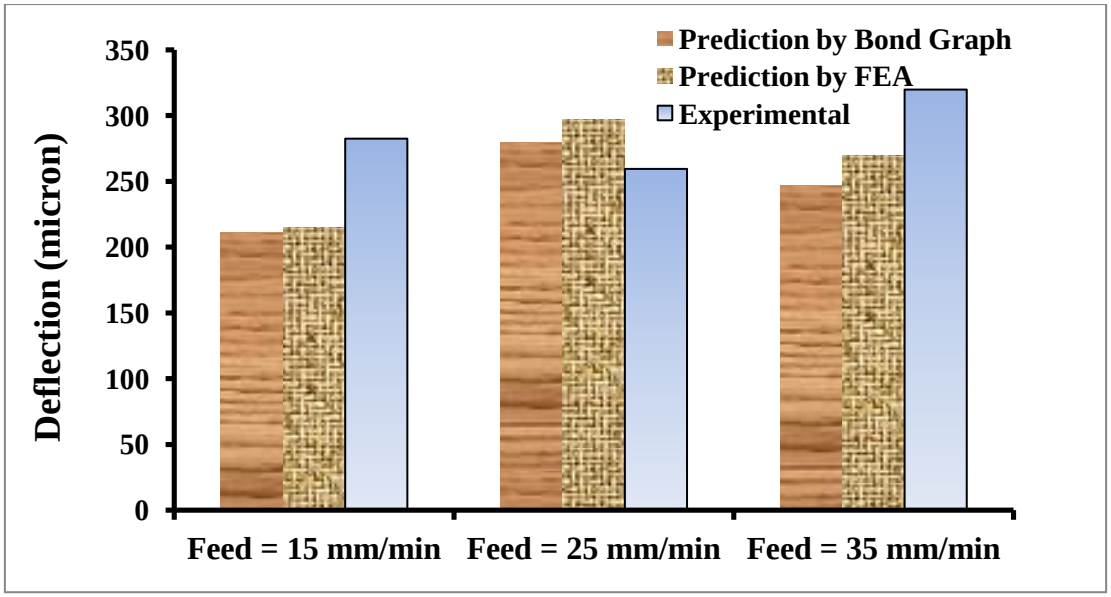

Fig. 5.30 Graphical representation of radial deflection due to feed by bond graph, FEA and experimental study for 9.5mm diameter tool
(constant Cutting speed = 350 rpm and constant DOC = 2 mm)

- **Tangential deflection due to feed**

Table 5.10 Tangential deflection due to feed
(constant Cutting speed = 350 rpm and constant DOC = 2 mm)

	Tangential Deflection		
	Bond Graph	FEA	Experimental
Feed = 15 mm/min	214.5	237	305
Feed = 25 mm/min	281.8	313.7	405
Feed = 35 mm/min	252.3	258	319

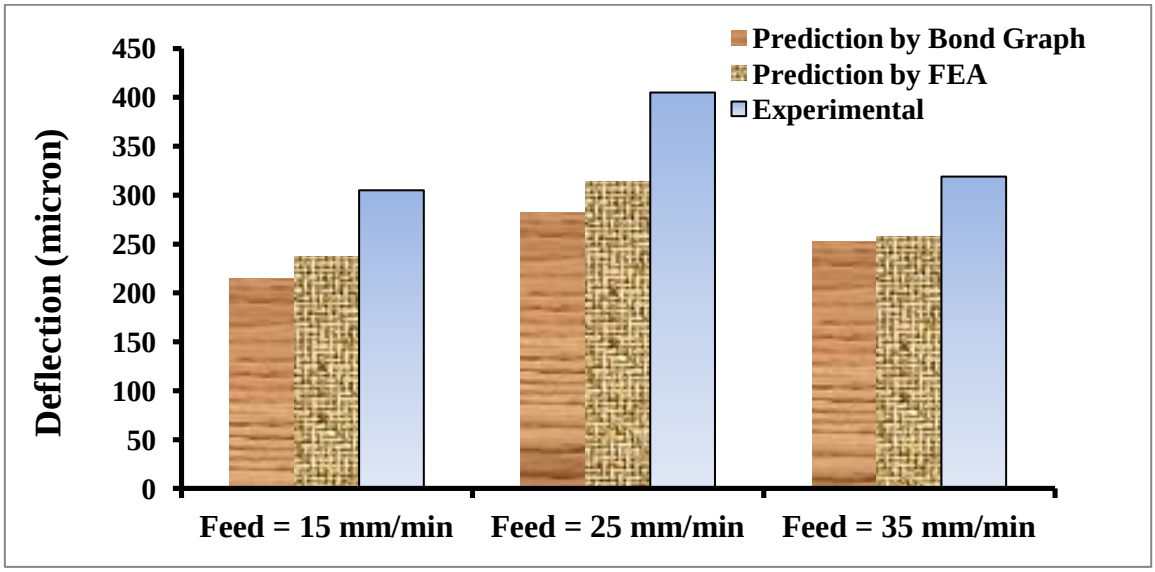

Fig. 5.31 Graphical representation of tangential deflection due to feed by bond graph, FEA and experimental study for 9.5mm diameter tool
(constant Cutting speed = 350 rpm and constant DOC = 2 mm)

- **Axial deflection due to feed**

Table 5.11 Axial deflection due to feed
(constant Cutting speed = 350 rpm and constant DOC = 2 mm)

	Axial Deflection		
	Bond Graph	FEA	Experimental
Feed = 15 mm/min	0.24	0.37	2
Feed = 25 mm/min	0.27	0.37	2
Feed = 35 mm/min	0.24	0.37	2

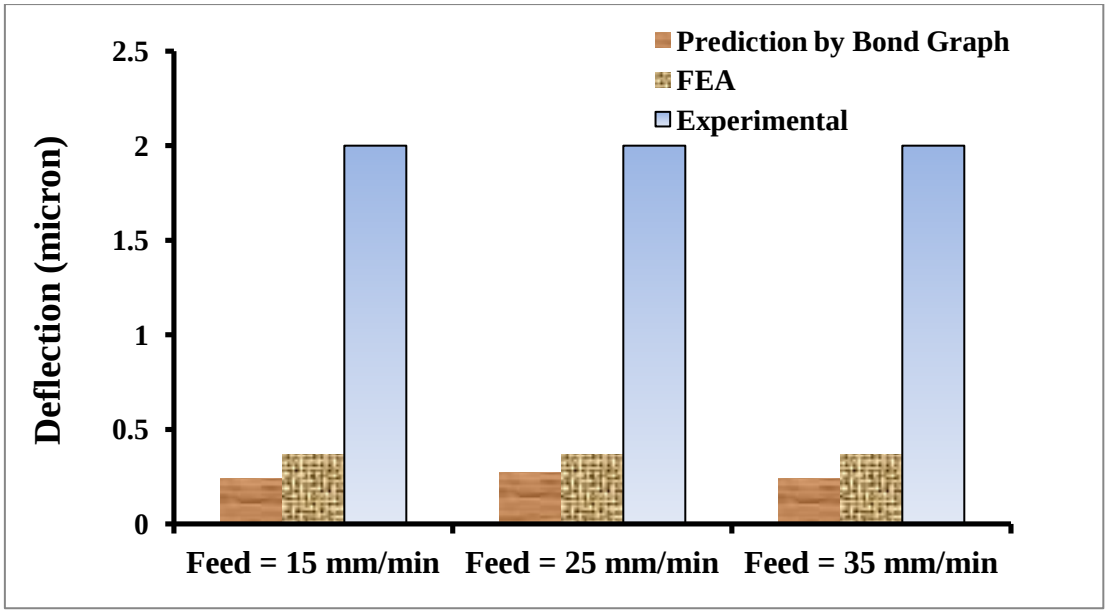

Fig. 5.32 Graphical representation of axial deflection due to feed by bond graph, FEA and experimental study for 9.5mm diameter tool
(constant Cutting speed = 350 rpm and constant DOC = 2 mm)

- **Radial deflection due to cutting speed**

Table 5.12 Radial deflection due to cutting speed
(constant feed = 35 mm/min and constant DOC = 4 mm)

	Radial Deflection		
	Bond Graph	FEA	Experimental
RPM = 350	579	578	648
RPM = 500	452	444	436
RPM = 650	371	359	414

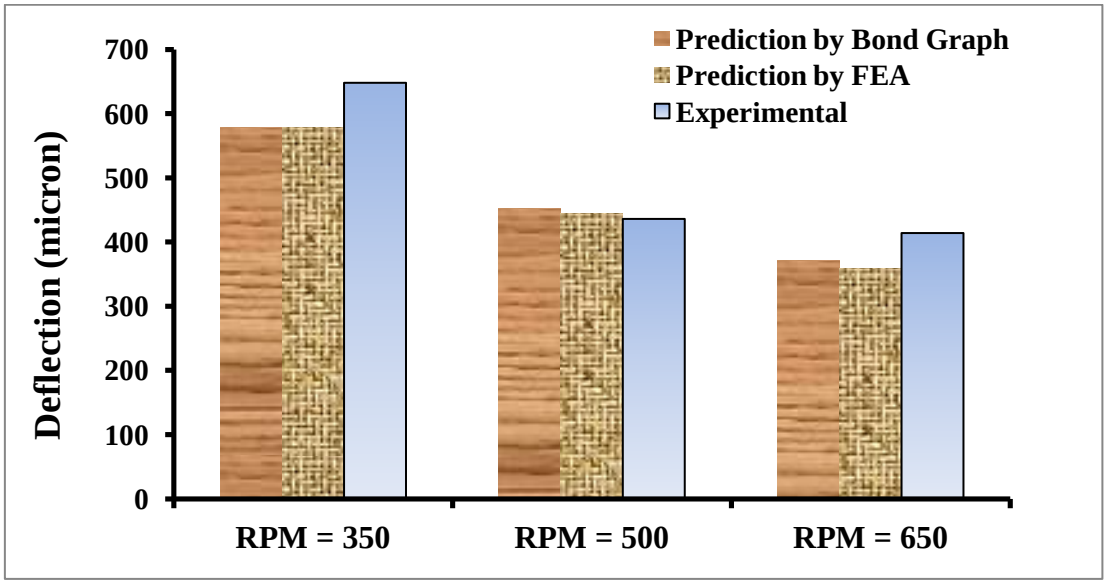

Fig. 5.33 Graphical representation of radial deflection due to cutting speed by bond graph, FEA and experimental study for 9.5mm diameter tool
(constant feed = 35 mm/min and constant DOC = 4 mm)

- **Tangential deflection due to cutting speed**

Table 5.13 Tangential deflection due to cutting speed
(constant feed = 35 mm/min and constant DOC = 4 mm)

	Tangential Deflection		
	Bond Graph	FEA	Experimental
RPM = 350	492.2	559.9	752
RPM = 500	388	444.7	518
RPM = 650	378	367	479

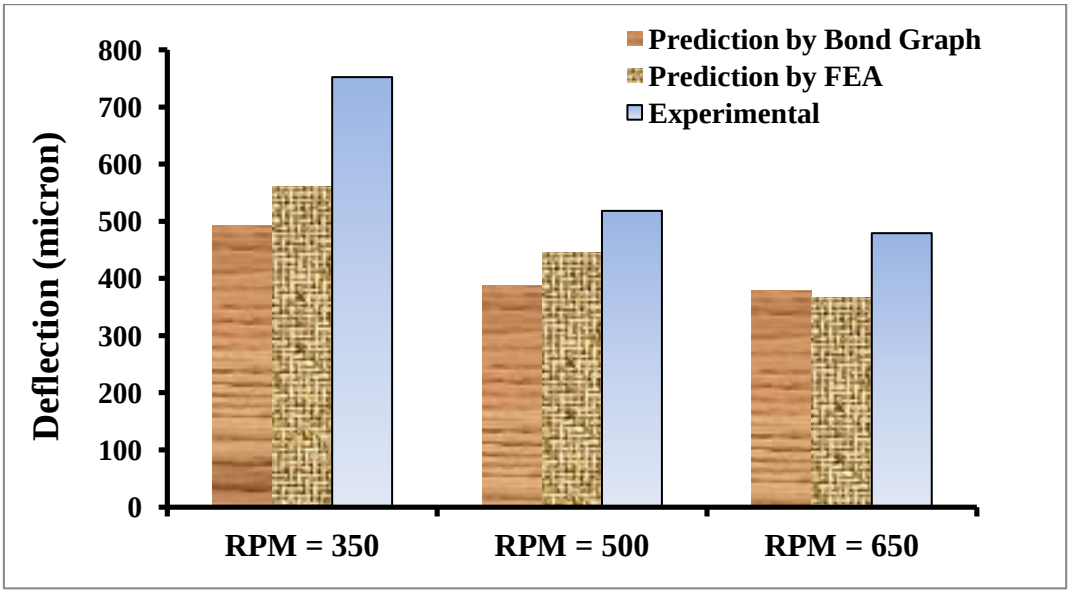

Fig. 5.34 Graphical representation of tangential deflection due to cutting speed by bond graph, FEA and experimental study for 9.5mm diameter tool
(constant feed = 35 mm/min and constant DOC = 4 mm)

- **Axial deflection due to cutting speed**

Table 5.14 Axial deflection due to cutting speed
(constant feed = 35 mm/min and constant DOC = 4 mm)

	Axial Deflection		
	Bond Graph	FEA	Experimental
RPM = 350	0.35	0.55	5
RPM = 500	0.52	0.83	6
RPM = 650	0.24	0.37	3

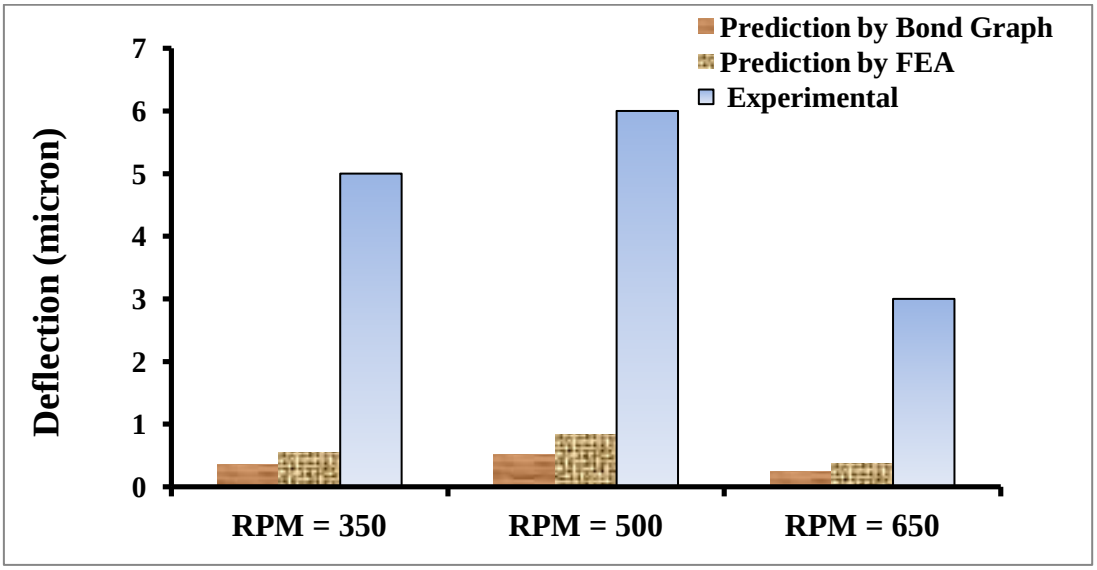

Fig. 5.35 Graphical representation of axial deflection due to cutting speed by bond graph, FEA and experimental study for 9.5mm diameter tool
(constant feed = 35 mm/min and constant DOC = 4 mm)

5.4.2 *For 14 mm tool diameter*

- **Radial deflection due to depth of cut**

Table 5.15 Radial deflection due to depth of cut
(constant Cutting speed = 250 rpm and constant feed = 20 mm/min)

	Radial Deflection		
	Bond Graph	FEA	Experimental
DOC = 2 mm	305.9	194	225
DOC = 3 mm	485.8	450.5	438
DOC = 4 mm	503.8	398	451

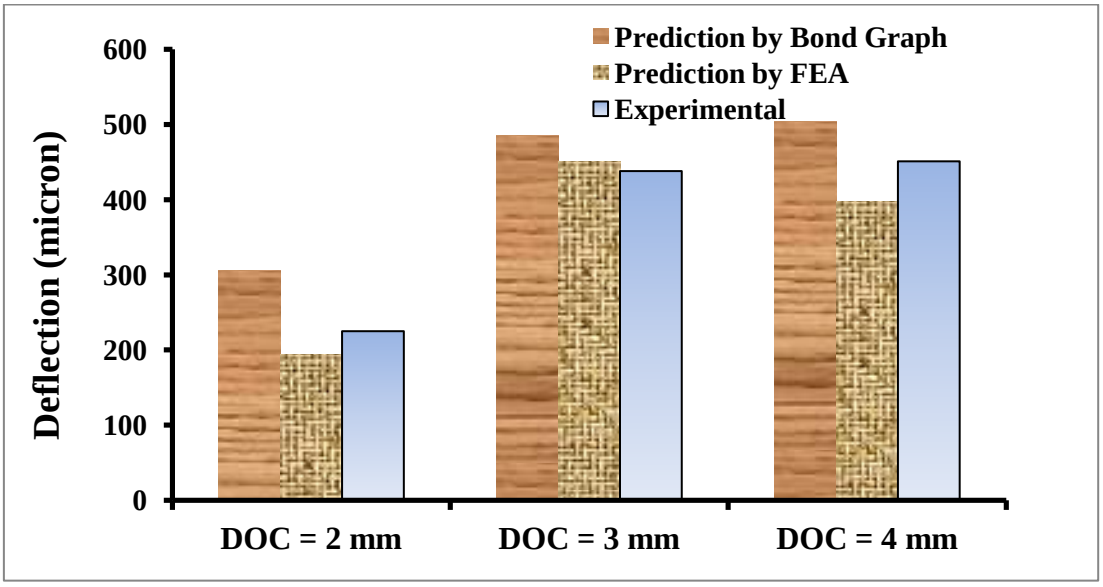

Fig. 5.36 Graphical representation of radial deflection due to depth of cut by bond graph, FEA and experimental study for 14 mm diameter tool
(constant Cutting speed = 250 rpm and constant feed = 20 mm/min)

- **Tangential deflection due to depth of cut**

Table 5.16 Tangential deflection due to depth of cut
(constant Cutting speed = 250 rpm and constant feed = 20 mm/min)

	Tangential Deflection		
	Bond Graph	FEA	Experimental
DOC = 2 mm	354.1	254	280
DOC = 3 mm	477.9	445	517
DOC = 4 mm	534.8	557	512

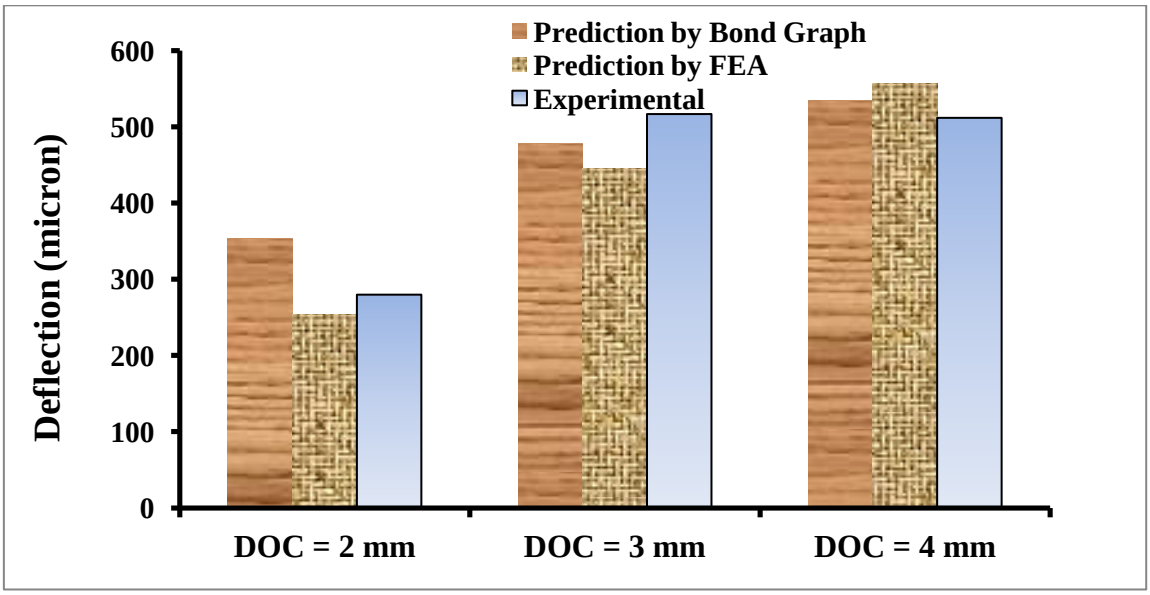

Fig. 5.37 Graphical representation of tangential deflection due to depth of cut by bond graph, FEA and experimental study for 14 mm diameter tool
(constant Cutting speed = 250 rpm and constant feed = 20 mm/min)

- **Axial deflection due to depth of cut**

Table 5.17 Axial deflection due to depth of cut
(constant Cutting speed = 250 rpm and constant feed = 20 mm/min)

	Axial Deflection		
	Bond Graph	FEA	Experimental
DOC = 2 mm	0.18	0.25	0.25
DOC = 3 mm	0.26	0.25	0.25
DOC = 4 mm	0.31	0.36	0.36

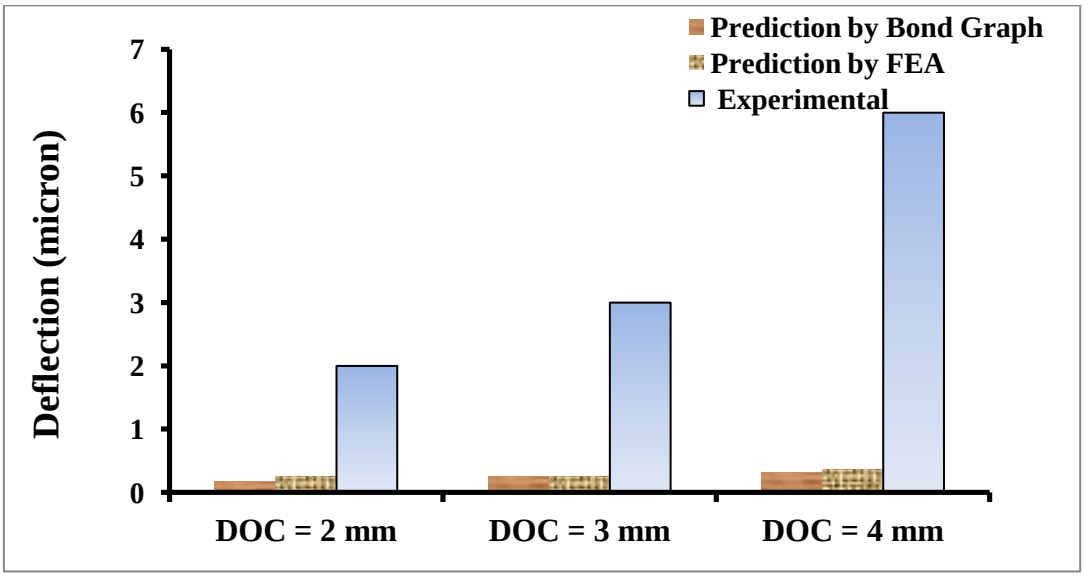

Fig. 5.38 Graphical representation of axial deflection due to depth of cut by bond graph, FEA and experimental study for 14 mm diameter tool
(constant Cutting speed = 250 rpm and constant feed = 20 mm/min)

- **Radial deflection due to feed**

Table 5.18 Radial deflection due to feed
(constant Cutting speed = 350 rpm and constant DOC = 2 mm)

	Radial Deflection		
	Bond Graph	FEA	Experimental
Feed = 15 mm/min	269.9	191	221
Feed = 25 mm/min	197.9	145	161.5
Feed = 35 mm/min	341.9	240	268.5

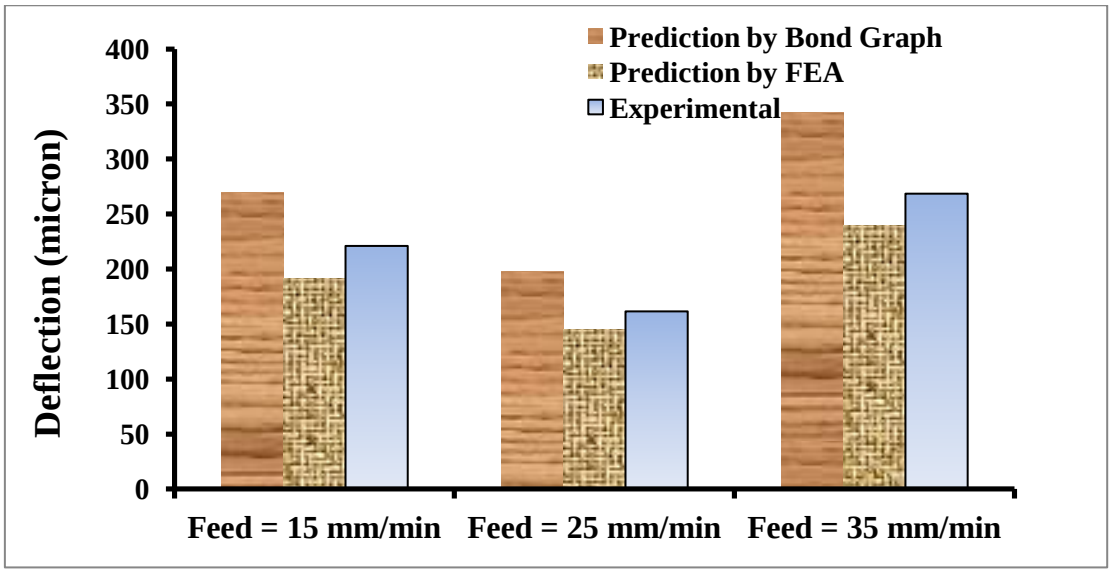

Fig. 5.39 Graphical representation of radial deflection due to feed by bond graph, FEA and experimental study for 14 mm diameter tool
(constant Cutting speed = 350 rpm and constant DOC = 2 mm)

- **Tangential deflection due to feed**

Table 5.19 Tangential deflection due to feed
(constant Cutting speed = 350 rpm and constant DOC = 2 mm)

	Tangential Deflection		
	Bond Graph	FEA	Experimental
Feed = 15 mm/min	279.2	294	306
Feed = 25 mm/min	199.7	217	185
Feed = 35 mm/min	370.7	379	383

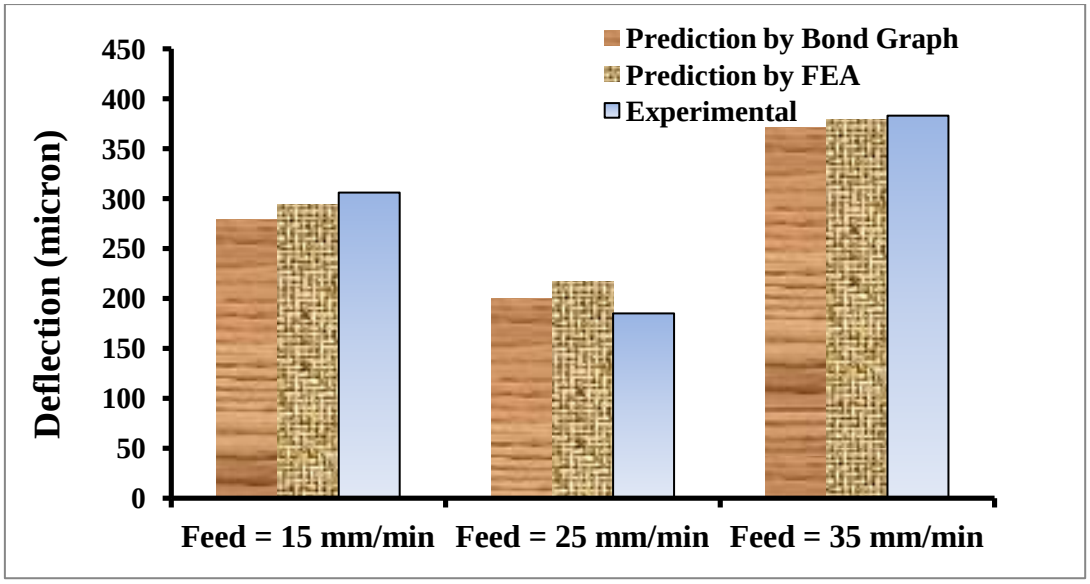

Fig. 5.40 Graphical representation of tangential deflection due to feed by bond graph, FEA and experimental study for 14 mm diameter tool
(constant Cutting speed = 350 rpm and constant DOC = 2 mm)

- **Axial deflection due to feed**

Table 5.20 Axial deflection due to feed
(constant Cutting speed = 350 rpm and constant DOC = 2 mm)

	Axial Deflection		
	Bond Graph	FEA	Experimental
Feed = 15 mm/min	0.26	0.38	3
Feed = 25 mm/min	0.26	0.38	3
Feed = 35 mm/min	0.26	0.38	2

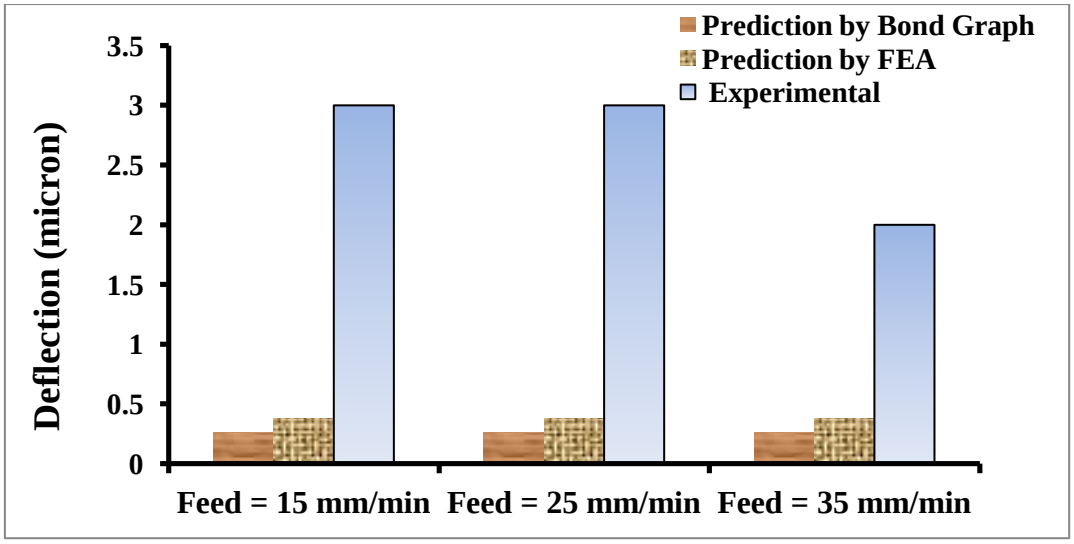

Fig. 5.41 Graphical representation of axial deflection due to feed by bond graph, FEA and experimental study for 14 mm diameter tool
(constant Cutting speed = 350 rpm and constant DOC = 2 mm)

- **Radial deflection due to cutting speed**

Table 5.21 Radial deflection due to cutting speed
(constant feed = 35 mm/min and constant DOC = 4 mm)

	Radial Deflection		
	Bond Graph	FEA	Experimental
RPM = 350	521.8	410	447.3
RPM = 500	629.8	494	557
RPM = 650	539.8	430	497

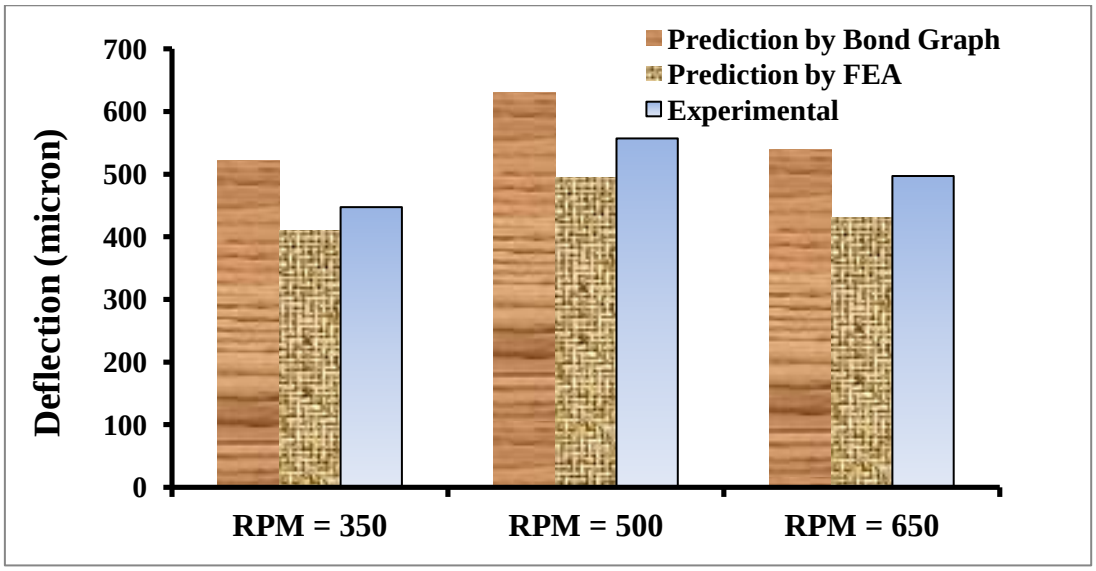

Fig. 5.42 Graphical representation of radial deflection due to cutting speed by bond graph, FEA and experimental study for 14 mm diameter tool
(constant feed = 35 mm/min and constant DOC = 4 mm)

- **Tangential deflection due to cutting speed**

Table 5.22 Tangential deflection due to cutting speed
(constant feed = 35 mm/min and constant DOC = 4 mm)

	Tangential Deflection		
	Bond Graph	FEA	Experimental
RPM = 350	522.9	587	607
RPM = 500	655	723	644
RPM = 650	547	615	556

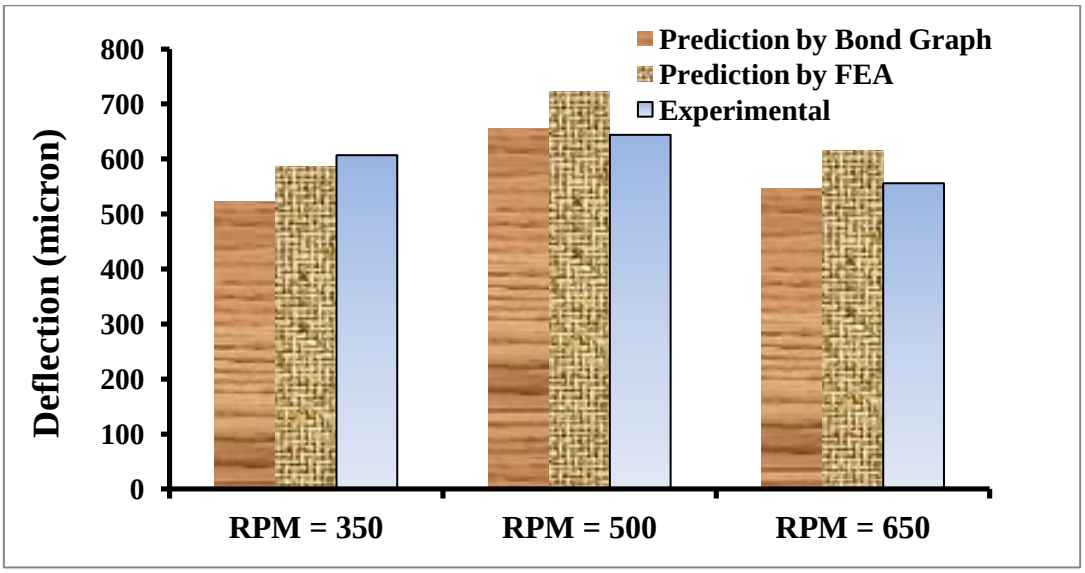

Fig. 5.43 Graphical representation of tangential deflection due to cutting speed by bond graph, FEA and experimental study for 14 mm diameter tool
(constant feed = 35 mm/min and constant DOC = 4 mm)

- **Axial deflection due to cutting speed**

Table 5.23 Axial deflection due to cutting speed
(constant feed = 35 mm/min and constant DOC = 4 mm)

	Tangential Deflection		
	Bond Graph	FEA	Experimental
RPM = 350	0.26	0.38	5
RPM = 500	0.39	0.56	7
RPM = 650	0.47	0.68	3

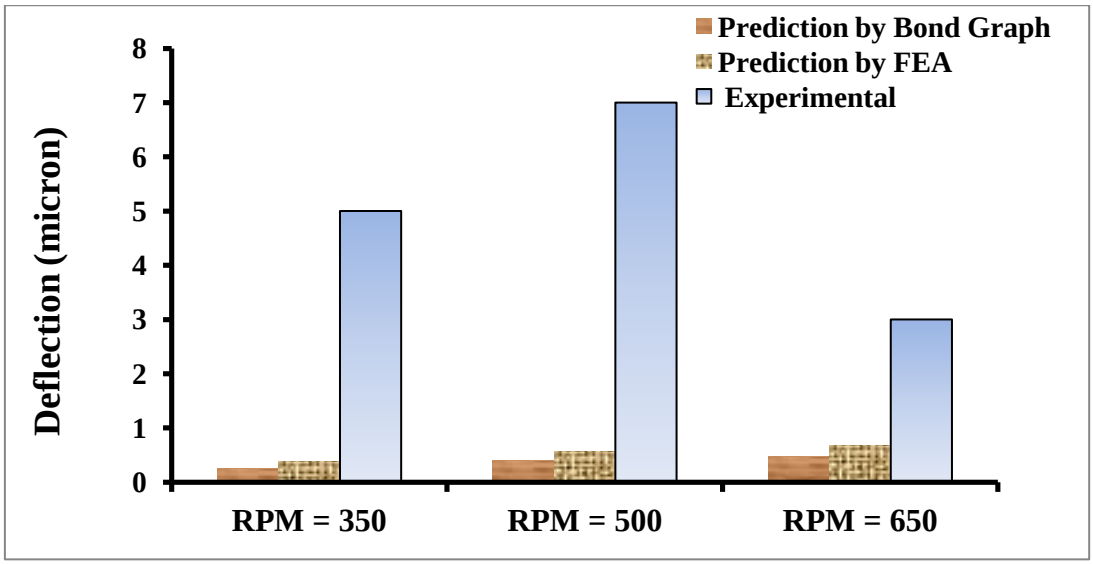

Fig. 5.44 Graphical representation of axial deflection due to cutting speed by bond graph, FEA and experimental study for 14 mm diameter tool
(constant feed = 35 mm/min and constant DOC = 4 mm)

CHAPTER 6

Conclusions And Scope Of Future Work

6.1 Conclusions

Deflection of cutter due to different cutting forces is predicted by FEA and bond graph approach and validated with experiment. The cutting forces exerted by the cutting tool on the work piece during a machining has been identified in order to control the tool deflection, and improve the accuracy of the geometry required. The aim of study is to predict the effects of cutting parameters on the variations of cutting forces to measure the tool deflection during end milling operation on medium carbon steel.

.The experiment has been performed by varying parameters. The critical analysis of results shows that when depth of cut varies by keeping others parameter constant, the deformation values seemed to be more sensitive to it. It means the value of cutting force increases with increase in depth of cut, which increases the tool deflection. When speed was varied the cutting forces will decrease, similarly there is less tool deflection. It has been calculated when feed rate is varied the variation in cutting forces also increases, similarly deflection also increases.

Similarly the FEA analysis shows that the tool deflection depends upon the cutting forces, higher the cutting force higher will be the value of tool deflection. From the results it was concluded that a deflection value varies throughout the tool. It is maximum at tool tip and minimum at holding position. From the experiment it has been concluded that when cutting force on the tool is high then surface finish is very less.

- Prediction of cutter deflection by FEM and bond graph closely match with experimental values.
- Error of machined surface is mostly contributed by the radial and tangential forces.
- Axial force has marginal effects on the workpiece (in depth direction).
- Depth of cut has the most significant influence on profile deviations.
- Predictions by bond graph simulation takes significantly less computational time and space.

6.2 Scopes for Future Work

Based on this thesis, the following areas of work are suggested for further exploration.

- Generation of an analytical model for prediction of deflection directly.
- Tool compensation methodology can used to improve the accuracy.
- Increasing the parameter repetition to validate the optimum conditions and find best tool material for different grades of material for machining.
- Increasing the slices in FEA modeling will also increase the accuracy of results. But automatically it will take more memory and time for post processing.

References

- Budak, E. (2005) Analytical models for high performance milling. Part I: cutting forces, structural deformation and tolerance integrity, *International Journal of Machine Tool & Manufacture*, 46: 1478 – 1488.
- Brown, (1914) Practical treatise on milling and milling machines. *Brown & Sharpe Manufacturing company*, Retrieved 2013, 01 – 28.
- Bhattacharya, A. (1998) Metal cutting theory and practices. *New Central Book Agency (p) Ltd*., 87 – 88.
- Chattopadhyay, A.K. *IIT Kharagpur Course*, Access from NPTEL Lecture.
- Desai, K.A.; Rao, P.V.M. (2012) On cutter deflection surface error in peripheral milling. *Journal of material processing technology*, 212**:** 2443 – 2454.
- Kivanc. E.B.; Budak, E. (2004) Structural modeling of end mill for form error and stability analysis. *Int. J. Mach. Tool Manufacture*, 44: 1151 – 1161.
- Armarego, E.J.A.; Brown, R.H. (1969) The Machining of Metals, Prentice Hall, englewood Cliffs, NJ.
- Rivin, E. (1999) Stiffness and Damping in Mechanical Design, *marcel Dekker, New York*
- Hyoung.; Ryu, S. (2012) An analytical expression for end milling forces and tool deflection using Fourier series. *Int J Adv Manuf Technol*, 59: 37 – 46.
- Tlusty, J.; Macneil, P. (1975) Dynamics of cutting forces in end milling. *Ann. CIRP* 24, 1, 21 – 25.
- Ohio. (1992) A treatise on milling and milling machines. *Cincinnati Milling Machine Company* Retrieved 2013, 01– 28.
- Lacalle, L.N Lopez.; Lamikiz. D.; Salgado, M.A. (2007) Tool path selection based on minimum deflection cutting forces in the programming of complex surface milling. *International Journal of Machine Tool & Manufacture*, 47: 388 – 400.
- Rao, V.S.; Rao, P.V.M. (2004) Modeling of tooth trajectory and process geometry in peripheral milling of curved surf. *International Journal of Machine Tool & Manufacture*, 45: 617 – 630.
- Rao, V.S.; Rao, P.V.M. (2006) Tool deflection compensation in peripheral milling of curved geometries. *International Journal of Machine Tool & Manufacture*, 46: 2036 – 2043.

- Rao, V.S. (2005) Effect of work piece curvature on cutting forces and surface error in peripheral milling. *Journal of Engineering, Manufacturing, Proceedings of the Institution of Mechanical Engineers*. UK, submitted for publication.
- Srinath, L.S. (2009) Advanced mechanics of solids. tata *mchraw hill education private limited, new delhi*, 3: 216–219
- Saffer, R. J.; Rajfar, M.R.; Zarai, O. (2008) Simulation of three-dimension cutting force and tool deflection in the end milling operation based on finite element method, *Simulation Modeling Practice and Theory*, 16: 1677–1688.
- Kline, W.A.; Devor, R.E.; Shareef, I.A. (1982) The prediction of surface accuracy in end milling. *Transactions of ASME Journal of Engineering for Industry*, 104: 272–278.
- Woodbury, Robert S. (1972) History of the Milling Machine. In Studies in the History of Machine Tools. *Cambridge, Massachusetts, USA, and London, England, MIT Press, ISBN*, 978: 0–262.
- Myeong, Woo. Cho. (1999) Tool trajectory based on tool deflection effects in Flat-end milling process, *KSME International Journal*, 13: 738 –751.
- Altintas, Y. (2000), Manufacturing automation, *Cambridge university press, Cambridge.*
- Singh, J. (2013) Dynamic Analysis and Control of Semi Active Suspension System for a Heavy Vehicle: A Bond Graph Approach. ME thesis, Thapar University, India.

WEB REFERENCES

- Nomenclature of milling cutter
  http://www.mechlook.com (assessed January 2013)
- Strain energy due to shear deformation,
  http://www.facweb.iitkgp.ernet.in/~baidurya/CE21004/online_lecture_notes/m1l2.pdf (2009, assessed on September 2013)
- Strain energy due to torsional deformation,
  http://www.freestudy.co.uk/statics/complex/t5.pdf (2009, assessed on September 2013).